# Athens Journal of Technology & Engineering

*Quarterly Academic Periodical, Volume 8, Issue 3, September 2021*
*URL: https://www.athensjournals.gr/ajte*
*Email: journals@atiner.gr*
*e-ISSN: 2241-8237 DOI: 10.30958/ajte*

## Front Pages

# Athens Journal of Technology & Engineering

*Published by the Athens Institute for Education and Research (ATINER)*



*******************************************************************************

*ATINER is an Athens-based World Association of Academics and Researchers based in Athens. ATINER is an independent and non-profit Association with a Mission to become a forum where Academics and Researchers from all over the world can meet in Athens, exchange ideas on their research and discuss future developments in their disciplines, as well as engage with professionals from other fields. Athens was chosen because of its long history of academic gatherings, which go back thousands of years to Plato's Academy and Aristotle's Lyceum. Both these historic places are within walking distance from ATINER's downtown offices. Since antiquity, Athens was an open city. In the words of Pericles, Athens"…is open to the world, we never expel a foreigner from learning or seeing". ("Pericles' Funeral Oration", in Thucydides, The History of the Peloponnesian War). It is ATINER's mission to revive the glory of Ancient Athens by inviting the World Academic Community to the city, to learn from each other in an environment of freedom and respect for other people's opinions and beliefs. After all, the free expression of one's opinion formed the basis for the development of democracy, and Athens was its cradle. As it turned out, the Golden Age of Athens was in fact, the Golden Age of the Western Civilization. Education and (Re)searching for the 'truth' are the pillars of any free (democratic) society. This is the reason why Education and Research are the two core words in ATINER's name.*

******************************************************************************************

The ***Athens Journal of Technology & Engineering (AJTE)*** is an Open Access quarterly double-blind peer reviewed journal and considers papers from all areas engineering (civil, electrical, mechanical, industrial, computer, transportation etc), technology, innovation, new methods of production and management, and industrial organization. Many of the papers published in this journal have been presented at the various conferences sponsored by the Engineering & Architecture Division of the Athens Institute for Education and Research (ATINER). All papers are subject to ATINER's Publication Ethical Policy and Statement.

The Athens Journal of Technology & Engineering
ISSN NUMBER: 2241-8237- DOI: 10.30958/ajte
Volume 8, Issue 3, September 2021
Download the entire issue (PDF)

# Athens Journal of Technology & Engineering
# Editorial and Reviewers' Board

# President's Message

All ATINER's publications including its e-journals are open access without any costs (submission, processing, publishing, open access paid by authors, open access paid by readers etc.) and is independent of presentations at any of the many small events (conferences, symposiums, forums, colloquiums, courses, roundtable discussions) organized by ATINER throughout the year and entail significant costs of participating. The intellectual property rights of the submitting papers remain with the author. Before you submit, please make sure your paper meets the basic academic standards, which includes proper English. Some articles will be selected from the numerous papers that have been presented at the various annual international academic conferences organized by the different divisions and units of the Athens Institute for Education and Research. The plethora of papers presented every year will enable the editorial board of each journal to select the best, and in so doing produce a top-quality academic journal. In addition to papers presented, ATINER will encourage the independent submission of papers to be evaluated for publication.

The current issue is the third of the eighth volume of the *Athens Journal of Technology & Engineering (AJTE),* published by the Engineering & Architecture Division of ATINER.

Gregory T. Papanikos, President, ATINER.

# Athens Institute for Education and Research
*A World Association of Academics and Researchers*

## 12th Annual International Conference on Civil Engineering
## 20-23 June 2022, Athens, Greece

The Civil Engineering Unit of ATINER is organizing its **12th Annual International Conference on Civil Engineering, 20-23 June 2022, Athens, Greece** sponsored by the Athens Journal of Technology & Engineering. The aim of the conference is to bring together academics and researchers of all areas of Civil Engineering other related areas. You may participate as stream leader, presenter of one paper, chair of a session or observer. Please submit a proposal using the form available (https://www.atiner.gr/2022/FORM-CIV.doc).

### Academic Members Responsible for the Conference

- **Dr. Dimitrios Goulias**, Head, Civil Engineering Unit, ATINER and Associate Professor & Director of Undergraduate Studies Civil & Environmental Engineering Department, University of Maryland, USA.

### Important Dates

- Abstract Submission: **22 November 2021**
- Acceptance of Abstract: 4 Weeks after Submission
- Submission of Paper: **23 May 2022**

### Social and Educational Program

The Social Program Emphasizes the Educational Aspect of the Academic Meetings of Atiner.

- Greek Night Entertainment (This is the official dinner of the conference)
- Athens Sightseeing: Old and New-An Educational Urban Walk
- Social Dinner
- Mycenae Visit
- Exploration of the Aegean Islands
- Delphi Visit
- Ancient Corinth and Cape Sounion

### Conference Fees

Conference fees vary from 400€ to 2000€
Details can be found at: https://www.atiner.gr/fees

# Athens Institute for Education and Research

*A World Association of Academics and Researchers*

**10th Annual International Conference on Industrial, Systems and Design Engineering, 20-23 June 2022, Athens, Greece**

The Industrial Engineering Unit of ATINER will hold its **10th Annual International Conference on Industrial, Systems and Design Engineering, 20-23 June 2022, Athens, Greece** sponsored by the Athens Journal of Technology & Engineering.The aim of the conference is to bring together academics, researchers and professionals in areas of Industrial, Systems, Design Engineering and related subjects. You may participate as stream leader, presenter of one paper, chair of a session or observer. Please submit a proposal using the form available (https://www.atiner.gr/2022/FORM-IND.doc).

**Important Dates**

- Abstract Submission: **22 November 2021**
- Acceptance of Abstract: 4 Weeks after Submission
- Submission of Paper: **23 May 2022**

**Academic Member Responsible for the Conference**

- **Dr. Theodore Trafalis**, Director, Engineering & Architecture Division, ATINER, Professor of Industrial & Systems Engineering and Director, Optimization & Intelligent Systems Laboratory, The University of Oklahoma, USA.

**Social and Educational Program**

The Social Program Emphasizes the Educational Aspect of the Academic Meetings of Atiner.

- Greek Night Entertainment (This is the official dinner of the conference)
- Athens Sightseeing: Old and New-An Educational Urban Walk
- Social Dinner
- Mycenae Visit
- Exploration of the Aegean Islands
- Delphi Visit
- Ancient Corinth and Cape Sounion

More information can be found here: https://www.atiner.gr/social-program

**Conference Fees**

Conference fees vary from 400€ to 2000€

Details can be found at: https://www.atiner.gr/fees

*Athens Journal of Technology and Engineering - Volume 8, Issue 3, September 2021 – Pages 199-216*

# Assessment of Miniature Piezoelectric Travelling-Wave Beam and Plate Robots

*By Adel Razek*[*]

*Different up-to-date utilizations have found several benefits in condensing the size of autonomous robots. Miniature traveling wave piezoelectric robots have proven to be appropriate for many of these applications. The principles of locomotion embraced in these robots are mainly inspired by natural biological locomotion and could be categorized by their movement through a specific medium. In this article, after having highlighted the amplifying effect of piezoelectric actuators generating the locomotion necessary for robotic requests, we will review the different types of such locomotion. Next, we will discuss the traveling wave piezoelectric resonant robots. Succeeding, we will look at the operation and usages of piezoelectric beam and plate robots. Finally, we will discuss the modeling aspects implicated in these robots and more generally, the modeling of piezoelectric patches stuck on thin structures.*

**Keywords:** *piezoelectric, miniature, travelling-wave, locomotion, beam and plate robots*

## Introduction

Various recent applications have found many advantages in reducing the size of autonomous robots. We can cite, for example, the storage of cells, research objects in narrow areas, the behavior of swarms, surveillance for security, medical applications. Such miniaturization allows the robot to access restricted scenes such as, water pipes (Zhu 2007), in the middle of debris (Casper and Murphy 2003, Zhang et al. 2012), implanting the human body (Dolghi et al. 2011, Razek 2018, Razek 2019). In addition, due to modest power demands, it is likely that a miniature robot will operate from physical energy sources such as light, electric fields, magnetic fields, or vibration (Paradiso and Starner 2005). One can encounter several difficulties related to the design of a miniature robot. The reduced size of the robot amplifies the complication of the robot's power supply, mechanical scheme, sensors and control. To remedy this, we can reduce the number of actuators or the robot's degrees of freedom.

Piezoelectric actuators are potential allowing technology for autonomous micro robots with locomotion aptitudes matching biological practices. Many piezoelectric robots that move on a solid substrate (smooth and flat ground) have been investigated. Many designs and mechanisms can be found in literature (Avirovik et al. 2014, Baisch 2013, Zhou et al. 2013, Zesch et al. 1995, Cimprich et al. 2006, Simu and Johansson 2002, Ishihara et al. 1995, Uchino 2006, Hariri et

[*]Emeritus Research Director, C.N.R.S. & Honorary Professor, CentraleSupelec, GeePs, University of Paris-Saclay and Sorbonne University, France.

al. 2010, Hariri et al. 2018, Hariri et al. 2015a, Hariri et al. 2015b, Bernard et al. 2014a, b). The sizes of mobile miniature robots are generally of less than one $dm^3$ and a motion range of at least several times the robots body length.

Piezoelectric materials power miniature robots. Multilayer piezoelectric actuators and bending piezoelectric actuators potentially improve the performance of piezoelectric materials and make them among the most commonly used in miniature mobile robots. Piezoelectric actuators are responsible for movement and are characterized by two energy transformations. These are electrical to mechanical conversion and mechanical-to-mechanical conversion. The first transformation reflects the reverse piezoelectric effect that results in little movement of the mobile miniature robot. The second holds a specific locomotion that amplifies the movement of the miniature robot. The involved locomotion principles are mostly inspired from natural locomotion and could be categorized by their displacement through a fluid medium or on a solid substrate (Hariri 2012).

In this paper, after pointing out the amplifying effect of piezoelectric actuators engendering locomotion that is necessary for robotic applications, we will review the different types of such locomotion. Then, we will discuss the functioning of traveling wave piezoelectric resonant robots. Following this, we will consider the operation and applications of piezoelectric beam and plate robots. Finally, we will discuss the modeling aspects involved in these robots.

## Locomotion Principles and Miniature Robots

As mentioned before, the amplifying effect of piezoelectric actuators engenders locomotion is necessary for robotic applications. In this section, we are going to discuss the two categories of locomotion, displacements on solid surfaces and through fluids.

### *Locomotion on a Solid Substrate*

The forces associated to on-ground motion involve the gravity, the normal reaction, the friction force and the active force that generates the motion. Locomotion on a solid surface of a mobile miniature robot comprises different types. These are wheeled, walking, inchworm, inertial drive, resonant drive and friction drive.

#### Wheeled Locomotion

The principle of this locomotion is founded on small actuators operating wheels. These actuators can be DC motors, step motors, or piezoelectric ones. Cases for wheeled locomotion in miniature robots operated by piezoelectric materials could be found in (Uchino 2006, Epson 2010).

Walking Locomotion

This locomotion uses legs that are the drive elements to realize a movement like that of a biological entity. In walking mechanisms of mobile miniature robots, the legs are fastened on the robot by pairs in which each leg can maintain alone the robot equilibrium. The legs perhaps thermal, polymer, electrostatic or piezoelectric drives components. In the last case, piezoelectric actuators are generally multilayer benders or monolithic multilayer. Note that walking is principally a quasi-static locomotion. Different piezoelectric miniature robots involving walking locomotion are given in e.g., Rembold and Fatikow (1997), Simu and Johansson (2002) and Snis et al. (2004).

Inchworm Locomotion

The inchworm principle is based on operating clampers and extensors actuations permitting displacements (Sunyoto et al. 2006). An inchworm mechanism consists of three actuators, two clampers and one extensor. The extensor one is always between the two clampers. The clamper is used to clamp the device into the substrate while the extensor generates the stroke required for the displacement. Examples of inchworm locomotion in piezoelectric miniature robots are given in Fuchiwaki and Aoyama (2002), Koyanagi et al. (2000), Torii et al. (2001), Yan et al. (2005) and Wood (2008).

Inertial Drive

The inertial drive notion is engendered in asymmetric actuation situations, i.e., in the case of rapid extension (or contraction) and slow contraction (or extension) of the actuator. Consequently, the control signal of the actuator must be a saw tooth one. Piezoelectric actuators hold high bandwidth that permit such functioning and so, most of miniature robots based on inertial drive principle are actuated by piezoelectric actuators. Two sorts of inertial drive principles can be distinguished: the stick-slip one and the impact drive one (Figure 1). A stick-slip situation consists of an inertial mass that is the main body with legs which are the piezoelectric drive elements. These last are fixed in the inertial mass from one side and exercise the contact surface on the other. An impact drive design consists of an inertial mass connected to the main body via a piezoelectric element (Driesen 2008). Examples of piezoelectric miniature robots based on the inertial drive principles are shown in Rembold and Fatikow (1997), Simu and Johansson (2006), Ikuta et al. (1991) and Zesch et al. (1995).

**Figure 1.** *Stick-Slip (left) and Impact Drive (right) Designs*

Resonant Drive

Resonant drive motion modes are often used in the case of ultrasonic motors (USM). In the case of mobile miniature robot, the resonant motion is linked to the standing wave type that is defined e.g., in Driesen (2008) by inertial slip generation using contact force variation. So, the motion is generated by variation of the contact force, which is the inertial effect of a vertical vibration, which results from the back -and-forth motion of the robot body. This could be abbreviated that the inertial force is engendered by the horizontal vibration of the robot body. Therefore to intensify the inertial force, the horizontal vibration must be increased. This requires increasing the frequency of feet vibration. The motion occurs when this inertial force becomes greater than the maximum feet to substrate friction force. Therefore, it is needed to increase the frequency until a threshold where motion occurs. Examples of piezoelectric mobile miniature robots using this mode could be found in Edqvist et al. (2008), Ferreira and Minotti (1997), Son et al. (2006) and Cimprich et al. (2006).

Friction Drive

In this case, the origination of motion is due to the change of friction coefficient all through horizontal vibration of the robot body. The variation of friction coefficient results from a no perpendicular contact angle between robot feet and substrate. This is different from the resonant drive. In the case of the resonant drive the horizontal vibration generates the inertial vibration that in turn generates the motion of the robot. While in the friction drive, no inertial force vibration occurs during horizontal vibration but a change in the friction coefficient. This causes a motion in the direction of low friction without involvement of the inertial force. Examples of piezoelectric miniature robots using this mode are given in Aoshima et al. (1993), Ishihara et al. (1995) and Matsuoka et al. (1993).

*Locomotion through Fluids*

We consider here locomotion in water and in air (Hariri et al. 2010). The movement in liquid is entirely inspired from natural locomotion and is distributed into locomotion inside liquid and at the liquid surface. For the case inside water, a description of fish swimming modes can be found in Sfakiotakis et al. (1999). Some piezoelectric miniature robots like swimming fishes are developed e.g., in Fukuda et al. (1994), Tzeranis and Papadopoulos (2003), Borgen et al. (2003), Deng and Avadhanula (2005), Kodati et al. (2007), Wiguna et al. (2006) and Hu et al. (2006), where piezoelectric actuators are used for producing the movements for miniature robots. In addition, piezoelectric actuators are used in Kosa et al. (2007) and Kosa et al. (2008) for creating the travelling wave needed for the movements of swimming microorganisms. Concerning the case of water surface an example of water strider miniature robot walking on water is given in Suhr et al. (2005).

The movement in air for mobile robots is classified into two groups: active air vehicle and passive air vehicle. The first group is divided into three different locomotion principles: flapping, rotary and fixed wing. Different examples for piezoelectric flapping wings are given e.g., in Sitti (2001), Campolo et al. (2003), Park et al. (2006), Nguyen et al. (2007) and Aiguo et al. (2008).

**Traveling Wave Piezoelectric Resonant Robots**

The linear traveling wave ultrasonic motor inspires the idea of these robots (Sashida and Kenjo 1993, Ueha and Tomikawa 1993). This is applied to robotic systems to progress all of the system instead of moving the slider in the case of ultrasonic motors. Various designs were reported in the literature to excite traveling waves in finite structures. Among them we can cite the one mode excitation (see e.g., Kuribayashi et al. 1985) and, the two-mode excitation presented in e.g., Loh and Ro (2000). Both methods are presented for ultrasonic linear motors. Additional methods used to generate traveling waves in finite beam structures, like the feedback control method, active control method and adaptive control method are also present in the literature. Interested readers can refer to Gabai and Bucher (2009), which presents an important review of the excitation of traveling waves in finite beam structures.

Other examples of traveling waves generated on finite beam structures using two Langevin piezoelectric transducers have been investigated. In Hernandez (2010) and Hernandez et al. (2013a) two Langevin piezoelectric transducers are used to create a traveling wave on a finite beam; the traveling wave is created by actuating the two piezoelectric transducers (vibrator–vibrator: two mode excitation) and also by actuating one transducer while the other is used as an absorber (vibrator–absorber: one mode excitation). This was used to realize a prototype of a linear pump system (Hernandez et al. 2010, Hernandez et al. 2013b). Figure 2 illustrates the basis of the mechanical component of this pump that is a linear ultrasonic traveling wave actuator. It is composed of two piezoelectric transducers connected by a metallic flexural beam on which a mechanical traveling wave is induced. Figure 3 shows the fluid-containing component of the pump that is bonded onto the beam. It is composed of three layers of plastic forming two reservoirs connected by a channel whose base is in direct contact with the flexural beam. In Kim et al. (2009) two piezoelectric Langevin transducers were used as vibrators to create a traveling wave on a finite beam. In Loh and Ro (2000) it was demonstrated experimentally the possibility to generate a traveling wave on a finite length using two piezoelectric Langevin transducers as vibrators (two mode excitation). Another type of traveling wave linear ultrasonic motors using piezoelectric patches bonded on an elastic structure as actuators instead of Langevin actuators is also presented in the literature. These types of motors use many piezoelectric patches bonded on one or both sides of the elastic structure and teeth on the structure to generate the traveling wave. As examples of this type of motors, we can cite Bein et al. (1997) and Roh et al. (2001). Dual piezoelectric actuators for the traveling wave ultrasonic motor are presented in Suybangdum et al. (2009).

**Figure 2.** *Principle of the Mechanical Component of the Pump: π-Like Structure of a Linear Actuator*

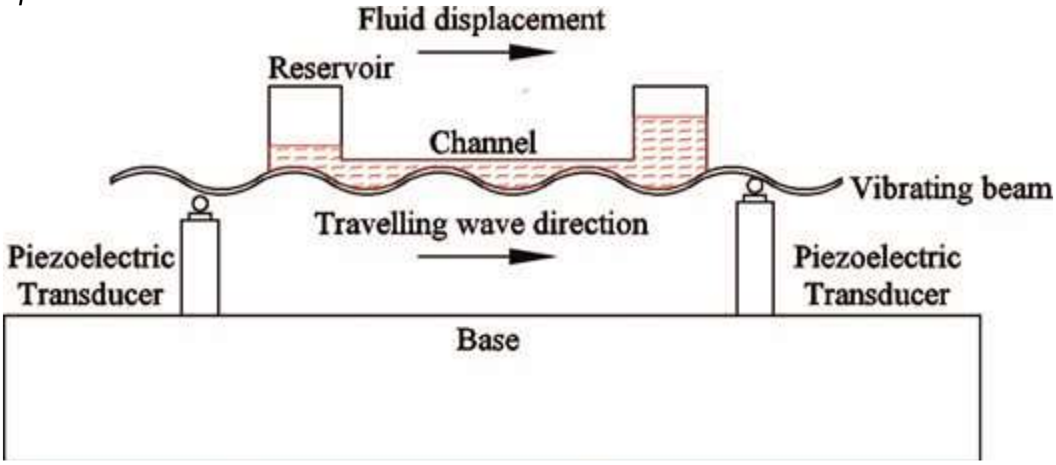


*Source:* Hernandez 2010.

**Figure 3.** *Fluid-Containing Component of the Pump: (a) Channel Composition and (b) Cross-Sectional View*

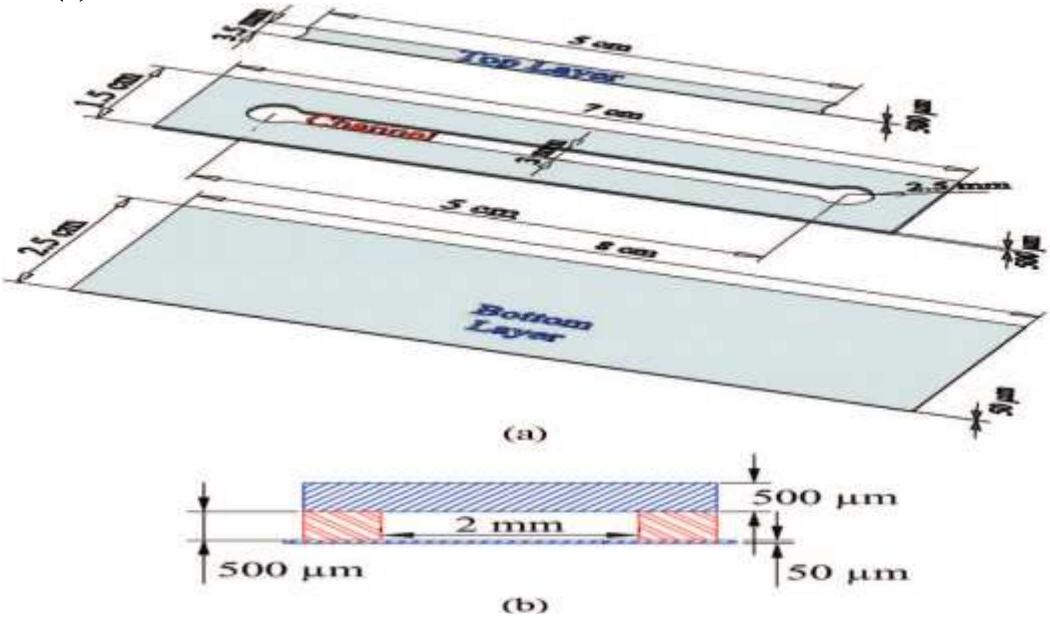


*Source:* Hernandez 2010.

## Thin Structures Involving Piezoelectric Materials

In general, thin structures containing piezoelectric materials are widely used to control vibrations, for detecting damage in the structure, to design sensors and for energy harvesting. Also to design actuators as: inchworm actuators, micro pumps, valves, miniature robots, motors,…, (Hariri et al. 2010, Hariri et al. 2018, Hernandez et al. 2010, Bernard et al. 2014a, b, Tian et al. 2011, Hariri et al. 2011). Two large branches are studied in the literature due to their domain of applications, namely beam and plate structures. On the other hand, these systems may be symmetrical or asymmetrical where the piezoelectric materials are collocated or not on the thin beam/plate. In a symmetrical system, the piezoelectric materials are bonded face-to-face on both sides of the beam/plate while in an asymmetrical one the piezoelectric materials are bonded only on one side surface of the structure. This non-collocated structure is generally the situation concerned by applications interesting our subject.

## Piezoelectric Beam Robots

In the last sections, we have seen different methods for generating traveling waves in finite beam structures. Concerning applications involving robotics, few works were reported. Nevertheless, in Hariri et al. (2010) and Hariri (2012) a general outline of locomotion principles for piezoelectric miniature robots is detailed. In Son et al. (2006) a robot using standing wave with legs to generate motion, it consists of a piezoelectric layer bonded on a metal layer. Such an organization does not permit the generation of a traveling wave on the beam to move entirely the system. Conversely, in Hariri et al. (2014) a robot consists of only two piezoelectric patches bonded on a beam layer permit, without using teeth or legs, to generate the traveling wave. In such a case, compared to the mentioned robot of Son et al. (2006) and generally the linear ultrasonic motors, the originality lies in the fact that in robotic applications we need to move the entire system and not for e.g., a slider on beam. The motion could be generated using one or two-mode excitation. Figure 4 shows the piezoelectric miniature robot of Hariri (2012) and Hariri et al. (2014) for the case of motion generated using two-mode excitation. Figure 5 shows the case of one-mode excitation.

**Figure 4.** *Schematic Diagram of the Piezoelectric Miniature Beam Robot with Two-Mode Excitation*

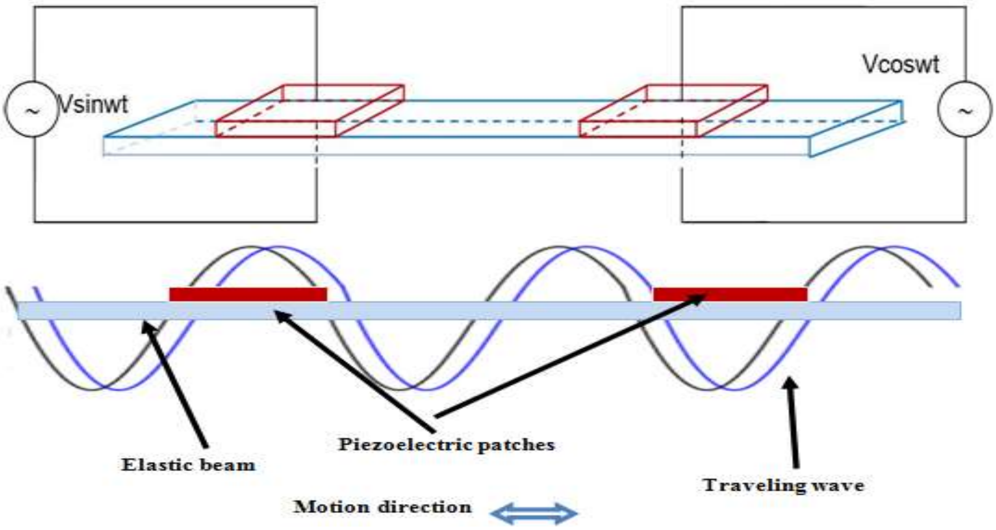


*Source:* Hariri 2012.

**Figure 5.** *Beam Robot with One-Mode Excitation*

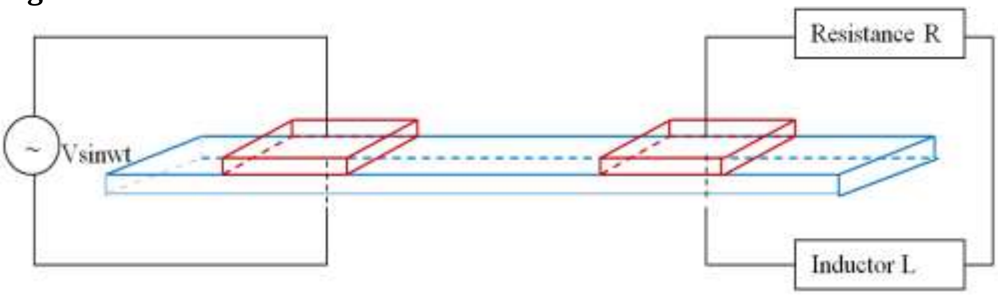


Let us examine theoretically the excitation modes of the miniature piezoelectric beam robot involving two non-collocated piezoelectric patches bonded on the beam surface. In the one-mode excitation, one patch is used as an actuator to engender vibration on the beam while the other is used as a sensor to transform the mechanical vibration into heating and so to generate a traveling wave on the beam. In the two-mode excitation, the two patches are used as actuators to generate the mechanical vibration of the beam in order to create the traveling wave. The details of performing these modes in realistic structures will be illustrated in the next lines.

Pure linear traveling waves are usually observed on long structures. In finite structures similar to beams, the excited vibration wave is partially reflected when it strikes the boundaries. Two approaches can be found in the literature to excite traveling wave in finite structures.

In the first approach one piezoelectric transducer is excited (generally) at the resonance frequency and used to generate the traveling wave on a beam and a second piezoelectric transducer is used to prevent the reflection of the wave by means of a passive electrical circuit. The passive electrical circuit used in this approach can be replaced by active control methods like feedback control or adaptive control to regulate the vibrating wave along the beam (El Moucary et al. 2002). In this case, we have a one-mode excitation at resonance. Therefore, one patch produces the mechanical displacement of the beam by applying an electrical voltage, while the other converts this mechanical displacement into electrical energy, which is then dissipated e.g., through a passive RL electrical network to avoid wave reflection. Note that the inversion of the roles of the two patches leads to inverse the motion direction. The patches positions, the source frequency and the parameters of the dissipative element permit to control the nature of the traveling wave and hence the motion.

The second approach belongs to the active control methods and consists of generating a traveling wave in finite structure. It resides in generating a traveling wave on the structure by one piezoelectric transducer and removes the reflected wave at its boundaries by applying forces using the other piezoelectric transducer. In this two-mode excitation, the two piezoelectric patches produce the mechanical displacement of the beam by applying simultaneously two neighboring natural mode shapes of the beam at the same frequency but with a phase difference of 90°. So, the principle of two-mode excitation is based on the excitation of the two patches at a frequency between two resonance frequencies. At the resonance frequency, two progressive waves with the same amplitude propagating in

opposite directions cancel each other, resulting in a standing wave on the beam that will stop moving. Below or above the resonance frequency, one progressive wave is excited more than the other is. The resulting waves propagate in the same direction as the waves with the greater amplitude propagate. Note that the motion direction can be reversed by changing phase difference from 90° to -90°.
It has been shown in Hariri et al. (2014) and Hariri (2012), that the two-mode excitation shows higher velocity compared to the one- mode case, however the one-mode is better in terms of homogeneity (see Figure 6). This is because that, in the one-mode we excite at the resonance frequency while we excite between two resonance frequencies in the two-mode excitation.

**Figure 6.** *Robot Speed versus Applied Voltage on a Smooth Glass Flat Surface for the One-Mode and Two-Mode Excitation*

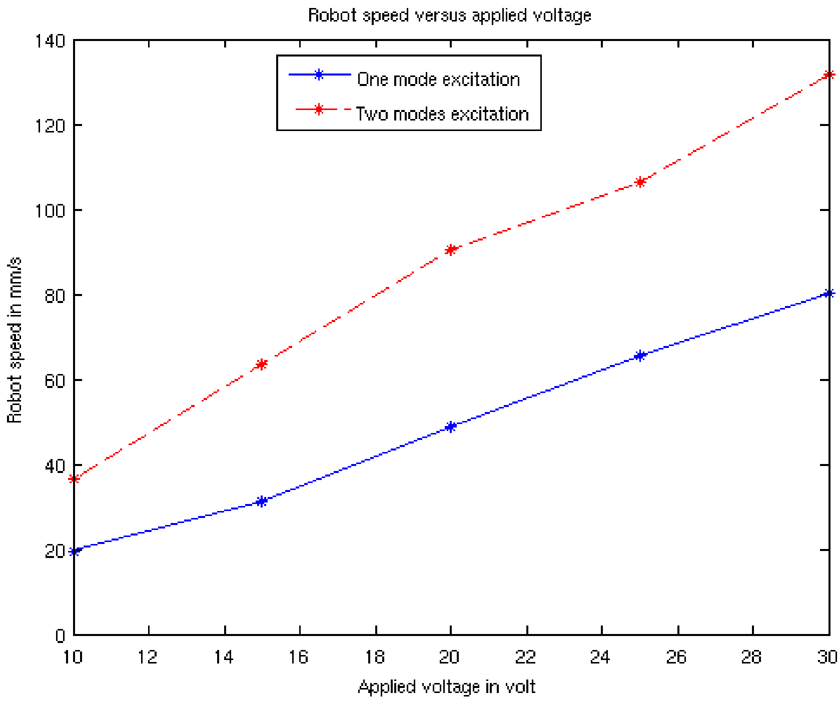


*Source:* Hariri 2012.

## Piezoelectric Patches Bonded on a Plate

As in the case of beam robots, a miniature piezoelectric plate robot is inspired by linear ultrasonic motors with the difference that there is no slider and the vibrator itself moves like a whole robot and in several directions. Such a robot is within the reach of those who move on a solid substrate (Hariri et al. 2010). We are interested in the mechanism that uses wave propagation to generate movement and control the direction of movement. Two types of waves are used for the propulsion of miniature piezoelectric robots on a solid substrate, the standing wave and the traveling wave. A miniature traveling wave piezoelectric robot is more suited to miniaturization than a standing wave robot, the one using legs. For this reason, we will only consider the case of the miniature traveling wave piezoelectric robot.

All of the traveling wave miniature piezoelectric robots mentioned in the last section use a 1D traveling wave on a beam structure for propulsion. However, in this section, a 2D traveling wave on a plate structure is used for propulsion. Such a 2D traveling wave generated on a plate structure is recently reported in Musgrave et al. (2016) for future drag reduction manipulation and to control the interaction between a fluid and the plate structure to improve the efficiency of the systems studied and not to propel the whole system. There is no evidence in this work if this 2D traveling wave can be used as a driven mechanism to propel the entire system. The objective is to generate a mechanical traveling wave in a finished flexible plate structure to propel the plate in different directions using piezoelectric patches (Hariri et al. 2018). Figure 7 shows non-collocated (stuck on the same side) piezoelectric patches bonded on a plate. The objective in Hariri et al. (2018) is to generate a traveling wave in a plate structure to move it on a solid substrate using piezoelectric patches stuck on the same face of the plate surface.

**Figure 7.** *Non-Collocated Piezoelectric Patches Bonded on a Plate*

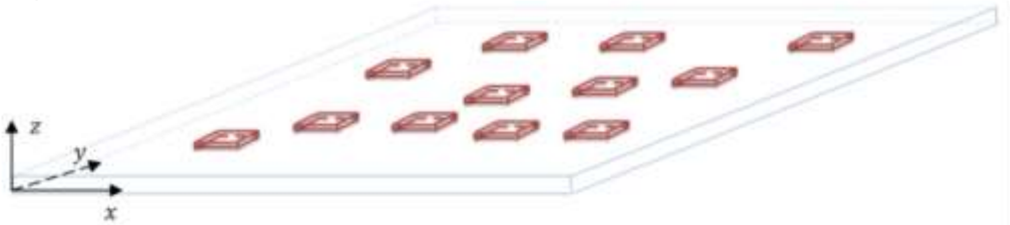


*Source:* Hariri 2012.

The design proposed in Hariri et al. (2018) consists of an elastic thin plate structure, with four non-collocated piezoelectric patches bonded to its surface. This system is called traveling wave driven piezoelectric plate robot for planar motion. The traveling wave on the plate is generated using the "two-mode excitation" method defined in the last section. The piezoelectric patches are used in this case to excite the plate at a frequency between two resonant frequencies in order to generate a traveling wave on the plate. The traveling wave is at the origin of the frictional forces exerted at the level of the contact lines between the plate and the ground that lead to the movement of the robot in different directions.

The design process in Hariri et al. (2018) consists in determining the optimal geometry and the mechanical properties of the plate robot that lead to optimize the generation of the traveling wave on it. It involves determining the optimal shape and geometry of the piezoelectric plate and patches, the material used for the plate and piezoelectric patches, and the locations of the piezoelectric patches. The type of material used for the plate is studied in Hariri et al. (2015a) where a comparison is made between steel, aluminum, brass and acrylic. It has been found that at a plate thickness of 0.5 mm, aluminum is the best elastic material, which presents the best compromise between maximum transverse displacement and maximum locking force. The effect of the positions of the patches on the performances of the traveling wave is studied in Hariri et al. (2015b) in the case of a beam structure. It has been found that locating the patches near the ends of the beam structure would lead to better performance and that the traveling wave is mainly generated over the distance between the patches. The difference in traveling wave performance for different patch positions was due to the establishment of the patches relative to nodes and anti-nodes of a given frequency.

It has been shown in Hariri et al. (2018) and Hariri (2012) that in the case of plates a traveling wave generated on a thin plate using distributed piezoelectric patches can move the plate in multi degree of freedom.

## Modeling of Piezoelectric Patches Bonded on Thin Structures

In the last two sections, we studied the cases of piezoelectric patches bonded on beams and plates. In the case of plates, we discussed the case of an elastic thin plate structure, with non-collocated piezoelectric patches bonded to its surface. The design and optimization of such structure needs 2D modeling of non-collocated patches bonded on thin structure (Hariri et al. 2015a).

For symmetrical or asymmetrical beam structures with respectively collocated or non-collocated piezoelectric materials, a 1D analytical or numerical model can be used to model such system (see Figure 6). In the case of plate structures, 2D or 3D Finite Element Method (FEM) can be used to model the system (Ouchetto et al. 2007, Ren and Razek 1990, Rapetti et al. 2002, Carpes et al. 2000, Razek 2019). In the 3D approach, volume elements are used while in the 2D case surface elements are used while the third dimension is introduced in the model equations. It is obvious that the second approach is faster but a little more complicated in model formulation. An example illustrating such 2D modeling is given in Hariri (2012) and Hariri et al. (2015a). The studied device consists of a thin structure with several piezoelectric patches bonded on one side of its surface i.e., non-collocated piezoelectric patches (asymmetrical system). Examples of such asymmetric systems finite element meshes are shown in Figure 8 where four colored rectangles stand for piezoelectric patches are bonded on one side of rectangular and circular thin structures with and without holes. It is worthy to note that all modeling tools are supposed to be validated by observation experience (Razek 2020).

**Figure 8.** *Finite Element Meshes of Non-Collocated Piezoelectric Patches Bonded on Structures*

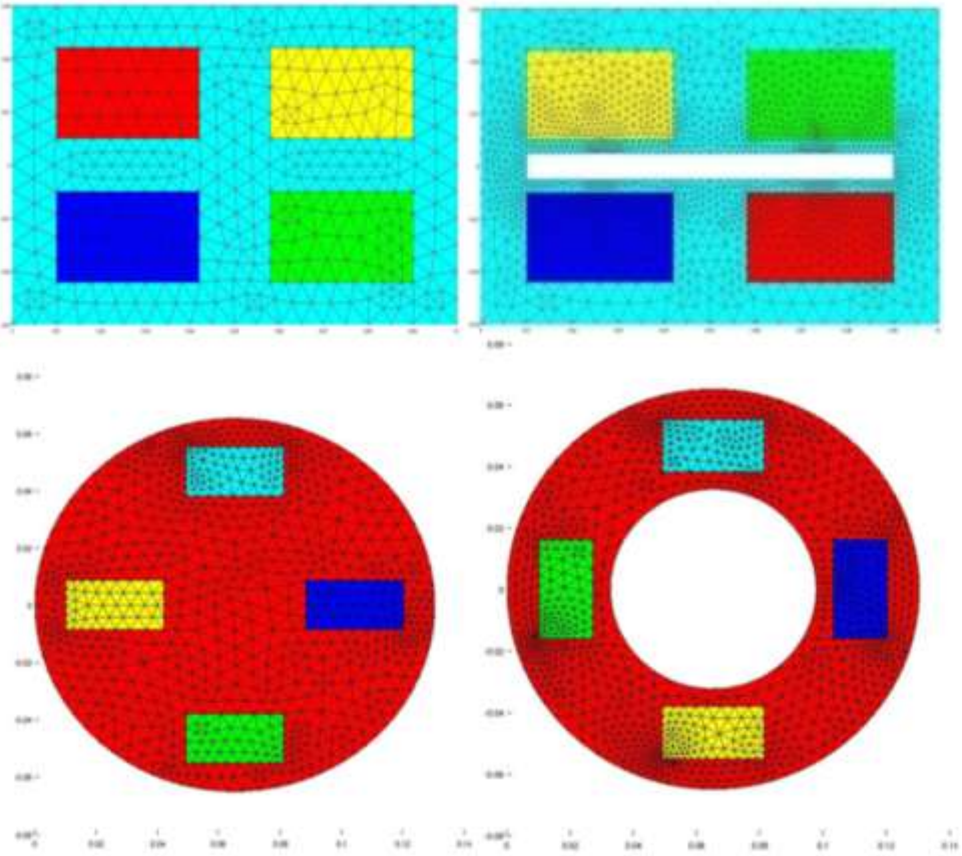

*Source:* Hariri 2012.

## Conclusions

This paper has reviewed the different types of locomotion perhaps used in robotics. The functioning of traveling wave piezoelectric resonant robots was discussed. The operation and applications of piezoelectric beam and plate robots have been assessed through numerous published works opting for those with innovative characteristics.

These use traveling waves practiced by non-collocated patches bounded on flexible thin beams or plates. These patches are activated by one or two-mode excitations. In the case of beams, the two-mode excitation shows higher velocity compared to the one-mode case, however the one-mode is better in homogeneity. This is because in the one-mode excitation we excite at the resonance frequency while we excite between two resonance frequencies in the two-mode excitation.

In addition, in the case of plates a traveling wave generated on a thin plate using distributed piezoelectric patches can move the plate in multi degrees of freedom.

The modeling aspects involved in these robots and more generally, the modeling of piezoelectric patches bonded on thin structures have exposed realistic tools.

**References**

Aiguo M, Yawen H, Fukushima Y, Shimojo M (2008) Development of an active flapping wing using piezoelectric fiber composites. In *IEEE International Conference on Robotics and Biomimetics ROBIO*, 2144–2149.

Aoshima SI, Tsujimura T, Yabuta T (1993) Miniature mobile robot using piezo vibration for mobility in a thin tube. *Journal of Dynamic Systems, Measurement and Control, Transactions of the ASME* 115(2 A): 270–278.

Avirovik D, Butenhoff B, Priya S (2014) Millipede-inspired locomotion through novel U-shaped piezoelectric motors. *Smart Materials and Structures* 23(3): 1–5.

Baisch AT (2013) *Design, manufacturing and locomotion studies of ambulatory micro-robots*. PhD Thesis. Cambridge, Massachusetts: Harvard University.

Bein T, Breitbach EJ, Uchino K (1997) A linear ultrasonic motor using the first longitudinal and the fourth bending mode. *Smart Materials and Structures* 6(1997): 619–627.

Bernard Y, Hernandez C, Razek A (2014a) Radial traveling wave ultrasonic motor design. *Actuator* 2014(Jun): 663–666.

Bernard Y, Hariri H, Razek A (2014b) *Mobile piezoelectric device* . Patent, WO Patent n°: EP2014/072867 and WO2015059283 A1.

Borgen MG, Washington GN, Kinzel GL (2003) Design and evolution of a piezoelectrically actuated miniature swimming vehicle. *IEEE/ASME Transactions on Mechatronics* 8(1): 66–76.

Campolo D, Sahai R, Fearing R (2003) Development of piezoelectric bending actuators with embedded piezoelectric sensors for micromechanical flapping mechanisms. In *IEEE International Conference on Robotics and Automation* 3: 3339–3346.

Carpes WP, Pichon L, Razek A (2000) A 3D finite element method for the modelling of bounded and unbounded electromagnetic problems in the time domain. *International Journal of Numerical Modelling: Electronic Networks, Devices and Fields* 13(6): 527–540.

Casper J, Murphy RR (2003) Human-robot interactions during the robot-assisted urban search and rescue response at the World Trade Center. *IEEE Transactions on Systems, Man, and Cybernetics. Part B, Cybernetics* 33(3): 367–85.

Cimprich T, Kaegi F, Drieseu W, Ferreira A, Breguet J (2006) Ultrasonic monolithic piezoelectric multi DOF actuators for mobile micro robots. In *ACTUATOR '06*. Bremen, DE.

Deng X, Avadhanula S (2005) Biomimetic micro underwater vehicle with oscillating fin propulsion: system design and force measurement. In *Proceedings of the 2005 IEEE International Conference on Robotics and Automation ICRA*, 3312–3317.

Dolghi O, Strabala KW, Wortman TD, Goede MR, Farritor SM, Oleynikov D (2011) Miniature in vivo robot for laparoendoscopic single-site surgery. *Surgical Endoscopy* 25(10): 3453–3458.

Driesen W (2008) *Concept, modeling and experimental characterization of the modulated friction inertial drive (MFID), locomotion principle: application to mobile microrobots*. PhD Thesis. Lausanne, Switzerland: Swiss Federal Institute of Technology Lausanne.

Edqvist E, Snis N, Sjölund M, Murase T, Söderberg A, Johansson S (2008) The assembly of millimeter sized mass producible autonomous robots. In *Proceedings of the International Conference on New Actuators, ACTUATOR '08*, 304–307.

El Moucary C, Mendes E, Razek A (2002) Decoupled direct control for PWM inverter-fed induction motor drives. *IEEE Transactions on Industry Applications* 38(5): 1307–1315.

Epson (2010) *News release: Epson to unveil a prototype microrobot with ultra-thin ultrasonic motor and power-saving Bluetooth module*. Epson.

Ferreira A, Minotti P (1997) Control of a multidegree of freedom standing wave ultrasonic motor driven precise positioning system. *Review of Scientific Instruments* 68(4): 1779–1786.

Fuchiwaki O, Aoyama H (2002) Piezo based micro robot for microscope instrument. In *Proceedings of the International Conference on Mechatronics Technology, ICMT '02*, 499–503.

Fukuda T, Kawamoto A, Arai F, Matsuura H (1994) Mechanism and swimming experiment of micro mobile robot in water. In *Proceedings of 1994 IEEE International Conference on Robotics and Automation* 1, 814–819.

Gabai R, Bucher I (2009) Excitation and sensing of multiple vibrating traveling waves in one-dimensional structures. *Journal of Sound and Vibration* 319(1–2): 406–425.

Hariri H (2012) *Design and realization of a piezoelectric mobile for cooperative use*. PhD Thesis. Paris, France: Université Paris Sud-XI (GeePs).

Hariri H, Bernard Y, Razek A (2010) Locomotion principles for piezo- electric miniature robots. In *Proceedings of ACITUATOR 10*, 1015–1020. Bremen, DE.

Hariri H, Bernard Y, Razek A (2011) Analytical and finite element model for unimorph piezoelectric actuator: actuator design. In *Piezo2011*, 71–75. Sestriere, Italy.

Hariri H, Bernard Y, Razek A (2014) A traveling wave piezoelectric beam robot. *Smart Materials and Structures* 23(2): 025013.

Hariri H, Bernard Y, Razek A (2015a) A two dimensions modeling of non-collocated piezoelectric patches bonded on thin structure. *Curved and Layered Structures* 2(1): 15–27.

Hariri H, Bernard Y, Razek A (2015b) Dual piezoelectric beam robot: the effect of piezoelectric patches' positions. *Journal of Intelligent Material Systems and Structures* 26(18): 2577–2590.

Hariri H, Bernard Y, Razek A (2018) 2-D Traveling wave driven piezoelectric plate robot for planar motion. *IEEE/ASME Transactions on Mechatronics* 23(1): 242–251.

Hernandez C (2010) Realization of piezoelectric micro pumps. PhD Thesis. Paris, France: University Paris sud-XI (GeePs).

Hernandez C, Bernard Y, Razek A (2010) A global assessment of piezoelectric actuated micro-pumps – A review. *The European Physical Journal Applied Physics* 51(2): 20101.

Hernandez C, Bernard Y, Razek A (2013a) Design and manufacturing of a piezoelectric traveling-wave pumping device. *IEEE Transactions on Ultrasonic, Ferroelectrics, and Frequency Control* 60(9): 1949–1956.

Hernandez C, Bernard Y, Razek A (2013b) *Ultrasonic traveling wave micro pump for liquid*. US Patent App. Patent n°: US-2013-02423627.

Hu T, Wang G, Shen L, Li F (2006) A novel conceptual fish-like robot inspired by Rhinecanthus Aculeatus. In *Ninth International Conference on Control, Automation, Robotics and Vision ICARCV '2006*, 1–5.

Ikuta K, Kawahara A, Yamazumi S (1991) Miniature cybernetic actuators using piezoelectric device. In *Proceedings IEEE Micro Electro Mechanical Systems, MEMS '91*, 131–136.

Ishihara H, Fokuda T, Kosuge K, Arai F, Hamagishi K (1995) Approach to distributed micro robotic system development of micro line trace robot and autonomous micro robotic system. In *IEEE International Conference on Robotics and Automation, ICRA.95 1*, 375–380.

Kim GH, Park JW, Jeong SH (2009) Analysis of dynamic characteristics for vibration of flexural beam in ultrasonic transport system. *Journal of Mechanical Science and Technology* 23(May): 1428–1434.

Kodati P, Hinkle J, Deng X (2007) Micro Autonomous Robotic Ostraciiform (MARCO): design and fabrication. In *IEEE International Conference on Robotics and Automation*, 960–965.

Kosa G, Shoham M, Zaaroor M (2007) Propulsion method for swimming micro robots. *IEEE Transactions on Robotics* 23(1): 137–150.

Kosa G, Jakab P, Hata N, Jolesz F, Neubach Z, Shoham M, et al. (2008) Flagellar swimming for medical micro robots: theory, experiments and application. In *2nd IEEE RAS & EMBS International Conference on Biomedical Robotics and Biomechatronics BioRob*.

Koyanagi T, Fukui R, Torii A, Ueda A (2000) Miniature robots with three degrees of freedom. In *Proceedings of the IEEE International Symposium on Micromechatronics and Human Science MHS'00*, 207–212.

Kuribayashi M, Ueha S, Mori E (1985) Excitation conditions of a flexural traveling waves for a reversible ultrasonic linear motor. *The Journal of the Acoustical Society of America* 77(4): 1431–1435.

Loh BG, Ro PI (2000) An object transport system using flexural ultrasonic progressive waves generated by two modes excitation. *IEEE Transactions on Ultrasonic, Ferroelectric, and Frequency Control* 47(4): 994–999.

Matsuoka T, Asano M, Fukushima H, Okamoto H, Uchida M, Matsui T (1993) Mechanical analysis of micro mobile machine with piezoelectric element. In *Proceedings of the IEEE/RSJ International Conference on Intelligent Robots and Systems IROS '93*, 1685–1690.

Musgrave PF, Malladi VNS, Tarazaga PA (2016) Generation of traveling waves in a 2D plate for future drag reduction manipulation. In *Book on Special Topics in Structural Dynamics, 6, Part of the Series Conference Proceedings of the Society for Experimental Mechanics Serie*s, 129–138.

Nguyen QV, Park HC, Goo NS, Byun D (2007) A flying insect-like flapper actuated by a compressed LIPCA. In *IEEE International Conference on Robotics and Biomimetics ROBIO*, 19–24.

Ouchetto O, Zouhdi S, Bossavit A, Griso G, Miara B, Razek A (2007) Homogenization of structured electromagnetic materials and metamaterials. *Journal of Materials Processing Technology* 181(1–3): 225–229.

Paradiso J, Starner T (2005) Energy scavenging for mobile and wireless electronics. *IEEE Pervasive Computing* 4(1): 1 –27.

Park HC, Syaifuddin M, Goo NS, Byun D, Yoon KJ (2006) An insect-mimicking flapping system actuated by a piezo ceramic actuator. In *IEEE International Conference on Robotics and Biomimetics*, 451–456.

Rapetti F, Maday Y, Bouillault F, Razek A (2002) Eddy-current calculations in three-dimensional moving structures. *IEEE Transactions on Magnetics* 38(2): 613–616.

Razek A (2018) Towards an image-guided restricted drug release in friendly implanted therapeutics – Review. *The European Physical Journal of Applied Physics* 82(3): 31401.

Razek A (2019) Assessment of supervised drug release in cordial embedded therapeutics. *Athens Journal of Technology and Engineering* 6(2): 77–91.

Razek A (2020) The observable, the theory, and prospective revised models for societal concerns. *Athens Journal of Sciences* 7(1): 1–14.

Rembold U, Fatikow S (1997) Autonomous microrobots. *Journal of Intelligent and Robotic Systems* 19(4): 375–391.

Ren Z, Razek A (1990) A coupled electromagnetic-mechanical model for thin conductive plate deflection analysis. *IEEE Transactions on Magnetics* 26(5): 1650–1652.

Roh Y, Lee S, Han W (2001) Design and fabrication of a new traveling wave-type ultrasonic linear motor. *Sensors and Actuators A: Physical* 94(3): 205–210.

Sashida T, Kenjo T (1993) An Introduction to Ultrasonic Motors. (Oxford: Clarendon).

Sfakiotakis M, Lane DM, Davies JBC (1999) Review of fish swimming modes for aquatic locomotion. *IEEE Journal of Oceanic Engineering* 24(2): 237–252.

Simu U, Johansson S (2002) Fabrication of monolithic piezoelectric drive units for a miniature robot. *Journal of Micromechanics and Microengineering* 12(5): 582–589.

Simu U, Johansson S (2006) Analysis of static and dynamic motion mechanisms for piezoelectric miniature robots. *Journal of Sensors and Actuators* 132(2): 632–642.

Sitti M (2001) PZT actuated four-bar mechanism with two flexible links for micromechanical flying insect thorax. In *Proceedings ICRA. IEEE International Conference on Robotics and Automation* 4, 3893–3900.

Snis N, Simu U, Johansson S (2004) Piezoelectric drive platform for cm3 sized autonomous robot. In *Proceedings of the International Conference on New Actuators, ACTUATOR '04*, 106–109.

Son K, Kartik JV, Wickert JA, Sitti M (2006) An ultrasonic standing-wave-actuated nano-positioning walking robot: piezoelectric-metal composite beam modelling. *Journal of Vibration and Control* 12(12): 1293–1309.

Suhr SH, Song YS, Lee SJ, Sitti M (2005) Biologically inspired miniature water strider robot. In *Proceedings of the Robotics: Science and Systems I*, 319–325. Boston, U.S.A.

Sunyoto S, Bernard Y, Razek A (2006) Design and realization of a linear piezoelectric actuator for orthopedic applications. *Journal of Advanced Science* 18(1/2): 162–165.

Suybangdum P, Smithmaitrie P, Laoratanakul P (2009) Dual piezoelectric actuators for the traveling wave ultrasonic linear motor. In *Fourth International Conference on Experimental Mechanics*.

Tian Y, Hernandez C, Bernard Y, Razek A (2011) Self moving stick slip piezoelectric actuator design and modeling. In *Piezo11*. February 2011, Sestriere, Italy.

Torii A, Kato H, Ueda A (2001) A miniature actuator with electromagnetic elements. *Denki Gakkai Ronbunshi/Electrical Engineering in Japan* 134(4): 70–75.

Tzeranis D, Papadopoulos E (2003) On the design of an autonomous robot fish. In *Proceedings of 11th Mediterranean Conference on Control and Automation MED*, 17–20.

Uchino K (2006) Expansion from IT/Robotics to ecological/energy applications. In *ACTUATOR06*, 48. Bremen, DE.

Ueha S, Tomikawa Y (1993) *Ultrasonic motors, theory and applications*. Oxford Science.

Wiguna T, Heo S, Park HC, Goo NS (2006) Mechanical design of biomimetic fish robot using lipca as artificial muscle. In *Key Engineering Materials*, volume: *Experimental Mechanics in Nano and Biotechnology*, 1443–1446.

Wood RJ (2008) The first takeoff of a biologically inspired at-scale robotic insect. *Transactions on Robotics* 24(2): 341–347.

Yan S, Zhang F, Qin Z, Wen S (2005) A 3-DOFs mobile robot driven by a piezoelectric actuator. *Smart Materials and Structures*: Technical Note 15 (No. 1).

Zesch W, Bychi R, Codourey A, Siegwart R (1995) Inertial drive for micro and nan robots: two novel mechanics. In Lynne B. Parker (ed.), *Proceedings in Microrobotics and Micromechanical Systems* 2593, 80–88.

Zhang L, Huang Q, Li Y, Gao J, Li H, Wu L (2012) Research and development of throw able miniature reconnaissance robot. In *2012 IEEE International Conference on Mechatronics and Automation*, 1254–1259.

Zhou M, Tuo Y, Cheng L, Liu WT, Fu X (2013) A biomimetic earthworm-like micro robot using nut-type piezoelectric motor. In *Sixth International Conference on Intelligent Robotics and Applications ICIRA 2013*.

Zhu C (2007) In-pipe robot for inspection and sampling tasks. *Industrial Robot: An International Journal* 34(1): 39–45.

*Athens Journal of Technology and Engineering - Volume 8, Issue 3, September 2021 – Pages 217-236*

# A Waste Energy Recovery Management for Electricity Generation from Two Temperature Grades of Energy Sources in Subcritical Organic Rankine Systems

*By Ali H. Tarrad*[*]

*Waste energy represents one of the most critical issues for the economic utilization and management of energy in modern industrial fields. This article outlines a scheme to utilize two different source temperature levels within the envelope of higher than 200 °C zones. Two regenerative organic Rankine cycles (RORC) were implemented to construct a compound regenerative organic Rankine cycle (CRORC) to improve the energy management of the sources. These two mini-cycles were integrated throughout an intermediate economizer circuit to extract a certain amount of energy from the high-temperature level mini-cycle. R-123 was circulated in the high-temperature cycle due to its high critical temperature at evaporation and condensation temperatures of 160 °C and 50 °C, respectively. R-123, R-21, and hydrocarbon R-600 were used as working fluids for the low-temperature cycle at evaporation and condensation temperatures of 130 °C and 35 °C, respectively. The R-123 fluid in the high-temperature mini-cycle was superheated to 170-240 °C, whereas the fluid in the low-temperature level was superheated to 180 °C. The results showed that the independent system (IRORC) requires more energy recovery than the compound system by a maximum of 2% to achieve the same net power output. This corresponds to the enhancement of 2% for the system net thermal efficiency of the compound (CRORC) system compared to the independent (IRORC) one. The compound (CRORC) system revealed a net thermal efficiency in the range of 14% and 15.6% for the test conditions. The mini-cycle net thermal efficiency of the low-temperature in the compound system was enhanced by a range of 2.5-5% compared to that of the independent arrangement. R-123/R-123 and R-123/R-21 systems exhibited higher net thermal efficiencies than the R-123/R-600 one by 3% and 2%, respectively. Increasing the superheat degree of the high-temperature mini-cycle from 10 °C to 80 °C for the compound system has improved the thermal efficiency by 7.6-7.9% for the examined fluid pairs and operating conditions.*

**Keywords:** *compound cycle, regenerative, energy management, energy recovery, organic fluids*

## Introduction

Astina (2010) compared the direct expansion steam turbine, binary cycle (Organic Rankine Cycle, ORC), and heat pumped geothermal power plant performance. The ORC with working fluids R-134a and R-600a performs better than the direct expansion cycle when operated at lower geothermal source

[*]Professor, University of Lorraine, CNRS, LEMTA, F-54000 Nancy, France.

temperature. He concluded that the direct expansion cycle performs better when the steam temperature is higher than 150 °C. Therefore, including a gas turbine system in a geothermal power plant can improve the system's efficiency. Shengjun et al. (2011) investigated the utilization of an organic Rankine cycle (ORC) working at 80-100 °C. Their results proved that R-600a demanded the lowest cost to produce electricity, and the R-152 unit is more compactable. Vankeirsbilck et al. (2011) found that the (ORC) can be operated on low-temperature heat sources grades with low to moderate evaporation pressure and still achieve a better performance than that of a steam cycle under the same conditions.

Xi et al. (2013) compared the performance of different (ORC) technologies. They found that the double-stage regenerative cycle produced the best thermal and exergy efficiency under the optimal operating conditions. It was followed by the single-stage regenerative system (RORC), and the simple organic Rankine cycle (SORC) has the worst efficiencies. Molés et al. (2014) investigated the performance of R-1233zd-E, R-1336mzz-Z, and R-245fa fluids in an (ORC). They concluded that R-1233zd-E requires 10.3% to 17.3% lower pump power and provides up to 10.6% higher cycle efficiency than R-245fa over the tested range of cycle conditions. They also postulated that the turbine size for R-1233zd-E would be about 7.5% to 10.2% larger than for R-245fa. Jung et al. (2015) studied the performance of a zeotropic fluid mixture of R-245fa and R365mfc (48.5%/51.5% on a mole basis) in a lab-scale ORC. They found that the electricity generated at a steady state was about 70% of the nominal capacity of the scroll expander. The ORC system efficiency resulting from the experiment was approximately 3.9%.

Javanshir et al. (2017) investigated a regenerative organic Rankine cycle (RORC) performance using dry working fluids. R-600, R-600a, and R113 offer the highest specific net of work output. They concluded that the circulated fluid's specific heat and critical temperature affect the thermal performance of the cycle. The higher cycle net of work output and thermal efficiency correspond to the working fluids that possess higher specific heat and higher critical temperature, respectively. Mishra and Khan (2017) performed the exergy and energy analysis of the organic Rankine cycle with the solar heating source, and bleeding regeneration was implemented in the (RORC). The system's performance was compared with different organic fluids such as R134a, R407C, R404A, and R410A at different organic Rankine cycle maximum temperatures and pressures. R410A showed a maximum efficiency by regeneration around 64%. R410A showed the maximum organic Rankine cycle efficiency of 16.51%. They concluded that thermal efficiency for the plant increases with the inlet temperature increase of the expander.

Yazdi (2017) evaluated analytically three different ORC cycles; they were basic ORC, regenerative ORC, and ORC with an internal heat exchanger (IHE). The IHE heats the working fluid from the pump outlet to the open feed organic heater inlet condition and cools the saturated vapor of working fluid from the outlet condition of the turbine to the condenser inlet condition. In addition, flashing pressure and extraction pressure optimization of these cycles was performed. According to this study, the best cycle, which gives maximum thermal and exergy efficiency to a flash-binary power plant, is a regenerative ORC with

IHE, which is on average 1.22% higher than basic ORC. Yuan and Zhang (2019) investigated the thermal performance of eight candidate working fluids R-123, R-245fa, R-114, R-236ea, R-236fa, RC318, R-227ea, and R-1234yf with a low heat source grade of 100-150 °C. They concluded that the heat source temperature and its allowable minimum temperature at the outlet port influence the optimal turbine inlet condition state. Further, the optimal condition state is also affected by the critical temperature of the working fluid.

Pandey et al. (2018) studied the zeotropic mixture of R-600a/DME at different composition values. They found that R600a/DME (0.8/0.2) gives the maximum net of work output corresponding to (70) °C inlet temperature to the evaporator. Among all selected proportions, R600a/DME (0.6/0.4) has both maximum thermal efficiency and maximum exergy efficiency corresponding to 100 °C inlet temperature to the evaporator. Da Cunha and Souza (2020) simulated a regenerative organic Rankine cycle (RORC) with fluid bleeding at the turbine; R-134a was chosen as a working fluid. The evaporation temperature was ranged between 60 °C and 100 °C with superheated temperatures of 120 °C, 200 °C, and 300 °C. They concluded that the maximum thermal efficiency and turbine output increase with the evaporation temperature. The turbine output power showed an augmentation with increasing superheat temperatures, and the thermal efficiency exhibited a declination with superheat temperature increase. Tarrad (2020a) investigated the thermal performance of a simple organic Rankine cycle (SORC) when circulated various organic fluids at low-temperature levels. He found that the thermal efficiencies of R-134a, R-123, R-245fa, R-1233zd-E, and R-1234ze-E were higher than that of R-290 by 10-14%, 11-12%, 9-12%, 4-7%, and 1-3%, respectively. R-290 exhibited thermal efficiencies close to R-1233zd-E and R-1234ze-E in the superheat degree range of 5-15 °C.

Tarrad (2020b) investigated the performance of a regenerative (RORC) cycle arrangement when it is circulating R-123, R-1233zd-E, R-245fa, and R600a as candidate working fluids at boiling and condensation temperatures of 130 °C and 45 °C, respectively. The (RORC) showed higher thermal efficiency than that of the simple one (SORC) by the range of 8-15% for the test fluids and operating conditions. The attained maximum and minimum cycle thermal efficiencies were 12% and 10.7% for R-600a and R-1233zd-E, respectively, at 15 °C superheat degree. Tarrad (2021) investigated the performance of a compound system where two temperature levels existed for the heat sources. The lower part of the compound cycle represents the low-temperature cycle. One of the R-123, R-245fa, R-1233zd-E, or R-600a fluids was circulated in the low-temperature level of 130 °C and 35 °C evaporation and condensation temperatures, respectively. R-123 was circulated at the high-temperature level of the system at 150 °C and 50 °C evaporation and condensation temperatures, respectively. His study showed that the independent system needed energy consumption of about 2% higher than that of the compound system when operating under the same conditions to produce the same net power output.

This work compared the thermal performance of a compound regenerative organic Rankine cycle (CRORC) system to that of the independent regenerative organic Rankine cycle (IRORC) system under the same operating conditions.

Three organic fluids, R-123, R-21, and R-600, were studied as candidate working fluids. Three fluid pairs were utilized to evaluate the thermal performance of the postulated system as R-123/R-123, R-123/R-21, and R-123/R-600. A hypothetical organic Rankine cycle of nominal heat recovery of 100 kW was implemented to evaluate the cycle performance. The low-temperature waste heat source was suggested to be available at a level higher than 200 °C. The superheat degrees of 10-80 °C and 50 °C were utilized for the high-temperature and low-temperature levels of the fluids in the mini-cycles, respectively.

*Compound Cycle*

This cycle was initially postulated by Tarrad (2021), as presented in Figure 1. The suggested scheme outlined two regenerative (RORC) cycles integrated and combined by an intermediate economizer for energy management purposes. The upper part of the system is a regenerative cycle representing the high-temperature grade; R-123 was circulated at 160 °C and 50 °C evaporation and condensation temperatures, respectively. The lower part of the compound cycle represents the low-temperature grade where one of the R-123, R-21, or R-600 fluids was circulated at 130 °C and 35 °C evaporation and condensation temperatures, respectively.

An 8% of R-123 mass flow rate of the high-temperature cycle fluid was extracted at point (A), Figure 1, and passed through the economizer. This amount of fluid bypass was inferred from keeping a constant terminal temperature difference between condensate and the low-temperature fluid at the exit side of the condensation zone of the economizer, as shown schematically in Figure 2.

In the present work, a value of 2 °C was considered as a maximum terminal temperature difference $(\Delta T_{ter})$ to ensure a complete condensation of the bypassed fluid amount in the economizer and avoid any economic impact. More detailed process descriptions are to be found in Tarrad (2021).

**Figure 1.** *A Schematic Diagram of the Postulated Compound Cycle, Tarrad (2021)*

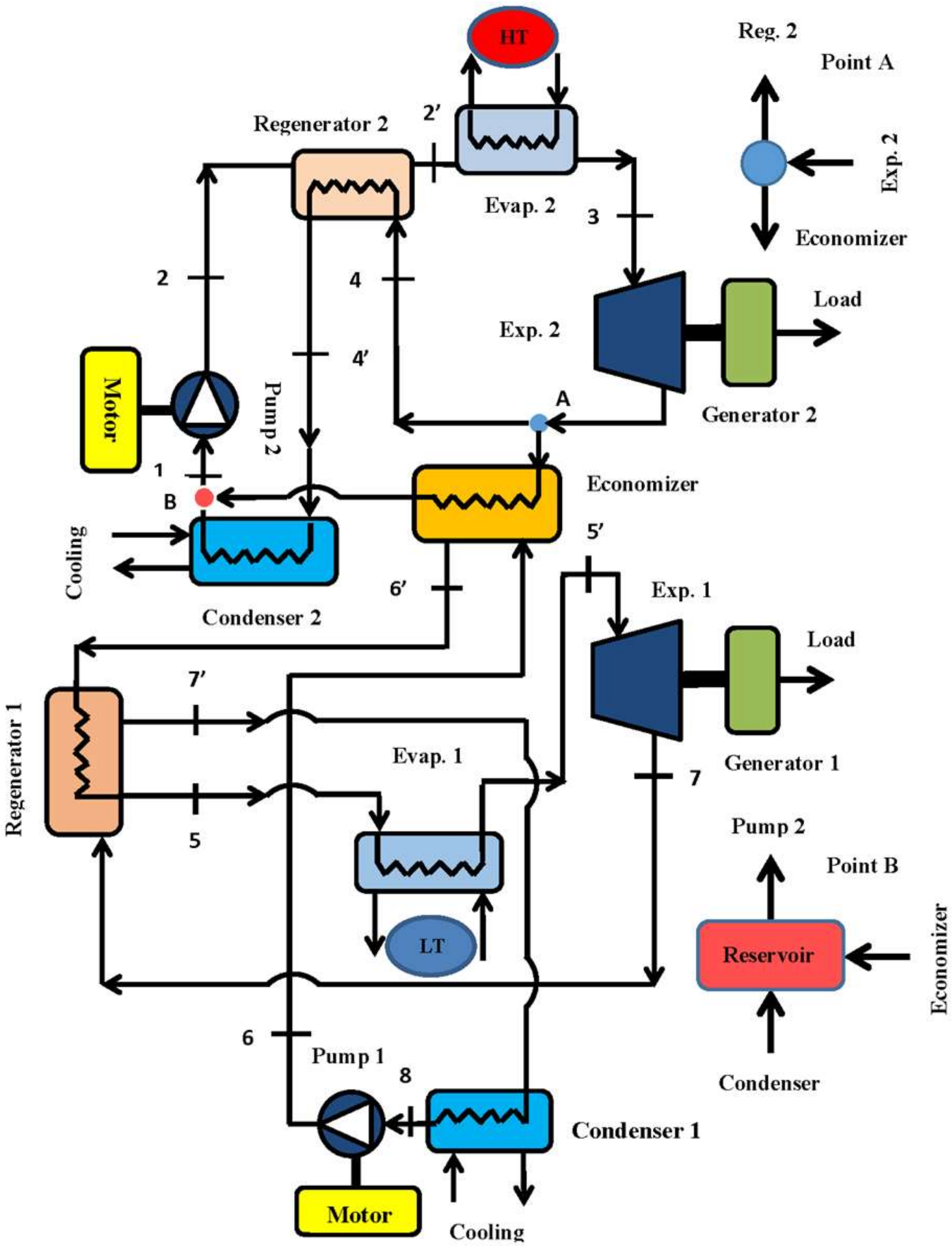

**Figure 2.** *Fluid Temperature Variation in the Economizer*

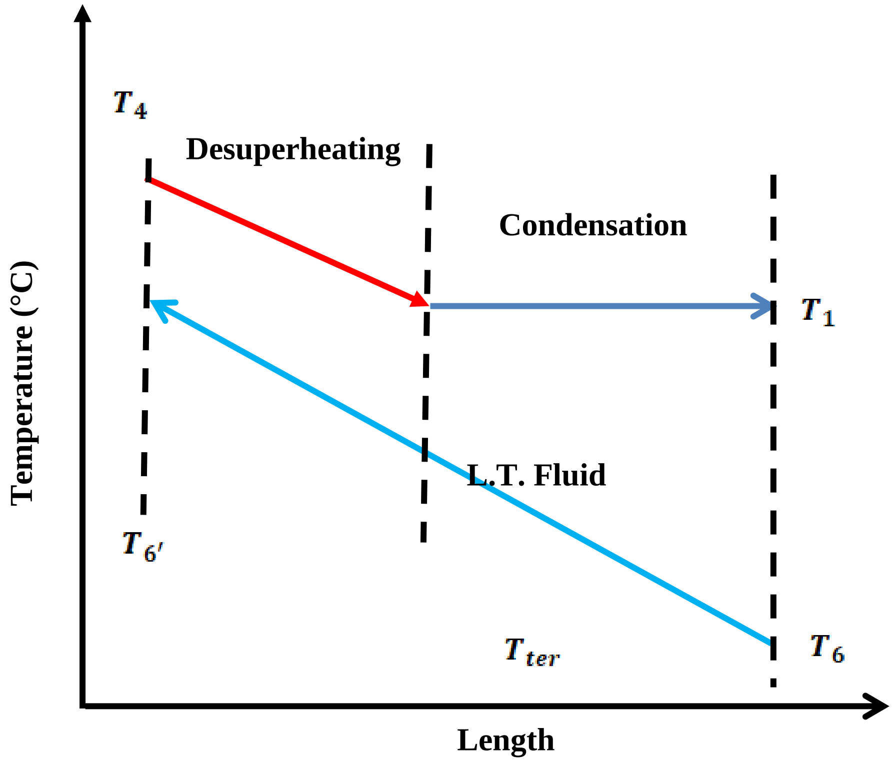


## Methodology

*Organic Fluids*

Table 1 shows some of the physical, safety, and environmental characteristics of the selected working fluids. Three organics were selected as working fluids to circulate in the suggested compound regenerative organic Rankine cycles (CRORC). The global warming potential (GWP), Ozone depletion potential (ODP), and critical point characteristics play an essential role in the choice process of the working fluids.

**Table 1.** Characteristics of Test Candidate Fluids

| Refrigerant | Chemical Formula | $T_c$ (°C) | $p_c$ (bar) | $M_w$ (gr/mol) | $T_{n,b}$ (°C) | Depletion | | Safety Group* |
|---|---|---|---|---|---|---|---|---|
| | | | | | | ODP | GWP | |
| R-123 | $CHCl_2CF_3$ | 183.68 | 36.618 | 152.93 | 27.82 | 0.02 | 77 | B1 |
| R-21 | $CHCl_2F$ | 178.5 | 51.68 | 102.9 | 9.35 | 0.04 | 151 | B1 |
| R-600 | $CH_3CH_2CH_2CH_3$ | 150.8 | 37.18 | 58.1 | -0.5 | 0 | 20 | A3 |

*ANSI/ASHRAE Standard 34 (2016).

Tables 2 a and b depict some thermodynamics properties of the test fluids for both of the high-temperature and low-temperature cycles fluids.

**Table 2a.** *Thermodynamics Properties of the Candidate Working Fluid R-123 for the Higher Temperature Level Cycle*

| Refrigerant | Pressure (bar) | | Liquid Density (kg/m$^3$) | | Liquid Enthalpy (kJ/kg) | | Vapor Enthalpy (kJ/kg) | |
|---|---|---|---|---|---|---|---|---|
| | 50 °C | 160 °C | 50 °C | 160 °C | 50 °C | 160 °C | 50 °C | 160 °C |
| R-123 | 2.134 | 20.992 | 1397.8 | 974.28 | 248.92 | 378.5 | 409.97 | 459.97 |

**Table 2b.** *Thermodynamics Properties of Working Fluids for the Low-Temperature Level Cycle*

| Refrigerant | Pressure (bar) | | Liquid Density (kg/m$^3$) | | Liquid Enthalpy (kJ/kg) | | Vapor Enthalpy (kJ/kg) | |
|---|---|---|---|---|---|---|---|---|
| | 35 °C | 130 °C | 35 °C | 130 °C | 35 °C | 130 °C | 35 °C | 130 °C |
| R-123 | 1.31 | 14.638 | 1437.61 | 1132.9 | 233.29 | 340 | 400.81 | 452.44 |
| R-21 | 2.534 | 23.713 | 1341.20 | 1080.5 | 236.68 | 350.52 | 464.19 | 495.15 |
| R-600 | 3.257 | 26.284 | 562.270 | 417.14 | 283.17 | 554.35 | 631.96 | 746.4 |

The R-123 and R-600 fluids were selected according to their excellent thermal performance in organic Rankine cycles (ORC), Javanshir et al. (2017), Yuan and Zhang (2019), and Tarrad (2020a, b, 2021). In addition, R-21 was investigated due to its high critical point characteristics, temperature, and pressure.

## Thermal Analysis

The thermal analysis of the present compound cycle is summarized in Table 3.

**Table 3.** *Thermal Analysis of the Compound Regenerative Organic Rankine Cycle (CRORC)*

| *Component* | *Analysis* |
|---|---|
| 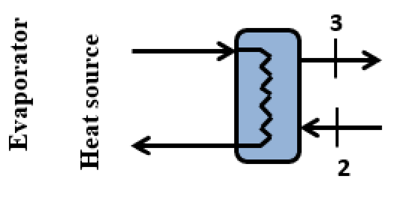  | $\dot{Q}_{evap,H.T} = \dot{m}_{H.T}\,(h_3 - h_{2'})$ (1.a)<br>$\dot{Q}_{evap,L.T} = \dot{m}_{L.T}\,(h_{5'} - h_5)$ (1.b) |
| 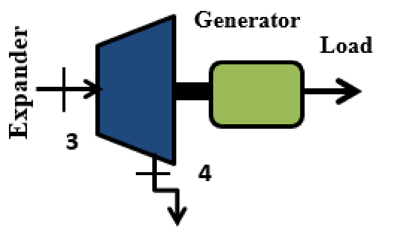  | $\eta_{is,ex,H.T} = \frac{h_3 - h_4}{h_3 - h_{4,is}}$ (2.a)<br>$\eta_{is,ex,L.T} = \frac{h_{5'} - h_7}{h_{5'} - h_{7,is}}$ (2.b)<br>$\dot{W}_{ex,H.T} = \eta_{m,ex}\,\eta_{v,ex}\,\dot{m}_{H.T}\,(h_3 - h_4)$ (3.a)<br>$\dot{W}_{ex,L.T} = \eta_{m,ex}\,\eta_{v,ex}\,\dot{m}_{L.T}\,(h_{5'} - h_7)$ (3.b) |

**Table 3.** *(Continued)*

| *Component* | *Analysis* |
|---|---|
| **Regenerator** 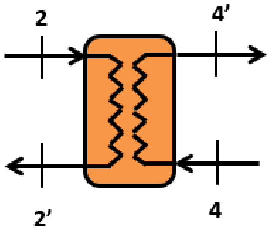  | $\varepsilon = \frac{T_4 - T_{4'}}{T_4 - T_2}$ (4.a)<br>$\varepsilon = \frac{T_7 - T_{7'}}{T_7 - T_{6'}}$ (4.b)<br>$h_{2'} = h_2 + h_4 - h_{4'}$ (5.a)<br>$h_5 = h_{6'} + h_7 - h_{7'}$ (5.b) |
| **Condenser** **Cooling Medium** 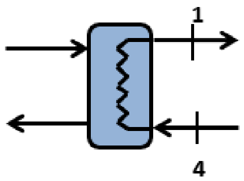  | $\dot{Q}_{cond,H.T} = 0.92\, \dot{m}_{H.T}\, (h_{4'} - h_1)$ (6.a)<br>$\dot{Q}_{cond,L.T} = \dot{m}_{L.T}\, (h_{7'} - h_8)$ (6.b) |
| **Economizer** 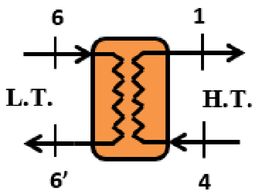  | $\dot{Q}_{Econ} = 0.08\, \dot{m}_{H.T}\, (h_4 - h_1)$ (7)<br>$h_{6'} = h_6 + \frac{\dot{Q}_{Econ}}{\dot{m}_{L.T}}$ (8) |
| **Pump** 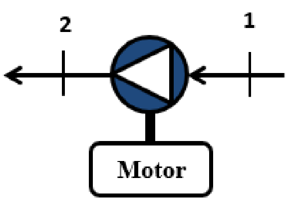  | $\eta_{is,p,H.T} = \frac{h_{2,is} - h_1}{h_2 - h_1}$ (9.a)<br>$\eta_{is,p,L.T} = \frac{h_{6,is} - h_8}{h_6 - h_8}$ (9.b)<br>$\dot{W}_{p,H.T} = \dot{m}_{H.T}(h_1 - h_2)/\eta_{m,p}$ (10.a)<br>$\dot{W}_{p,L.T} = \dot{m}_{L.T}\, (h_6 - h_8)/\eta_{m,p}$ (10.b) |

The first law of thermodynamics efficiency is defined as:

$$\eta_{net} = \frac{\dot{W}_{ex} - \dot{W}_p}{\dot{Q}_{evap}} \quad (11)$$

Hence, the compound cycle net thermal efficiency is estimated from:

$$\eta_{net.com} = \frac{(\dot{W}_{ex,H.T} + \dot{W}_{ex,L.T}) - (\dot{W}_{p,H.T+p,L.T})}{\dot{Q}_{evap,H.T} + \dot{Q}_{evap,L.T}} \quad (12)$$

The corresponding net thermal efficiency for the two independent cycles is calculated by:

$$\eta_{net,ind} = \frac{(\dot{W}_{ex,H.T} + \dot{W}_{ex,f}) - (\dot{W}_{p,H.T} + \dot{W}_{p,f})}{\dot{Q}_{evap,H.T} + \dot{Q}_{evap,f}} \quad (13)$$

The subscription ( $f$ ) refers to the working fluid circulating in the lower temperature mini-cycle; this includes any of the R-123, R-21, and R-600. The parameter $\eta_{net,ind}$ is the net thermal efficiency mean value when these cycles operate independently at the two temperature levels.

The mass flow rate of the circulated fluid was calculated for the hypothetical cycles of the total 100 kW nominal evaporation load, for a mini-cycle of the (CRORC) and independent systems, it corresponds to:

$$\dot{m} = \frac{50}{(h_{g,evap} - h_x)} \tag{14}$$

In this expression, the heating load of each mini-cycle of the (CRORC) and independent systems possesses half of the total system nominal heat load. The ($h_{g,evap}$) refers to the vapor enthalpy at the operating evaporator saturation temperature, Table 2. The enthalpy ($h_x$) corresponds to that at the pump discharge side; it is equal to ($h_2$) and ($h_6$) for the high and low-temperature mini-cycles, respectively, for the compound system. Thus, the same mass flow rates were circulated in both (CRORC) and (IRORC) systems.

$$\dot{Q}_{evap,t} = \dot{Q}_{evap} + \dot{Q}_{sup} \tag{15}$$

Table 4 illustrates the numerical values of the efficiencies of the expander and pump and the effectiveness of the regenerators.

**Table 4.** *The Numerical Values of Performance Parameters Utilized at the Present Work*

| **Parameter** | **Value** |
|---|---|
| Expander isentropic efficiency, $\eta_{is,ex}$ | 85% |
| Expander volumetric efficiency, $\eta_{v,ex}$ | 85% |
| Expander mechanical efficiency, $\eta_{m,ex}$ | 90% |
| Pump isentropic efficiency, $\eta_{is,p}$ | 85% |
| Pump mechanical efficiency, $\eta_{m,p}$ | 80% |
| Regenerator effectiveness, $\varepsilon$ | 80% |

The evaluation of the performance comparison between different test fluids under similar operating conditions was based on the discrepancy percentage defined as:

$$\beta_{\phi} = \frac{\phi_n - \phi_{ref}}{\phi_n} \times 100 \tag{16}$$

Here, the subscriptions (*n*) and ( *ref* ) refer to the compared fluid and reference fluid, respectively. The parameter ($\phi$) refers to the required characteristic variable for comparison, such as $\dot{W}_{pump}$, $\dot{W}_{exp}$, $\dot{Q}_{eavp}$, and $\eta_{net}$. This expression is valid for comparing the performance of the same fluid at different operating conditions such as volumetric efficiency or evaporation temperature change. The comparison of the compound regenerative organic Rankine cycle (CRORC) system and the independent regenerative organic Rankine cycle (IRORC) system performance parameters were deduced from:

$$\zeta_{\phi} = \frac{\phi_{com} - \phi_{ind}}{\phi_{com}} \times 100 \quad (17)$$

The parameter ($\phi$) has the same definitions as those in Eq. (16). Equation (17) is valid for all of the compared parameters, $\dot{W}_{pump}$, $\dot{W}_{exp}$, and $\eta_{net}$ except for the consumed energy one ($\dot{Q}_{eavp}$) which was inverted as:

$$\zeta_{\dot{Q}_{evap}} = \frac{\dot{Q}_{evap,ind} - \dot{Q}_{evap,com}}{\dot{Q}_{evap,ind}} \times 100 \quad (18)$$

## Results and Discussion

### *Energy Consumption*

Figure 3 illustrates a comparison of the extracted heating load from the waste for the compound and independent systems.

**Figure 3.** *Comparison of Energy Recovery Between the (CRORC) and (IRORC)*

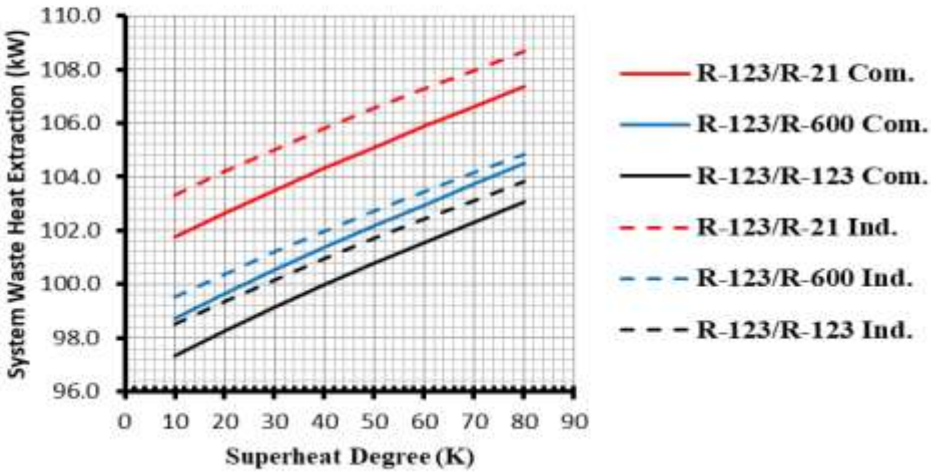


The results show that the compound system requires less energy than the independent arrangement to produce equal net output power. The pair R-123/R-21 absorbed the highest heating load for both systems, followed by the R-123/R-600 pair, and the R-123/R-123 system absorbed the minimum heat load. The increase of the energy extraction for the independent system was higher than that of the compound system, with 2% for all of the test pairs. Figure 4 depicts the heat load distribution percentage for each compound system pair at 80 °C superheat degree.

**Figure 4.** *The Compound System Energy Distribution at (80) °C Superheat Degree*

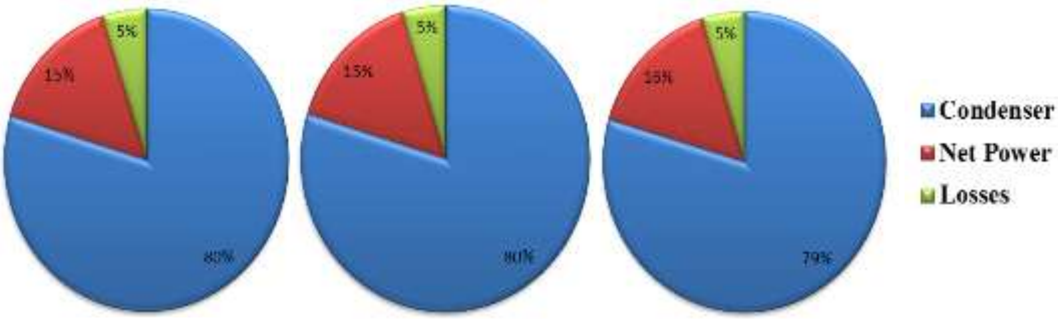


**Figure 4a.** *R-123/R-600* **Figure 4b.** *R-123/R-21* **Figure 4c.** *R-123/R-123*

These results show that the heat transfer domain is shared similarly for all of the test fluid pairs. The condensation load occupies about 80% of the total consumed energy in the boiler. The green sector corresponds to 5%; it refers to the losses that accompany the thermal and mechanical efficiencies of the actuators and the regenerators installed in the cycles. Figure 5 depicts the energy distribution of the independent system at 80 °C. The net power output of all test fluid pairs is equal; the R-123/R-123 exhibited the higher condensation and lower losses components as 82% and 3%, respectively.

**Figure 5.** *The Independent System Energy Distribution at 80 °C Superheat Degree*

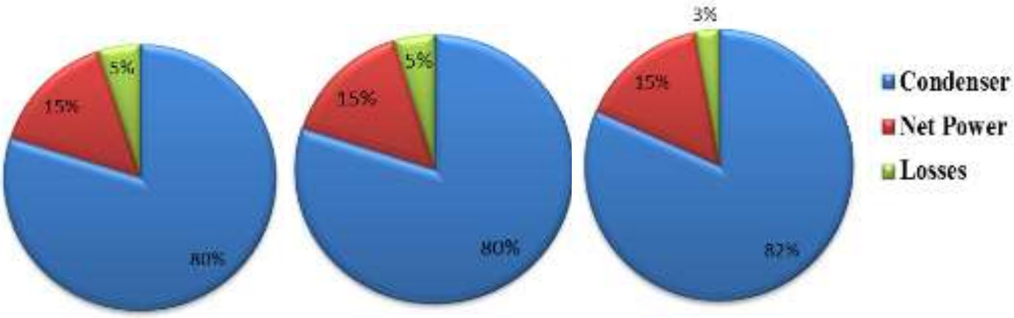


**Figure 5a.** *R-123/R-600* **Figure 5b.** *R-123/R-21* **Figure 5c.** *R-123/R-123*

The energy distribution of the compound system at 10 °C superheat degree in the high-temperature mini-cycle for all of the examined fluids was 5%, 14%, and 81% for the losses, net power output, and condensation load parts.

All of the tested pairs for the compound system showed similar values for energy distribution. The condensation load for the condenser of both mini-cycles occupies 81% of the total energy consumption in the boiler. Therefore, the rejected heat load in the condensers could be used with a suitable system arrangement to provide hot water for heating or daily human needs. The energy distribution in the high-temperature mini-cycle of the compound system is shown in Figure 6 at different superheat degrees.

**Figure 6.** *The High-Temperature Mini-Cycle Energy Distribution*

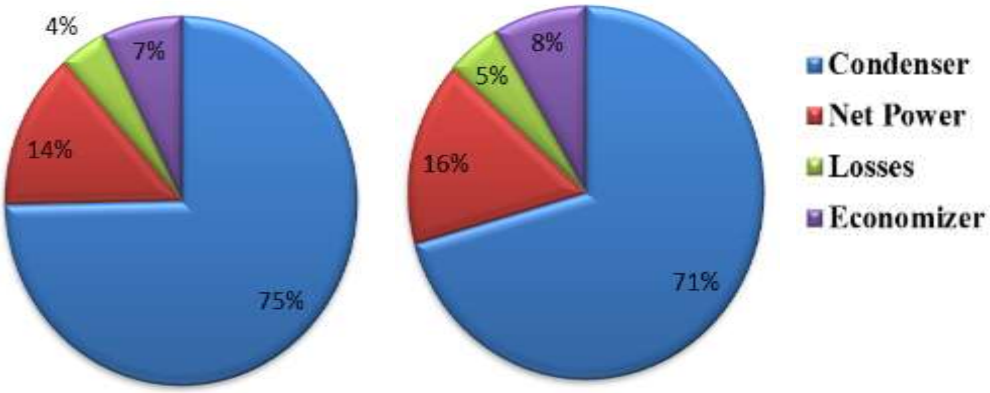


**Figure 6a.** $\Delta T_{sup}$=10°C **Figure 6b.** $\Delta T_{sup}$=80 °C

The economizer occupies the range of 7-8% of the total extracted waste energy in the boiler. This amount of energy is added to the low-temperature mini-cycle to minimize the total energy consumed by the system.

*Net Power Output*

Figure 7 illustrates the net power output of the examined compound systems for the tested fluid pairs and operating conditions.

**Figure 7.** *Comparison of System Net Power Output of (CRORC) for the Test Fluid Pairs*

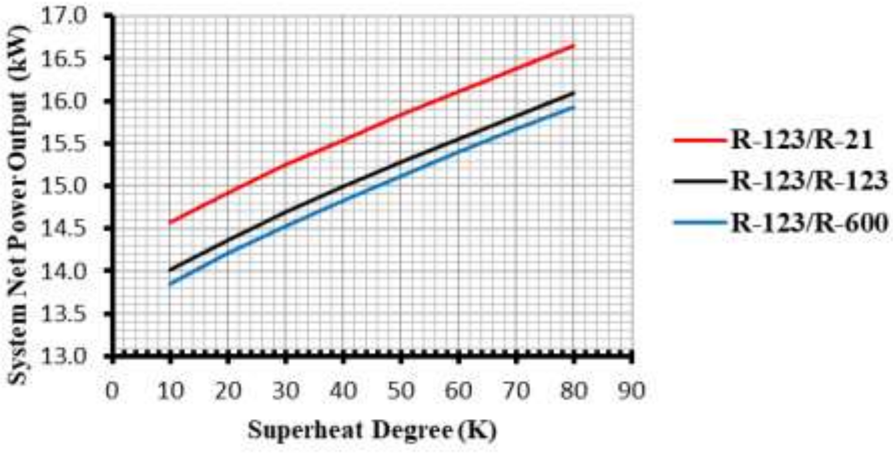


The system net power output showed an enhancement as the superheat degree increases. For example, as the superheat degree was increased from 10 °C to 80 °C, the system net power output for the R-123/R-123 and R-123/R-600 was augmented by 13%. The corresponding enhancement for the R-123/R-21 system was 12.5% for the same operating conditions. As a result, the maximum system net power output was produced by the R-123/R-21 system and approached a value of 16.6 kW at 80 °C superheat degree. At the same superheat degree, the R-123/R-123 and R-123/R-600 systems had 16.1 kW and 15.9 kW, respectively.

*Net System Efficiency*

A comparison of the system net thermal efficiency between both test systems, compound and independent, for the examined fluid pairs is shown in Figure 8.

**Figure 8.** *Comparison of System Net Power Efficiency of the (CRORC) and (IRORC) for Test Fluid Pairs*

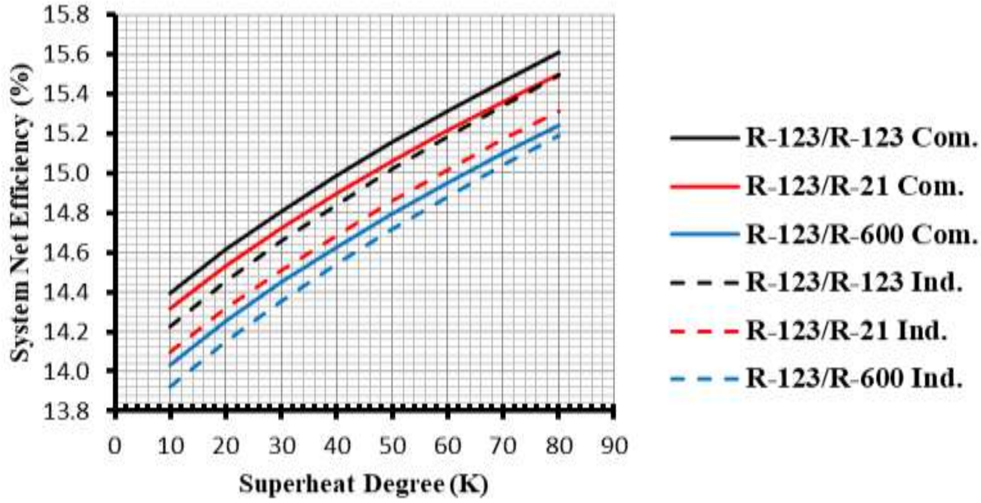


The compound system showed higher net thermal efficiency than the independent one with up to 2%. The R-123/R-123 and R-123/R-600 fluid pairs exhibited higher and lower thermal efficiency values, respectively, in both systems. The R-123/R-123 and R-123/R-21 compound systems revealed higher thermal efficiency than R-123/R-600 one by 3% and 2% respectively for the superheat degree range of 10-80 °C in the high-temperature mini-cycle. R-123/R-123 and R-123/R-600 systems produced a thermal efficiency in the range of 14.4-15.6 and 14-15.2%, respectively, for the superheat degree range of 10-80 °C, Figure 9. R-123/R-21 compound system achieved close results to those of the R-123/R-123 within the scope of 14.3-15.5%.

**Figure 9.** *A Comparison of the Compound System Net Thermal Efficiency at Different Superheat Degrees*

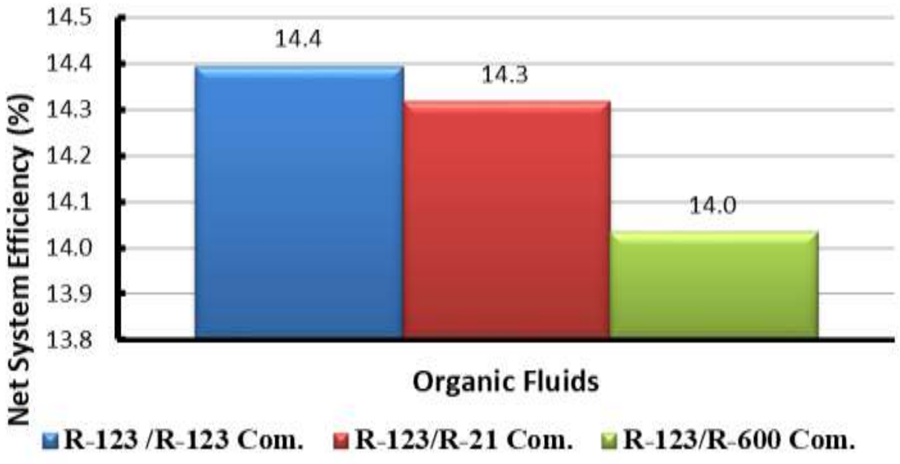


**Figure 9a.** $\Delta T_{sup} = 10\ °C$

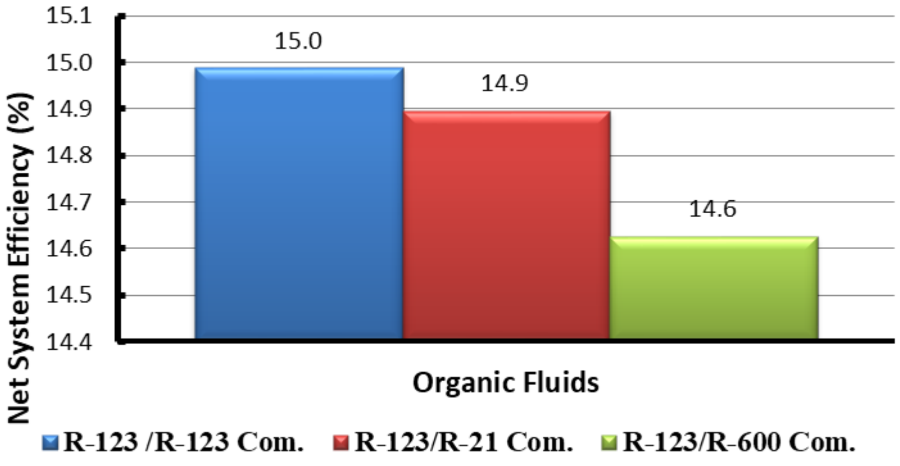


**Figure 9b.** $\Delta T_{sup} = 40\ °C$

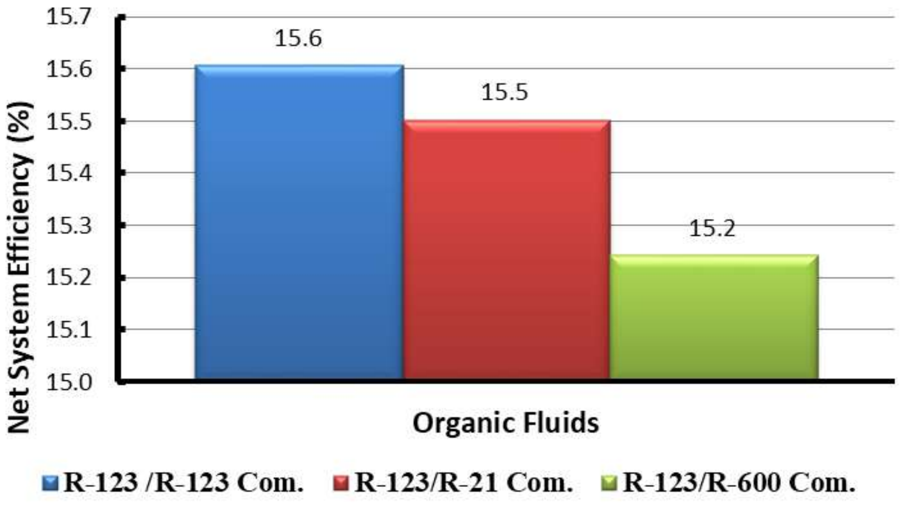


**Figure 9c.** $\Delta T_{sup} = 80\ °C$

The numeric values revealed that the thermal efficiency experienced an increase when the superheat degree was raised from 10 °C to 80 °C for the high-temperature mini-cycle fluid. R-123/R-600, R-123/R-123, and R-123/R-21 thermal efficiency at 80 °C superheat degree for the compound system were higher than those at 10 °C superheat degree ones by 7.9%, 7.8%, and 7.6%, respectively. The corresponding enhancement values were 8.4%, 8.2%, and 8% for R-123/R-600, R-123/R-123, and R-123/R-21, respectively, in the independent arrangement when the superheat degree was increased from 10 °C to 80 °C.

*Low-Temperature Mini-Cycle Efficiency*

Figure 10 illustrates a comparison of the thermal efficiency of the low-temperature mini-cycle of the compound cycle for the examined fluids.

**Figure 10.** *Comparison of the Net Thermal Efficiency of Low-Temperature Mini-Cycle in the Compound System for Test Fluids*

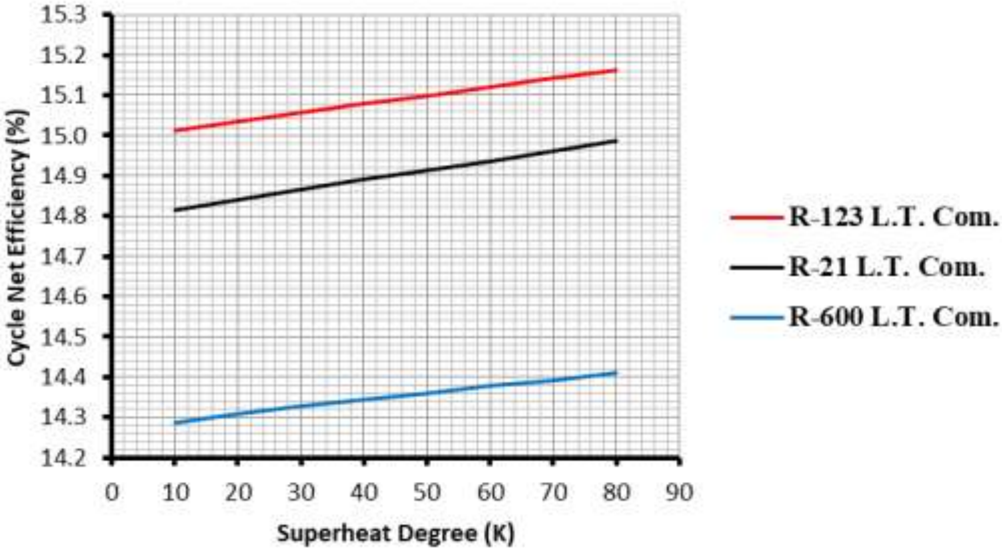


The R-123 fluid exhibited the highest thermal efficiency; it corresponds to the range of 15-15.2%. It is followed by the R-21 system, where it occupies 14.8-15%, whereas the R-600 fluid produced the lower thermal efficiency in the range of 14.3-14.4%, Figure 11.

**Figure 11.** *Comparison of Cycle Net Efficiency of the Low-Temperature Mini-Cycle at Different Superheat Degrees*

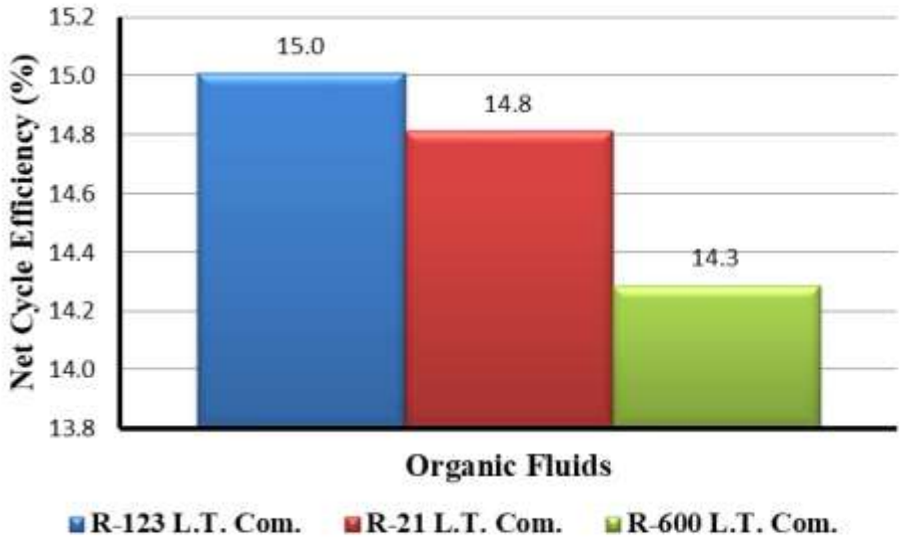


**Figure 11a.** $\Delta T_{sup} = 10\ °C$

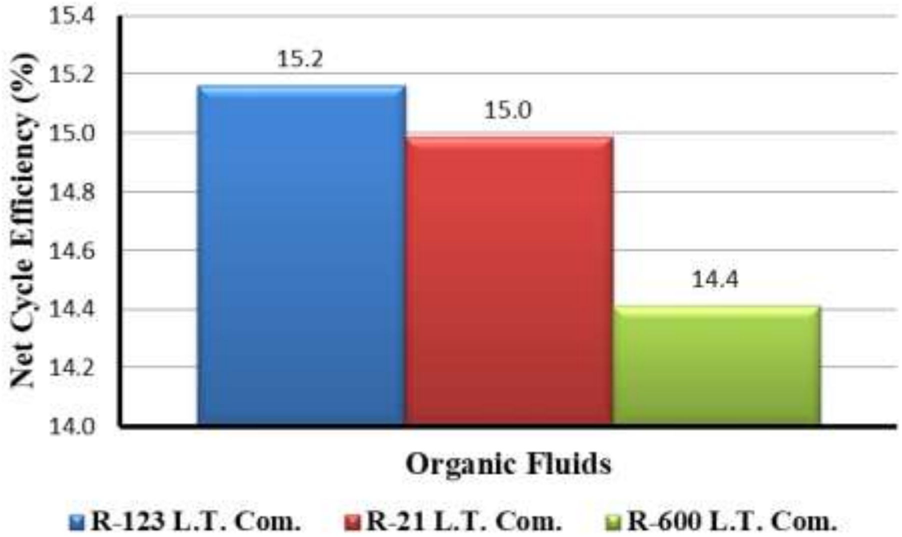


**Figure 11b.** $\Delta T_{sup} = 80\ °C$

The results showed that R-123 and R-21 provided higher net thermal efficiency than the R-600 for the examined operating conditions in the range of 4.7-5.3% and 3.4-4.2%, respectively. The compound low-temperature mini-cycle thermal efficiency was higher than that of the low-temperature independent system for all tested fluids. R-123, R-21, and R-600 fluids thermal efficiency in the compound system were higher than those of the independent cycle by the range of 3-4%, 3.6-4.7, and 2.3-3%, respectively.

## Conclusions

The present work revealed the importance of utilizing the compound system at low and moderate waste energy source temperatures. Therefore, the following facts were withdrawn as:

- The required energy extraction for the independent system to achieve similar net power output as that of the compound system was higher by a maximum of 2%.
- The net thermal efficiency of the compound system was higher than that of the independent system by a maximum of 2% when operates under similar operating conditions.
- The compound system provided a thermal efficiency of 14-15.6% for the examined fluid pairs. The R-123/R-123 provided the maximum thermal efficiency, followed by R-123/R-21 and the R-123/R-600 pair possessed the minimum.
- The low-temperature mini-cycle of the compound system showed thermal efficiency enhancement of 3-4%, 3.6-4.7, and 2.3-3% for the R-123, R-21, and R-600 fluids, respectively, when compared to those of the independent cycle.
- Increasing the superheat degree of the high-temperature mini-cycle from 10 °C to 80 °C for the compound system has improved the thermal efficiency by 7.9%, 7.8%, and 7.6% for the R-123/R-600, R-123/R-123, and R-123/R-21, respectively.

## Acknowledgments

The author would like to express his sincere thanks to the Laboratoire Énergies & Mécanique Théorique et Appliquée (LEMTA) of the University of Lorraine for their valuable support. Thanks are also extended to the administration of the (PAUSE) program of Collège de France for allowing the author to pursue his research activities.

## Nomenclature

| **Parameter** | **Definition** |
|---|---|
| $h$ | Fluid specific enthalpy, (kJ/kg) |
| $M_w$ | Fluid molecular weight, kg/kmol |
| $\dot{m}$ | Fluid mass flow rate, (kg/s) |
| $P$ | Fluid working pressure, (bar) |
| $\dot{Q}$ | Heat transfer rate, (kW) |
| $s$ | Fluid specific entropy, (kJ/kg) |
| $T$ | Fluid temperature, (°C) |
| $\dot{W}$ | Power, (kW) |

**Subscription**

| **Parameter** | **Definition** |
|---|---|
| *c* | Critical point |
| *com* | Compound |
| *cond* | Condenser |
| *evap* | Evaporator |
| *ex* | Expander |
| *g* | Gas condition |
| *H.T* | High-temperature side |
| *i* | Inlet side |
| *ind* | Independent |
| *is* | Isentropic |
| *L.T* | Low-temperature side |
| *n* | Fluid, normal point |
| *net* | Net value |
| *p* | Feed pump |
| *ref* | Reference fluid |
| *sup* | Superheated vapor |
| *t* | Total |
| *ter* | Terminal |
| *v* | Volumetric |

**Greek Letter**

| | |
|---|---|
| $\beta$ | Deviation percentage, (%) |
| $\varepsilon$ | Heat exchanger effectiveness, (%) |
| $\zeta$ | Deviation, (%) |
| $\eta$ | Cycle thermal efficiency, (%) |
| $\phi$ | Characteristic parameter |

**Abbreviations**

| **Parameter** | **Definition** |
|---|---|
| *CRORC* | Compound Regenerative Organic Rankine Cycle |
| *GWP* | Global Warming Potential |
| *IRORC* | Independent Regenerative Organic Rankine Cycle |
| *ODP* | Ozone Depletion Potential |
| *ORC* | Organic Rankine Cycle |

## References


ANSI/ASHRAE (2016) *Standard 34, designation and safety classification of refrigerants*.

Astina I (2010) Alternative systems for enhancing geothermal power plan. In *The 2nd AUN/SEED-Net Regional Conference on New and Renewable Energy*, 1–12. Faculty of Engineering, Burapha University, Thailand. January 21-22, 2010.

Da Cunha AFV, Souza SLS (2020) Analysis of R134a organic regenerative cycle. *Journal of Power and Energy Engineering* 8(5): 32–45.

Javanshir A, Sarunac N, Razzaghpanah Z (2017) Thermodynamic analysis of a regenerative organic Rankine cycle using dry fluids. *Applied Thermal Engineering* 123(May): 852–864.

Jung HC, Taylor L, Krumdieck S (2015) An experimental and modelling study of a 1 kW organic Rankine cycle unit with mixture working fluid. *Energy* 81(Mar): 601–614.

Mishra RS, Khan Y (2017) Exergy and energy analysis of modified organic Rankine cycle for reduction of global warming and ozone depletion. *International Journal of Research in Engineering and Innovation* 1(3): 1–12.

Molés F, Navarro-Esbrí J, Peris B, Mota-Babiloni A, Barragán-Cervera Á, Kontomaris KK (2014) Low GWP alternatives to HFC-245fa in organic Rankine cycles for low-temperature heat recovery: HCFO-1233zd-E and HFO-1336mzz-Z. *Applied Thermal Engineering* 71(1): 204–212.

Pandey S, Dwivedi A, Ahmad S, Arora A (2018) Parametric analysis of geothermal organic Rankine cycle working on zeotropic mixture of R600a/DME. *International Journal of Advanced Production and Industrial Engineering* 3(3): 33–46.

Shengjun Z, Huaixin W, Tao G (2011) Performance comparison and parametric optimization of subcritical organic Rankine cycle (ORC) and transcritical power cycle system for low-temperature geothermal power generation. *Applied Energy* 88(8): 2740–2754.

Tarrad AH (2020a) A steady-state evaluation of simple organic Rankine cycle (SORC) with low-temperature grade waste heat source. *Journal of Power and Energy Engineering* 8(7): 15–31.

Tarrad AH (2020b) A comparative study for the organic Rankine cycle coupled with low-temperature grade waste energy source. *International Journal of Latest Engineering Research and Applications (IJLERA)* 5(7): 11–26.

Tarrad AH (2021) A perspective evolution methodology of energy management in a subcritical regenerative organic Rankine cycles operate at two temperature levels. *Athens Journal of Technology and Engineering* 8(1): 9–26.

Xi H, Ming-Jia L, Chao X, Ya-Ling H (2013) Parametric optimization of regenerative organic Rankine cycle (ORC). *Energy* 58(Sep): 473–482.

Yazdi AJ (2017) Investigation of different models of combined parallel flash binary cycles. *International Journal of Engineering Sciences & Research Technology* 6(2): 139–147.

Yuan P, Zhang C (2019) Comparison on thermodynamic performances between basic and regenerative sub-critical organic Rankine cycles coupled with low-grade heat source. In *IOP Conf. Series: Materials Science and Engineering*, 473, Article ID: 012031.

Vankeirsbilck I, Vanslambrouck B, Gusev S, De Paepe M (2011) Organic Rankine cycle as efficient alternative to steam cycle for small scale power generation. In *8$^{th}$ International Conference on Heat Transfer, Fluid Mechanics, and Thermodynamics (HEFAT2011)*, 785–792. Pointe Aux Piments, Mauritius. 11-13 July 2011.

*Athens Journal of Technology and Engineering - Volume 8, Issue 3, September 2021 – Pages 237-258*

# E-Banking and Monetary Policy in Nigeria

*By Nathan Audu*[*]

*The goal of this paper is to assess the impact of e-banking, which are distinct from conventional banking systems, on central banks' monetary policy. E-banking poses a challenge to central banks' ability to control interest rates and it may also increase endogenous financial instability. The challenge to interest rate control stems from the possibility that e-banking may diminish the financial system's demand for central bank liability, rendering central banks unable to conduct meaningful open market operations. Increased financial instability could emerge from the increased elasticity of private money production and from the periodic runs out of e-banking into central bank money that generates liquidity crises. Similarly, the future of e-banking is dependent on its growth, regulation and increased technological advancements that would boost the security of the new instrument. It will directly impact the central bank's control of monetary policy unless it is included in its measurements of monetary aggregates. We therefore recommend that since the impact of e-banking on monetary policy depends solely on how fast it will spread and the extent to which it will substitute for cash, it is vital that Central Bank of Nigeria (CBN) considers taking steps to compensate the resulting decrease in its balance sheet. Also, CBN must have to impose special obligations with the money reserve on the e-banking issuer in case of any large increase in e-banking creativity that will affect the monetary policy at the end. The government must keep the rate of prices stable and with this condition, where e-banking will be equal to other forms of money which maintain by apportion percentage as a reserve ratio to the central bank. Similarly, if e-banking spreads moderately, there will be a decrease in the seigniorage income and thus, the decrease in the balance sheet of CBN will be limited. Hence, it must include e-banking in monetary aggregates that the spread of e-banking may lead to a change in the velocity of money.*

**Keywords:** *monetary policy, e-banking, technology, velocity of money*

## Introduction

Following the development of the Internet and the advancements in computer and telecommunications technology, a rising number of financial institutions are introducing and expanding their offerings of electronic banking products (Sciglimpaglia and Ely 2002). These new developments include; mobile banking, internet banking, telephone banking, electronic card, etc., thus the transition from metal currency through paper currency, and now electronic currency, has made transactions more convenient with or without the physical presence of economic agents in a banking hall. The broad acceptance and ease of carrying out transactions using electronic methods has also increased the use of bank card transfers, online

[*]Nigeria Country Economist, West African Monetary Institute, Ghana.

payments and other network-based transactions on a daily basis. The extension of these platforms at the enterprise level has further entrenched its use and changed the purchasing dynamics of economic agents, thus diminishing cash transactions.

Following these developments, modern banks have recognised the need to overhaul their payment service delivery and operations in order to survive and make profit in the 21st century (Opara et al. 2010). The employment of electronic banking (e-banking) and the application of its concepts, techniques, policies, and implementation strategies to banking services has drawn attention and become fundamental to all banks. Its importance has made it a pre-requisite for local and global competitiveness, as it directly affects aspects of banking such as management decisions, and products and services offered by banks, changing the way banks and the corporates relate worldwide and the variation of innovation of service delivery. Customers' avid appetite for fast, effective and efficient banking service has further added to the drive to advance and promote more radical transformation of banking business systems and models, especially in the delivery of cashless banking. Also, the outbreak of the COVID-19 pandemic and its attendant consequences of lockdown, social distancing and hygienic protocol have further exacerbated this.

E-banking has the potential to replace currency in circulation, however it raises a number of policy issues for central banks who are tasked with the responsibility of managing the financial stability of an economy via its policies (monetary) as well as its general interest in payment systems. Thus, extensive research has been done regarding the possible economic effects of e-banking on critical variables such as money supply, currency in circulation, interest rates and business profitability for various countries. While some economists focus on the pure costs and benefits from an economic standpoint, others have focused on the implication on monetary policy and the role of central banks in a cashless society. Some have opined that e-banking will make monetary policy more efficient, while others claim that it would cause central banks to lose their independence, making monetary policy less efficient. This has implications for the way e-banking is viewed worldwide, particularly in developing countries such as Nigeria; an indication that there are a myriad of issues and challenges surrounding the application of e-banking. It has also continued to elicit the reactions of many scholars with, varying and often, conflicting views on the fundamental issues at stake; how they can be resolved; and the importance of such resolution in the ever-changing banking system and its regulation.

It is against this backdrop that this paper seeks to assess the impact of e-banking services on monetary policy in Nigeria in a bid to understand its effectiveness and guard against the negative potentials of e-banking on the efficacy of the Central Bank of Nigeria's monetary policy. The major objective of this paper therefore is to evaluate the effectiveness of e-banking services on monetary policy as a major tool for the achievement of economic efficiency and price stability.

It is worthy to note that this paper is different from others in the following ways; (a) the works of Bamidele (2005), focused on the essence of e-banking deployment for monetary policy with a view of advocating necessary actions required for enhancing the effectiveness and efficiency of monetary policy implementation in Nigeria, while (b) Imiefoh (2012), evaluated the efficient businesses response to customers demand in Nigeria. The evaluation of these studies revealed that they were both reviews. However, this current study employed both descriptive and inferential statistics to assess the impact of e-banking services on monetary policy in Nigeria.

Following the introduction, Section 2 reviews relevant literature while Section 3 discusses the challenges of e-banking for monetary authorities. Section 4 evaluates the methodology and analysis of the estimation and findings. Section 5 concludes with recommendations.

## Literature Review

### *The Evolution of E-Banking*

The first consumer credit card was issued by the Western Union in 1914, but its root dates back to 1851 when central banks first manipulated book-entries to clear payment balances among themselves through telegraph (David and Glyn 1996). Diners Club issued the first plastic money credit card in 1950, which was accepted by many merchants. This launch by American Express led to a change in the financial landscape in the United States. However, after a year of its inception, nearly hundred banks began to issue their cards. In the United Kingdom, the credit cards was first issued in 1966. Despite all these innovations, the widespread use of electronic banking did not begin until the automated clearing house was set up by the Federal Reserve Bank of the United States in 1972 to provide the US Treasury and commercial banks with an electronic alternative to check processing. Similar systems emerged in Europe around the same time, so electronic banking has been widely used throughout the world on an institutional level for more than three decades. Today, it is used in nearly all of the deposit currencies in the world's banking systems (Wafa 2003, ECB 2000, Rahn 2000). However, Salawu and Salawu (2007) opined that e-banking was first introduced in Nigeria in the late 80s with the Automated Teller Machines (ATMs) at its rudimentary stage, but with a promising future given the size of the country's financial markets and the increased desire to embrace information and communications technology. Nonetheless, in August 2003, the CBN issued guidelines for compulsory practice of e–banking in the country. But, a number of measures were still needed to be put in place to avoid threats to the stability of the entire financial system and the nation's economy (CBN 2004). A survey conducted by CBN in 2002 to determine the level and types of e-banking activities carried out by banks in the country, revealed that 17 banks were offering internet banking, 24 were offering basic telephone, while 13 banks were offering other forms of e-banking. Twelve (12) banks indicated that their websites were hosted in Nigeria, while 22 were hosted outside Nigeria. Fourteen (14) of the websites were for information only, 11 for information transfer systems and 22 for transactional purposes. Furthermore, the survey suggested that 27 banks had security measures on e–banking, while 4 had none. Also, it was observed that 30 banks used authentication as a means of security control, 28 used firewalls, 16 cryptography, 8 digital signature, 14 digital certificate, 18 used secured socket layer, 15 public key infrastructure and 31 physical security (Audu 2011, CBN 2003). Currently all the twenty-two existing banks in the country are fully compliant with the CBN's guidelines (CBN 2019).

*The Impact of E-Banking on Monetary Policy*

In most developing economies such as Nigeria, one of the goals of monetary policy is the promotion of an efficient and sound financial sector. As such, the monetary authorities' avowed objective is to ensure banking soundness and financial sector stability aimed at improving the efficiency of the payments system and the effective transmission of monetary policy to the real sector. Others include ensuring the effective enforcement of market rules to enthrone the right market expectation (CBN 2017a, b). For optimum efficiency of monetary policy, it has to be executed in an atmosphere of financial stability to minimise macroeconomic losses. This means that the expected macroeconomic losses that arose from financial system disturbances should cover the probability of financial disturbance occurrence and the magnitude of macroeconomic costs of such disturbances when they crystalise (Kent et al. 2007, Miller 2000). Considering the link between the real sector and the financial sector of the economy, monetary authorities need to take cognizance of the potential for financial system stability that is vital for the conduct of monetary policy. This conforms to the tasks of monetary authorities' duty of ensuring that shocks from any part of the financial system do not ultimately threaten the health of the system and that of the economy as a whole (Tak 2002).

Also, customers' attitude of the usefulness, easiness and compatibility, is the main driver of consumers' intentions to the adoption of e-banking services. Consumers' perceptions of availability of knowledge, resources and opportunities necessary for using the service, and the pressure of interpersonal and external social contexts toward the use of e-banking are the other two, less important, adoption drivers, as these will reduce the e-banking threat to the financial system (Sandhu and Arora 2020, Giovanis et al. 2019, Foroughi et al. 2019, Singhraul and Garwal 2018). Despite the foregoings, e-banking has improved service-efficiency and cost-efficiency of business. Researchers have observed that different dimensions of customer satisfaction exist, as such both the fiscal and monetary authorities should pursue the digitization of banking, and reforming the security framework to develop trust with a higher acceptance rate amongst the customer (Khan et al. 2021, Pandian and Duraisingh 2021).

Therefore, the effect of any kind of banking transaction or the introduction of new products or services on the system must clearly be evaluated to ensure a healthy financial system (Ovia 2004). The danger arising from the high degree of substitution of currency in circulation with e-money is presented in a decrease in the central bank balance sheet, which hinders the positive influence of the monetary instruments. Also, the new incentives of electronic banking have triggered the basic changes in plan of action measurements like customers' value, market portion, cost structure and revenue sources (Chukwudi and Amah 2018). In order to avoid this negative influence in the near future, there is another possibility to be taken into consideration and that is the possibility for the central bank to impose reserve requirements on all issuers of electronic money.

According to previous analyses, the impact of the emergence of electronic money on monetary policy can mostly be expected in the following areas (Al Laham et al. 2009):

a) Decrease in the control of the central bank over money supply: Decreasing the central bank's control of money supply depends on the degree of substitution of currency in circulation with e-money. The currency in circulation is part of monetary aggregates, and if it is decreased as a result of wider use of e-money, it will produce difficulties in measurement of monetary aggregates and of the control of money supply by the central bank. Possible solutions for limitations of this effect are, for example, limitations of the use of e-money. But this will be in direct confrontation with the laws of technological progress and could produce negative external effects on banking in general. Because of that, there is need for intensified research on new opportunities to limit the adverse impacts of replacing cash with electronic money.
b) Increase in the velocity of money: The influence of e-money over monetary policy can be seen through monetary aggregates and the ability of the central bank to control money supply. In the future, impact should be seen through other indicators related to monetary aggregates, like the velocity of money. With the use of e-money, transactions are relatively cheaper which allows increase in the number of transactions, and increase in the speed of money. Generally speaking, it will be useful, but only to the extent that the central bank can control or measure the monetary aggregates.
c) Volatility in exchange rates: The change of the monetary multiplier is an important indicator. This indicator shows the share of currency in the money supply. As a result of e-money, the currency decreases producing effects to multiplier.
d) With the use of e-currency, the need for printing cash is decreasing, which influences the revenues of central banks in terms of seignorage, thereby affecting the balance sheet of the central banks.
e) E-money has a characteristic of easy portability and affordability which offers a wide use in trade among countries. It is assumed that the user of e-money, motivated with the cheaper foreign currency transactions, will prefer the transactions to be in the most powerful currency. So, through PayPal and other services, users from the country with weaker currency will prefer to transfer their money in higher currency. So in this way the dollarisation or euroisation will be a subject to clicking the mouse. Reynolds (2013) posits that this situation can weaken the central bank's control in the process of foreign currency exchange among the countries.

De Grauwe and Costa Storti (2005) argue that central banks and monetary policy will be negatively affected by a transition towards a cashless society. They claim that private institutions issuing money will not be able to control inflation and that central banks will lose their independence. They conclude that there will be no mechanism to control price stability if private institutions take on the role to create money. This is due to the problem of price indeterminacy, which can be illustrated by the equation for money market equilibrium, M=P(Y,r). According to this equation, there are infinite number combinations of the money stock, M, and price level, P, in which the money market is in equilibrium. Both of these are nominal variables, and assuming that private agents are free of money illusion (implying that they only care about relative prices, and not nominal variables), private agents have no incentive to control the nominal variables M and P. Today, central banks take on the responsibility to control the money stock in order to prevent inflation. However, in a cashless society central banks will no longer be able to maintain this role of protecting these nominal variables.

However, if a central bank is able to take on a supervisory role in a cashless society and control inflation by granting privately issued money, legal tender characteristics and imposing legal reserve requirements, they could succeed in remaining independent in a cashless society at the same time as controlling inflation. One recent study on the development of a cashless society in Nigeria by Odior and Banuso (2012) predicts monetary policy to become more efficient with less cash in circulation. In 2012, Nigeria implemented the "Cash-Less Nigeria Project" as a part of the goal of being one of the world's top-20 performing economies by 2020. The policy introduced cash handling charges with the goal to decrease the number of cash payments to prevent revenue leakage, improve efficiency, and reduce transaction costs and the risk for robbery. Studies suggest that implementing a similar cash handling fee in Sweden may better reflect the social cost of cash to make the Swedish payment system more efficient by reducing cash transactions (Moorthy et al. 2020, Bergman et al. 2007, Segendorf and Jansson 2012a, b, Arvidsson et al. 2019), while Martin et al. (2018) opined that a host of cultural and infrastructural issues have created major difficulties in e-banking implementation in Nigeria.

Rather than relying on inflation targeting, Nigeria will place a greater focus on open market operations and reserve requirements (Tolulope and Ajilore 2013, Migap 2011). Moreover, these studies predict that transaction costs will fall in Nigeria as a result of removing the central bank's monopoly in issuing currency, as it allows for competition in the financial sector. In addition, even though seignorage revenues for the central bank will fall, the cost savings from not printing currency will balance this loss. In turn, cashless banking is estimated to increase the velocity of circulation in the long-run which stimulates trade and commercial activities.

Hence, the introduction of e–banking in Nigeria had a salutary impact on monetary policy execution by reducing the non–bank public preference for cash. It is also a useful tool in advancing the integration of the domestic financial system with the international financial architecture. In addition, it serves as a robust payments system that satisfies the needs of economic agents, in areas of time-critical transactions which affects productivity and the overall economic activity. As such, if it is properly deployed, e-banking would enhance public confidence in both payments and financial systems in such a way that monetary policy would be transmitted in an unfitted manner. It is in this vein that the CBN has taken various measures in the banking industry to present them with opportunities to increase the tempo of e-banking in Nigeria, through product diversification of the industry.

## The Challenges of E-Banking for Monetary Policy in Nigeria

The application of Information and Communications Technology (ICT) in the Nigerian banking industry has resulted in improved business performance with positive impact on the domestic economy. In spite of the enormous benefits of electronic banking in promoting economic activity and its ability to promote monetary policy implementation by reducing the size of cash outside banks, it presents a great challenge to operators, regulators and supervisors. Most of these problems arise from its merits that endear it to public banking and the technology employed in its service delivery. Some of these include regulation, surveillance, seigniorage, operational system integrity and legal risk. Other problems faced by developing countries like Nigeria, include obsolescence and inadequate ICT and other infrastructure such as energy, inefficient payments system, information and data security. Bamidele (2005) opined that computers aid information acquisition, while information processing assists banks in providing customer-focused products/services, building beneficial and qualitative long-term relationships with customers, increasing revenue streams, as well as achieving profitability growth in a competitive environment. But, reliance on ICT to provide services could be problematic if requisite systems and infrastructure are either unreliable or unavailable in real-time on a daily basis. Most developing countries such as Nigeria import the required technologies and equipment. Therefore, the issue to contend with borders on the use of updated, secure, state-of-the-art technologies, coupled with the irregularity of power supply, could lead to inefficiencies, such as fraud, delays and breakdown in service delivery that would in turn erode public confidence in the industry, especially where time-critical transactions are involved. He also held that banking business is based on trust and confidentiality which places a fiduciary burden on the banker towards the customer, while security threats to financial information and customer net-worth which could originate from within and/or outside the system is ever-present and heightened in e-banking. This calls for all the regulatory agencies to put in place policies that would ensure standard practices to guarantee data and information confidentiality around-the-clock.

Audu (2011) observed that the efficient functioning of e-banking rests entirely on the adequacy of ICT infrastructure in terms of quality, volume and power to ensure its smooth operation. The reverse is the case in Nigeria with loss implication for the operators. When electronic banking transactions are significant in a sub-optimal ICT environment, the payments and financial systems could be adversely affected with serious implications for economic activity. Similarly, security breaches and disruption of efficient functioning of e-banking could damage not only a bank's reputation, but also the entire banking system. Hence, the efficacy of monetary policy in ensuring monetary stability rests partly on the assumption of a stable velocity of money and the reaction functions of the central bank, and the clearing banks and non-bank public under the classical quantity theory of money. Therefore, the advent of e-banking has changed the financial landscape and increased the potential for cross-border capital movements and capital flight. The implication of this is that the practice of electronic banking could lead to variability of velocity of money in both the short- and medium- term, owing to internet banking, especially where virtually all banks operate within the local economy.

## Methodology

### *Data Sources, Research Area and Sampling Technique*

The data for this study were obtained through primary and secondary sources. The primary source was through a field survey, while the secondary data were sourced from the CBN Statistical Bulletin and National Bureau of Statistics (NBS). The study covers the entire thirty-six states of Nigeria and the FCT, Abuja. In determining the samplings technique used for this study, we took into consideration the technical nature of the investigation which requires the responses of respondents with a good and related knowledge of the subject matter. To achieve this, a stratified random sampling method was employed for the study. The stratification was to ensure diversification of opinions. Customers and bankers from each state were stratified according to knowledge, and a sample size of 400 respondents was randomly selected from each geopolitical zone. It is hoped that the sample size will be statistically significant for inferential purposes. This method gives a more representative sample in this case than simple random sampling, because in the latter, certain strata may by chance be under- or over- represented in the sample. Hence, the stratified random sampling method guarantees representation of defined groups that are of of particular interest in the sample size. A sample of 2400 was drawn, 400 per zone (stratum).

### *Instrumentation and Data Collection Procedure*

The measurement instrument for the study is a two-point Likert-type scale questionnaire. The questionnaire was divided into two sections. The first section – 'A'—dealt with the respondents bio-data, while the second section – 'B' —- contained 27 items into two Likert-type questionnaires to measure the effectiveness of the existing e-banking services in Nigeria.

Both interviews and questionnaires were employed. The interviews were used to supplement the questionnaires. The e-banking survey was administered using the questionnaires, while interviews were used on key players in each zone. To validate survey instruments, 12 questionnaires were pretested on some bank customers and key players in each zone. The instrument was then reviewed and corrected as necessary. Twelve enumerators were recruited and trained to assist in administering the questionnaires on players in the industry.

*Data Analysis Method*

The survey questions were numerically coded and responses stored in computer spreadsheet software, Microsoft Excel Version 2010. The Chi-squares (non-parametric) test and descriptive tables were employed to describe existing relationships between e-banking variables. The formula for Chi-squares is given thus:

$$X^2 = \sum_{i=1}^{n} \frac{(OBS_i - EXP_i}{EXP_i} \quad (1)$$

$$DF = (R-1)(C-1) \quad (2)$$

where $X^2$ = Chi–Square, ∑=The sum of, n= Total number of observation, $OBS_i$=The Observed frequency, $EXP_i$=The expected frequency. DF=Degree of freedom, R=Total row, C=Total column

**Decision Rule:** If the value of $X^2$ calculated is greater than the value of $X^2$ critical, we reject the Null Hypothesis and accept the Alternative Hypothesis and vice versa.

The data on e-banking and customers were used to capture the impact of e-banking on monetary policy management in Nigeria from the survey data using statistical package for social sciences (SPSS) version 25 software. This would be achieved through the survey questionnaire.

*Data and Source*

The paper employed seven key variables; namely, debit card (DEC), internet banking (INTB), monetary base (MB), money supply (M2), mobile payment (MP), money multiplier (m) and velocity of money (v) for the period spanning 2010Q1 to 2020Q4. All the series were sourced from the CBN Statistical Bulletin and the Nigerian National Bureau of Statistics (NBS) data base, respectively.

*ARDL Approach*

The Autoregressive Distributed Lag (ARDL) model deals with single cointegration and was introduced originally by Pesaran and Shin (1999) and further extended by Pesaran et al. (2001). The ARDL approach has the merit that does not require all variables to be I(1) as the Johansen framework and it is still applicable if we have I(0) and I(1) variables in our set. The bounds test method cointegration has peculiar econometric advantages when compared to other methods of cointegration. These are:

- ✓ All the variables in the model are assumed to be endogenous.
- ✓ The bounds test method for cointegration is being applied irrespectively of the order of integration of the variables. They may be either integrated of

the first order or levels [I(1) or I(0)].
- ✓ The short-run and long-run coefficients of the model are estimated simultaneously.

This new approach to co-integration testing that is encompassing irrespective of whether the variables are I(0), I(1) or are mutually co-integrated was developed by Pesaran et al. (2001). The starting point of this test is a data generating process represented by a general VAR of order z which is rewritten in vector ECM form involving a vector σ of variables. They focus on the conditional modeling of the dependent scalar variable π. Therefore, the vector σ is partitioned into the scalar π and vector r of dependent variables (under the assumption that there is no feedback from π to r). The model can be written as the following conditional ECM model for $\Delta\pi$ thus:

$$\Delta\pi_t = \alpha' m + \beta_a \pi_{t-1} + \beta_{ar} r_{t-1} + \sum_{i=1}^{z-1} \gamma_i' \Delta\sigma_{t-i} + \vartheta' \Delta r_t + \varepsilon_t \qquad (3)$$

where m is a set of deterministic variables like the constant term, trend, seasonal dummies, etc. α is a vector of coefficients of deterministic variables $\varepsilon_t$ is the residual term.

To test the absence of a level relationship between π and r, the approach uses a Wald or F-statistics to test for the joint hypothesis that all coefficients of all (lagged) levels in the ECM equation are zero. Pesaran et al. (2001) x-rays six cases of deterministic ARDL approach to cointegration testing: the application to e-banking to monetary policy components are specified: no intercepts, no trends; restricted intercepts, unrestricted intercepts, restricted trends, unrestricted trends.

The resulting conditional ECMs' may be interpreted as autoregressive distributed models of orders (z, z,… z) or ARDL (z, z,…z) models. Pesaran et al. (2001) tabulated asymptotic critical value bounds for the F-statistic for all 6 conditional ECM models. If the computed F-statistic from the exclusion of levels in the conditional ECM's falls outside the critical value bounds, the test allows a conclusive inference without needing to know the integration/cointegration status of the underlying variables. But if the F-statistic falls inside the bounds, inference is inconclusive and knowledge of the order of integration of the underlying variables is required before conclusive inferences can be made. If the computed F-statistic lies below the 5 percent lower bound, the hypothesis that there is no level relationship is accepted at the 5 percent level. If the statistic falls within the 5 percent bounds, the test is inconclusive and when the F-statistic lies above the 5 per cent upper bound, the hypothesis of no level relationship is conclusively rejected.

Also in addition to the F-test, Pesaran et al. (2001), tabulates asymptotic critical value bounds of the t-statistic for testing the significance of the coefficient on the lagged dependent variable in the conditional ECM. Concerning the use of the F- and t-statistics, Pesaran et al. (2001) opined the following procedure: test $H_0$

using the bounds procedure based on the Wald or F-statistic. If $H_0$ is not rejected, proceed no further. If $H_0$ is rejected test the coefficient of the lagged dependent variables using the bounds procedure based on the t-statistics. A large value of t confirms the existence of a level relationship between π and r.

To test for the existence of a level relationship as in the previous section requires that the coefficients of the lagged changes remain unrestricted. But for the subsequent estimation of the ECM model, a more parsimonious approach is recommended, such as the ARDL approach to the estimation of the level relations discussed in Pesaran and Shin (1999). In practical terms an ARDL (z, z,… z) model is selected from a broader search analysis, testing the lag orders using information criteria such as AIC or SBC. In this respect, it is interesting that PSS note that the ARDL estimation procedure is directly comparable with the semi parametric Fully Modified OLS approach (FMOLS) of Phillips and Hansen (1990). From the parsimonious ARDL specification, the specification of the estimated levels relationship is then derived, as well as the associated ECM model.

We estimated this basic quarterly e-banking model using the ARDL technique along the lines suggested by Pesaran et al. (2001). The analysis starts from the assumption that the $MS_2$ in e-banking can be modeled by a semi log linear VAR (p) model, augmented with deterministic such as a constant and a time trend. Then using proofs in Pesaran et al (2001) the following conditional ECM was estimated:

$$\Delta MS_2 = \alpha' m + \beta_1 MS_{2t-1} + \beta_{2ar} r_{t-1} + \sum_{i=1}^{z-1} \gamma_i' \Delta\sigma_{t-i} + \vartheta' \Delta r_t + \varepsilon_t \quad (1)$$

Before the secondary data were collected from the CBN and were analyzed, key econometric assumptions were considered, and necessary tests were undertaken using EViews 10. A lot of effort was made to get the statistics about e-banking from the inception in Nigeria. The total number of debit card and master card (DEC), internet banking (INTB), point of sales (POS) and mobile payments (MP) from the year 2009 to 2015 as well as gross domestic product (GDP), money supply (M2), money base (MB), v and m were adopted on quarterly basis. Even though data on e-banking was available from 2009, we opted for year 2010 due to data consistency emanating from the rebasing of the country's GDP.

*Questionnaire Distribution*

The questionnaire response rate of the study is presented in Table 1. An evaluation of the study shows 1,695 respondents representing 70.6 percent response rate returned their completed questionnaire while 705 or 29.3 percent did not. Therefore, for the remainder of this study the 1,695 questionnaires retrieved would constitute the sample size.

**Table 1.** *Questionnaire Response Rate*

| Response | North Central | North East | North West | South East | South West | South South | Total | % |
|---|---|---|---|---|---|---|---|---|
| Retrieved | 250 | 300 | 245 | 300 | 300 | 300 | 1695 | 70.6 |
| Not Retrieved | 150 | 100 | 155 | 100 | 100 | 100 | 705 | 29.3 |
| **Total** | **400** | **400** | **400** | **400** | **400** | **400** | **2400** | **100** |

*Source:* Field Survey 2020.

*Gender Composition of Sample*

Table 2 is a representation of gender composition of respondents in Section A. Respondents in the male category represents 745 (44%), while respondents who are female constitute 950 (56%). Since it is our intention to analyze the data based on the six geo-political zones, the implication of the marginal difference between the six zones in terms of their responses to any question of importance would be highlighted in the analysis.

There was no intention to compare responses of each question of importance that relates to this study with the gender of our respondents. Even though Table 2 reveals a marginal difference between the genders, it has no implication on the result of the study. More so, no attempt was made to draw equal number of respondents from both sexes – male and female.

**Table 2.** *Distribution of Respondents by Sex*

| Sex | North Central | North East | North West | South East | South West | South South | Total | % |
|---|---|---|---|---|---|---|---|---|
| Male | 140 | 150 | 120 | 115 | 100 | 120 | 745 | 44 |
| Female | 110 | 150 | 125 | 185 | 200 | 180 | 950 | 56 |
| **Total** | **250** | **300** | **245** | **300** | **300** | **300** | **1695** | **100** |

*Source:* Field Survey 2020.

*Age Composition of Sample*

The pattern of responses as x-rayed in Table 2, indicates that 300 and 400 respondents representing 13% and 21% respectively are within 21-30 and 31-40 age bracket. The result also reveals that 800 and 660 respondents fall within the 41-50 and above 51 age brackets representing 36% and 29% respectively of the sample. We assume that most of the experienced bankers and seasoned customers would be found among this age bracket. It is vital to note that we do not intend to relate one's age with any question of importance in the research instrument, thus, no attempt was made to draw equal number of respondents from each age bracket.

*Composition of Respondents by Qualification*

**Table 3.** *Distribution of Respondents by Qualification*

| Qualification | South East | South West | South South | North Central | North East | North West | Total | % |
|---|---|---|---|---|---|---|---|---|
| SSCE/GCE/NCE/DIP. | 100 | 97 | 78 | 73 | 75 | 60 | 483 | 28.50 |
| B.Sc./BA/B.Ed/HND | 100 | 90 | 42 | 80 | 100 | 65 | 477 | 28.14 |
| MSc/MA/MEd/MBA | 100 | 115 | 162 | 130 | 92 | 90 | 689 | 30.97 |
| Ph.D. | 45 | 53 | 80 | 17 | 25 | 30 | 250 | 12.37 |
| **Total** | **300** | **300** | **300** | **250** | **300** | **245** | **1695** | **100** |

*Source:* Field Survey 2020.

From Table 3, 473 (21%) were holders of either SSCE or GCE or NCE or diploma certificates, 828 (37) of the sample were first degree holders while 698 (31%) of the total respondents were holders of a Master's degree. Only 250 (11%) of the sample are holders of Ph.D degrees. The degree holders include those whom obtained certificates in Banking and Finance, Insurance, Accounting, Business Administration and related disciplines.

*Analysis of E-Banking Efficiency Rating*

**Table 4.** *Respondents' Rating of E-Banking Efficiency in Nigeria*

| Responses | South East | South West | South South | North Central | North East | North West | Total | % |
|---|---|---|---|---|---|---|---|---|
| Efficient | 157 | 186 | 90 | 150 | 186 | 187 | 956 | 56.4 |
| Average | 61 | 76 | 132 | 89 | 94 | 41 | 493 | 29.1 |
| Insufficient | 82 | 38 | 78 | 11 | 20 | 17 | 246 | 14.5 |
| **Total** | **300** | **300** | **300** | **250** | **300** | **245** | **1695** | **100** |

*Source:* Field Survey 2020.

Table 4 analyses respondents rating of e-banking in Nigeria. The result reveals that 956 respondents representing 56.4 per cent are of the opinion that e-banking is efficient, 493 (29.1%) believed it is average while 246 (14.5%) respondents says it is inefficient. The implication of the result in Table 4 is that e-banking has made life easier for the people in the six geo-political zones.

**Table 5.** *Comparative Exploration between E-Banking and Conventional (Why do you Prefer E-Banking to Conventional Banking?)*

| Responses | South East | South West | South South | North Central | North East | North West | Total | % |
|---|---|---|---|---|---|---|---|---|
| Safe | 95 | 57 | 95 | 155 | 187 | 40 | 629 | 37.1 |
| Time saving | 57 | 105 | 57 | 29 | 41 | 145 | 434 | 25.6 |
| Convinient | 100 | 93 | 100 | 46 | 48 | 21 | 408 | 24.1 |
| Efficient | 48 | 45 | 48 | 20 | 24 | 39 | 224 | 13.2 |
| **Total** | **300** | **300** | **300** | **250** | **300** | **245** | **1695** | **100** |

*Source:* Field Survey 2020.

The respondents' preference for e-banking in Nigeria is presented in Table 5. The assessment of respondents' views reveals that 629 or 37.1 percent of the respondents are of the view that they prefer e-banking to conventional banking because it is safe; 434 (25.6%) held that they prefer e-banking to conventional banking because it is time-saving; while 408 or 24.1% and 224 (13.2%) held that they prefer e-banking to conventional banking because it is convenient and efficient, respectively. The implication of their responses in Table 5 is that the emanation of e-banking makes life more conducive in terms of business and financial transactions in the six geo-political zones.

*Investigation of the Positive Impact of E-Banking on Monetary Policy*

**Table 6.** *Does E–banking have any Positive Impact on Monetary Policy*

| **Responses** | **South East** | **South West** | **South South** | **North Central** | **North East** | **North West** | **Total** | **%** |
|---|---|---|---|---|---|---|---|---|
| Yes | 223 | 150 | 211 | 198 | 167 | 100 | 1049 | 61.9 |
| No | 77 | 150 | 89 | 52 | 133 | 145 | 646 | 38.1 |
| **Total** | **300** | **300** | **300** | **250** | **300** | **245** | **1695** | **100** |

*Source:* Field Survey 2020.

Table 6 presents the positive impact of e-banking on monetary policy in Nigeria. 61.9 percent of the respondents believed that e-banking has positive influence on monetary policy, while 38.1 disagreed and held that it does not. Given that majority of the respondents believe in the efficacy of e-banking, monetary authority should take cognizance of this while making policies to improve e-banking policies.

*Scrutiny of E-Banking in Nigeria*

**Table 7.** *Rating of E-Banking in Nigeria*

| **Responses** | **South East** | **South West** | **South South** | **North Central** | **North East** | **North West** | **Total** | **%** |
|---|---|---|---|---|---|---|---|---|
| Effective | 157 | 186 | 90 | 150 | 186 | 187 | 956 | 56.4 |
| Average | 61 | 76 | 132 | 89 | 94 | 41 | 493 | 29.1 |
| Ineffective | 82 | 38 | 78 | 11 | 20 | 17 | 246 | 14.5 |
| **Total** | **300** | **300** | **300** | **250** | **300** | **245** | **1695** | **100** |

*Source:* Field Survey 2020.

Respondents' rating of e-banking is analyzed in Table 7. The rating was categorized into three, thus, effective, average and ineffective, across the six geo-political zones in Nigeria. 56.4 percent of the respondents rated e-banking in the country as effective; 29.1 percent rated e-banking as average; while 14.5 rated it as ineffective. From the foregoing analysis, it is clear that e-banking has been accepted by the populace; therefore, monetary authority should make policies that will deepen its usage in the country.

*Examination of E-Banking Perception*

**Table 8.** *The Perception of E-Banking in Nigeria*

| Responses | South East | South West | South South | North Central | North East | North West | Total | % |
|---|---|---|---|---|---|---|---|---|
| Very strong | 160 | 122 | 91 | 187 | 145 | 82 | 767 | 46.7 |
| Strong | 45 | 90 | 121 | 35 | 98 | 100 | 469 | 28.6 |
| Weak | 45 | 68 | 63 | 9 | 33 | 43 | 261 | 15.4 |
| Very weak | 50 | 20 | 25 | 19 | 24 | 20 | 158 | 9.3 |
| **Total** | **300** | **300** | **300** | **250** | **300** | **245** | **1655** | **100** |

*Source:* Field Survey 2020.

The respondents' perception of e-banking in Nigeria is evaluated in Table 8. The valuation of respondents observation in Table 8, shows that 767 or 47 percent of the respondents believed that e-banking is very strong; 469 (29%) said it is strong; while 261 or 15% and 158 (9%) perceived e-banking as weak and very weak, respectively. The consequence of these responses in Table 10 is that the introduction of e-banking has made financial transaction for both business and other personal engagement easy for bank customers across the country.

*Evaluation of Problems Encountered in E-Banking Usage*

**Table 9.** *Problems Encountered by Bank Customers on the Use of E-Banking*

| Responses | South East | South West | South South | North Central | North East | North West | Total | % |
|---|---|---|---|---|---|---|---|---|
| Delay in reverting failed transaction | 70 | 68 | 56 | 75 | 55 | 49 | 373 | 22.0 |
| Fraud | 31 | 56 | 23 | 20 | 36 | 34 | 200 | 11.8 |
| Security issues | 13 | 48 | 50 | 12 | 32 | 15 | 170 | 10.0 |
| User error | 32 | 23 | 35 | 20 | 45 | 30 | 185 | 10.9 |
| Data protection | 23 | 16 | 29 | 21 | 15 | 35 | 139 | 8.2 |
| Bad internet connection | 36 | 15 | 20 | 14 | 21 | 22 | 128 | 7.6 |
| System error | 55 | 55 | 56 | 67 | 81 | 45 | 359 | 21.2 |
| Non reversal of failed transaction | 40 | 19 | 31 | 21 | 15 | 15 | 141 | 8.3 |
| **Total** | **300** | **300** | **300** | **250** | **300** | **245** | **1695** | **100.0** |

*Source:* Field Survey 2020.

The investigation of the problems encountered by bank customers on the use of e-banking is shown in Table 9. The examination of Table 9 indicated that 373 respondents representing 22 percent of the sampled population have experienced long delay in reverting failed transaction; 200 or 11.8% respondents said they have been defrauded; 10, 10.9 and 8.2 percent representing 170, 185 and 139 respondents, respectively, have problem with security, user error and data protection. Bad internet connection, system error and non-reversal of failed transaction accounting for 7.6, 21.2 and 8.3 per cent, respectively, representing

128, 359 and 141 respondents. The implication of this to monetary authority is that effort must be geared to reducing these identified problems by the customers.

The analysis of the effect of monetary policy on bank customers' choice for e-banking is presented in Table 10. The result reveals that 34.6 percent or 586 respondents believed that monetary policy affect bank customer's choice for e-banking directly, while 65 percent or 1,109 respondents, believed that monetary policy affect bank customer's choice for e-banking indirectly.

*Impact of Monetary Policy on Customer's Choice for E-Banking*

**Table 10.** *How does Monetary Policy Affect Bank Customer's Choice for E-Banking?*

| Responses | South East | South West | South South | North Central | North East | North West | Total | % |
|---|---|---|---|---|---|---|---|---|
| Directly | 83 | 105 | 108 | 92 | 107 | 91 | 586 | 34.6 |
| Indirectly | 217 | 195 | 192 | 158 | 193 | 154 | 1109 | 65.4 |
| **Total** | **300** | **300** | **300** | **250** | **300** | **245** | **1695** | **100** |

*Source:* Field Survey 2020.

The implication of the result on e-banking is that monetary policy being the anchor rate serves as a guide to deposit money banks to fix charges on their product, therefore, its impact on customers is indirect.

*Chi-square Statistical Analysis for Hypothesis Testing on the Positive Impact of E-Banking on Monetary Policy*

**Table 11.** *Chi-Square Statistical Analysis for Positive Impact of E-Banking on Monetary Policy Management in Nigeria*

| Responses | Bankers | Customers | Cal $x^2$ | Critical $x^2$ | DF | Total | % |
|---|---|---|---|---|---|---|---|
| YES | 629 (538.4) | 420(510.6) | 82.14 | 3.84 | 1 | **1049** | 61.9 |
| NO | 241 (331.6) | 405(314.4) | | | | **646** | 38.1 |
| **Total** | **870** | **825** | | | | **1695** | **100** |

Significance level = 0.05

*Source:* Field Survey 2020.

The dependent variable in this hypothesis is e-banking, while the independent variable is monetary policy. The statistical analysis used in testing the hypothesis was chi–square statistical analysis. The results of the analysis as presented in Table 11 reveals that the $x^2$ – value of 82.14 is greater than the critical $x^2$ – value of 3.84 at 0.05 level of significant with 1 degree of freedom. This means that the $x^2$ – value is statistically significant. This implies that the introduction of e-banking significantly influenced monetary policy management in Nigeria, thus, corroborating Martin et al. (2018), Odior and Banuso (2012), Audu (2011), Salawu and Salawu (2007) findings that e-banking has positive impact on monetary policy.

*KPSS Unit Root Test*

**Table 12.** *KPSS Unit Root Test Result*

| Variables | Levels | 1st Difference | Decision |
|---|---|---|---|
| DEC | 0.425088 | 0.578919 | I (0) |
| INTB | 0.254388 | 0.564930 | I (1) |
| $M_2$ | 0.303304 | 0.578304 | I (1) |
| MP | 0.254892 | 0.578668 | I (1) |
| MB | 0.254892 | 0.578668 | I (1) |
| *m* | 0.043329 | 0.566981 | I (1) |
| *v* | 0.191208 | 0.489849 | I (0) |
| *Critical values* | | | |
| *1%* | | *0.739000* | |
| *5%* | | *0.463000* | |
| *10%* | | *0.347000* | |

Note: Kwiatkowski et al. 1992.
*Source:* Author's computation.

*v (velocity of money)* $=\frac{GDP}{M_2}$, *m (Money Multiplier)* $=\frac{M_2}{MB}$ , *DEC = Debit card, MB = Monetary base,*
*$M_2$ = Money supply, GDP = Gross domestic product, INTB = Internet banking, MP = Mobile payments*

The econometric analysis of the secondary data of the results of the unit root test without trend of each variable is presented in Table 12. These results suggest that the null hypothesis of stationarity for all variables under consideration cannot be rejected at the 5 percent level of significance. But the results from the KPSS test indicate that apart from DEC and v, which are stationary at levels, all other variables are stationary at first difference at the 5 percent level of significance.

*Analysis of Descriptive Statistics on Study Variables*

**Table 13.** *Summary Statistics*

| Description | LM2 | LMB | LDEC | INTB | MP | POS | M | V |
|---|---|---|---|---|---|---|---|---|
| Mean | 16.453 | 14.920 | 4.994 | 4.204 | 10.931 | 11.455 | 4.846 | 1.290 |
| Median | 16.466 | 14.961 | 5.161 | 3.680 | 4.250 | 6.235 | 4.620 | 1.285 |
| Maximum | 16.765 | 15.625 | 5.837 | 8.120 | 39.820 | 34.860 | 7.160 | 1.450 |
| Minimum | 16.191 | 14.240 | 3.038 | 1.120 | 0.290 | 0.620 | 3.120 | 1.110 |
| Std. Dev. | 0.173 | 0.471 | 0.823 | 2.199 | 12.710 | 11.754 | 1.489 | 0.090 |
| Coeff. of Variation | 0.011 | 0.032 | 0.165 | 0.523 | 1.163 | 1.026 | 0.307 | 0.070 |
| Skewness | 0.106 | -0.080 | -1.175 | 0.492 | 0.968 | 0.800 | 0.295 | -0.033 |
| Kurtosis | 2.031 | 1.571 | 3.285 | 2.002 | 2.549 | 2.166 | 1.603 | 2.291 |
| Jarque-Bera | 0.902 | 1.895 | 5.139 | 1.800 | 3.626 | 2.984 | 2.109 | 0.465 |
| Probability | 0.637 | 0.388 | 0.077 | 0.407 | 0.163 | 0.225 | 0.348 | 0.792 |

*Source:* Author's computation.

Table 13, shows the summary of descriptive statistics of the variables employed to evaluate e-banking in Nigeria. The result reveals evidence of significant variation for five of the variables (DEC, INTB, MP POS and m). This is shown by the huge difference between the minimum and the maximum values, while that of MB, M2 and v have marginal differences between the minimum and the maximum values over the scope covered.

In terms of the statistical distribution of variables, M2, INTB, MP, POS and m, indicates the evidence of positive skewness implying that the right tail is extreme. In relation to kurtosis which compares the peakedness and tailedness of the probability distribution of a normal distributed series, it shows that all the variables are low peaked and thin tailed (platykurtic) than normal distribution. Similarly, the Jarque-Bera (JB) which uses the information from skewness and kurtosis to test for normality shows the evidence of normality for M2, INTB, MP, POS and m variables.

In addition, MB, DEC and v have a small and negative skewness statistics (i.e., leptokurtic), suggesting the presence of a left tail. However, the kurtosis statistics of MB and v revealed a low peaked and thin tail, while DEC with a kurtosis test statistics of greater than three suggests that the series is moderately peaked and moderately tailed (mesokurtic). Meanwhile, the Jarque-Bera (JB) statistic which measures normality of the distribution using both the skewness and kurtosis statistics show that we cannot reject the null hypothesis for normality for MB, DEC and v variables.

*Econometric Evaluation of the Impact of E-Banking on Monetary Policy*

**Table 14.** *The Regression Results of E-Banking on Monetary Variables in Nigeria*

| **Explanatory Variables** | **Dependent variables Parameter [Standard Error]** | | |
|---|---|---|---|
| | ***$MS_2$*** | ***m*** | ***v*** |
| *c* | –4.302321 [3.050598] | 9.713736 [1.291178] | 0.123837 [0.410674] |
| *$MS_2$(–1)* | 0.141114 [0.172676] | | |
| *m(–1)* | | 0.104378 [0.132601] | |
| *v(– 1)* | | | 0.683188 [0258723] |
| *MB* | 0.615473 [0.150775] | | |
| *MB(– 1)* | 0.740527 [0.161196] | | |
| *DEC* | –0.222650 [0.1100150] | –1.483763 [0.541683] | –0.460546 [0.170459] |
| *MP* | 0.015633 [0.004855] | 0.070851 [0.029734] | 0.004600 [0.002148] |
| *INTB* | 0.032723 [0.012268] | 0.223388 [0.050645] | –0.065886 [0.020199] |
| *POS* | –0.037017 [0.008617] | –0.156589 [0.043073] | 0.028587 [0.012158] |
| S.E. of Regression | 0.602171 | 0.424851 | 0.505179 |
| F–statistics | 72.65891 | 88.73931 | 4.796131 |
| Adjusted $R^2$ | 0.951413 | 0.728958 | 0.642623 |
| D.W. statistics | 1.861618 | 2.427820 | 2.151574 |

*Source:* Authors' computation using EVIEWS .

The unit root test in Table 12 shows that the various are a mixture of I (0) and I (1). In view of this, we employed the Autoregressive Distributed lag (ARDL) model for the estimation. The result of the ARDL is presented in Table 14. In order to confirm and validate the statistical properties of the model, we carried out a diagnostics test to ascertain the stability of our model and the results is shown in Table 15. The result of diagnostic tests of: (i) The Breusch-Godfrey LM test (BG) which is the appropriate autocorrelation test when a lagged dependent variable is a regressor, (ii) The Breusch-Pagan-Godfrey (BPG) for Autoregressive Conditional Heteroskedasticity (ARCH) LM test, and (iii) Ramsey's test for specification errors (RESET) (iv) Jarque-Bera test for normality as presented in Table 15 show that our model is stable was conducted to regression:

**Table 15.** *Summary of Diagnostics Result on E-Banking on Monetary in Nigeria*

| **Diagnostic Tests** | **F-Statistic (p-values)** | | |
|---|---|---|---|
| BG LM test | 2.234404 (0.2546) | 1.075939 (0.3774) | 0.807764 (0.4791) |
| BPG ARCH LM test | 1.101893 (0.4965) | 0.520830 (0.8195) | 0.940795 (05318) |
| Ramsey Reset test | 2.069562 (0.2237) | 0.865957 (0.3720) | 0.942355 (0.624267) |
| J–B normality test | 1.499651 (0.472449) | 2.258945 (0.323204) | 1.423473 (0.2633) |

*Source:* Authors' computation using EVIEWS .

*Synopsis of Econometric Assessment*

The impact of the various ARDL results and their diagnostic statistics as presented in Tables 14 and 15 are summarized thus:

i. The F-Statistics shows that the three linear models are statistically significant.
ii. The changes in e-banking (DEC) have a positive and significant effect on money supply. This implies that it will affect the liquidity management of the economy. This impact can either be negative or positive based on the position of the central bank;
iii. The increased use of e–banking has a positive and significant effect on money multiplier (*m*) and income velocity of money (*v*). This means that the rate of circulation will increase money supply, which will in turn have an implication for money management, either positively or negatively, depending on the central bank's stance.
iv. The results of the diagnostic tests indicate that the three ARDL regressions were well specified.
v. Also, in about two-thirds of the time, the explanatory variables explain the regressand (MS2, m and v) by exactly 60.2, 42.5 and 50.5 percents respectively.
vi. In addition, the goodness of fit ($R^2$) indicates that the models fit the data well.

## Conclusions

In the past decade, the sporadic advancement in information technology, coupled with the spread of e-banking, would weaken the Central Bank's control over the supply of bank reserves using the e-banking platform. The Central Bank's role as the monopoly issuer of money will be undermined by the emergence of non-bank competitors in the provision of payment services. As a result, CBN may be reduced to signaling their policy. Also, the future of e-banking is dependent on its growth, and increased technological advancements that would increase the security of this new instrument. In fact, since it has become widely accepted and used in Nigeria, it will directly impact the Central Bank's control of monetary policy, unless the Central Bank includes it in its measurement of monetary aggregates and regulates its growth as well as usage. There is no doubt that, with the spread of electronic trade, the CBN will have to shoulder new responsibilities because of its legal responsibility to monopolize the issuing of money. The most prominent of these responsibilities is: standing up to the results of the universality of e–payment systems and following it up with the development of e-banking products and services.

We therefore recommend that since the impact of e-banking on monetary policy depends solely on how fast it will spread and the extent to which it will substitute for cash, it is vital that CBN should consider taking steps to compensate the resulting decrease in their balance sheet. Furthermore, CBN must have to impose special obligations with the money reserve on the e-banking issuer in case of any large increase in e-banking activity that would affect the monetary policy at the end. The government, at all levels, must keep the rate of prices stable and with this condition, e-banking will be equal to other forms of money which it maintains by apportioning a percentage as a reserve ratio to the Central Bank. Similarly, if e-banking spreads moderately, the decrease in the seigniorage income and thus the decrease in the balance sheet of CBN will be limited. Hence, it must include e-banking in monetary aggregates that the spread of e-banking may lead to a change in the velocity of money.

## References

Al-Laham M, Abdallat N, Al-Tarawneh H (2009) Development of the electronic money and its impact on the central bank role and monetary policy. *Issues in Informing Science and Information Technology* 6: 339–349.

Arvidsson N, Jonsson S, Snickare LK (2019) The transaction-relationship paradox. *Managerial Finance* 45(9): 1253–1271.

Audu NP (2011) The dynamics of e-banking in the South-South region of Nigeria. *International Business Management* 5(6): 388–397.

Bamidele A (2005) The imperatives of e-banking for monetary policy in Nigeria. *CBN Economic and Financial Review* 43(1): 65–79.

Bergman M, Guibourg G, Segendorf BL (2007) The costs of paying-private and social costs of cash and card payments. In *Riksbank Research Paper Series*, 212.

CBN (2002) *Survey on electronic-banking in Nigeria*. Abuja: CBN Press.

CBN (2003) *Statistical bulletin.* Abuja: CBN Press.
CBN (2004) *Annual report and statement of account.* Abuja: CBN Press.
CBN (2017a) *Annual report and statement of account.* Abuja: CBN Press.
CBN (2017b) *Statistical bulletin.* Abuja: CBN Press.
CBN (2019) *Statistical bulletin.* Abuja: CBN Press.
Chukwudi D, Amah E (2018) Development of e-banking, its benefits and challenges in the Nigerian banking industry. *ASPL International Journal of Management Sciences* 7(2): 1–7.
David S, Glyn P (1996) *A history of money from ancient times to the present day.* London: University of Wales Press.
De Grauwe P, Costa Storti C (2005) *Is monetary policy in the Eurozone less effective than in the US?* CESifo Working Paper No. 1606, November.
ECB (2000) *Issues arising from the emerging of electronic money*. ECB Monthly Bulletin, November.
Foroughi B, Iranmanesh M, Hyun SS (2019) Understanding the determinants of mobile banking continuance usage intention. *Journal of Enterprise Information Management* 32(6): 1015–1033.
Giovanis A, Athanasopoulou P, Assimakopoulos C, Sarmaniotis C (2019) Adoption of mobile banking services. *International Journal of Bank Marketing* 37(5): 165–1189.
Imiefoh P (2012) Towards effective implementation of electronic banking in Nigeria. *African Research Review* 6(2): 290–300.
Kent C, Ossolinski C, Willard L (2007) The rise of household indebtedness. In C Kent, J Lawson (eds.), *The Structure and Resilience of the Financial System,* 123–163. Sydney: Reserve Bank of Austria.
Khan F, Chowdhury MSA, Haque A, Akter S, Ahsan SMH (2021) E-banking adoption in Bangladesh; present status and customer satisfaction: an evaluation. *Global Journal of Management and Business Research* 21(1–A).
Kwiatkowski D, Phillips PCB, Schmidt P, Shin Y (1992) Testing the null hypothesis of stationarity against the alternative of a unit root: how sure are we that economic time series have a unit root? *Journal of Econometrics* 54(1–3): 159–178.
Martin NC, Igboanugo D, Freeman E, Oddih CS, Sajjad M, Sajjad M (2018) A theoretical Insight on e-banking (internet banking) framework in developing countries. In *Proceedings of the International Conference on e-Learning, e-Business, Enterprise Information Systems, and e-Government (EEE)*, 68–75. The Steering Committee of The World Congress in Computer Science, Computer Engineering and Applied Computing (WorldComp).
Migap JP (2011) Is monetary policy the best instrument for inflation targeting in the Nigerian economy? *Journal of Business* 3: 34–45.
Miller SM (2000) *Monetary policy delegation, contract costs, and contract targets*. Working Paper 2000-2001. Connecticut, USA: University of Connecticut.
Moorthy K, Chun T'ing L, Chea Yee K, Wen Huey A, Joe In L, Chyi Feng P, et al. (2020) What drives the adoption of mobile payment? A Malaysian perspective. *International Journal of Finance and Economics* 25(3): 349–364.
Odior ESO, Banuso FB (2012) Cashless banking in Nigeria: challenges, benefits and policy implications. *European Scientific Journal*.
Opara CB, Ayopoo O, Darego WM (2010) Analysis of impact of technology on relationship marketing orientation and bank performance. *European Journal of Scientific Research* 45(3): 291–300.
Ovia J (2004) E-money: instruments and techniques. Paper presented at the *9th CBN Monetary Policy Forum Held at International Conference Centre*. Abuja, May 6th.

Pandian SH, Duraisingh V (2021) The cashless society: consumer perception of payment methods. *PalArch's Journal of Archaeology of Egypt/Egyptology* 18(7): 856–864.

Pesaran MH, Shin Y (1999) An autoregressive distributed lag modelling approach to cointegration analysis. Paper Presented at *Econometrics and Economics Theory in the 20th Century: The Ragnar Frisch Centennial Symposium*. Cambridge: Cambridge University Press.

Pesaran MH, Shin Y, Smith R (2001) Bounds testing approaches to the analysis of level relationships. *Journal of Applied Econometrics* 16(3): 289–326.

Phillips PC, Hansen BE (1990) Statistical inference in instrumental variables regression with I (1) processes. *The Review of Economic Studies* 57(1): 99–125.

Rahn RW (2000) *On the future of electronic payments*. CATO Congressional Testimony. CATO Institute.

Reynolds G (2013) Electronic money and monetary policy. In *Southwestern Economic Proceedings*.

Salawu RO, Salawu MK (2007) The emergence of internet banking in Nigeria: an appraisal. *Information Technology Journal* 6(4): 490–496.

Sandhu S, Arora S (2020) Customers' usage behaviour of e-banking services: interplay of electronic banking and traditional banking. *International Journal of Finance & Economics* (Oct).

Sciglimpaglia D, Ely D (2002, January) Internet banking: a customer-centric perspective. In *Proceedings of the 35th Annual Hawaii International Conference on System Sciences*, 2420–2429.

Segendorf B, Jansson T (2012a) Cards or cash. How should we pay? *Sveriges Riksbank Economic Review* 3(Oct): 43–57.

Segendorf B, Jansson T (2012b) *The cost of consumer payments in Sweden* (No. 262). Sveriges Riksbank Working Paper Series.

Singhraul BP, Garwal YS (2018) Cashless economy challenges and opportunities in India. *Pacific Business Review International* 10(9): 54–63.

Tak S (2002) *A study on the effects of the development of e-money on monetary policy in Korea*. Economic Papers, Bank of Korea.

Tolulope AO, Ajilore T (2013) Inflation targeting monetary policy rule in Nigeria: estimates of the policy reaction function. *International Journal of Economics and Finance 5*(7): 139–144.

Wafa ABM (2003) E-money markets: opportunities, threats and horizons. *Contemporary Egypt Journal* 471/472: 123–145.

*Athens Journal of Technology and Engineering - Volume 8, Issue 3, September 2021 – Pages 259-282*

# A Software Model for Parameters Affecting the Dimensions of Reinforced Concrete Prefabricated Facade Elements

*By Mustafa Tosun[*] & Enes Yasa[±]*

*In this study, a model software of a computer program related to determining dimensional behavior, which will contribute to the multi-layered units used on the facade of industrial buildings to be standardized, has been prepared. By means of this model software, the factors determining the width (A), the height (h) and the section (d) of the units of a building facade, could be evaluated. These factors, at the same time, from the dimensions of building facade units providing "thermal insulation, sound insulation statically behavior and coordination dimension of facade unit." In the program (named as MT2 Prefabrike), these four factors could be evaluated by providing the optimization in sequence and within themselves. Thus, by developing a new method of approach in the standardizing of facade units, apart from the visible characteristics of the units, the idea of standardizing the performance and behavior expected from the units, are put forward. In the model program formed with this idea, before producing of the facade units, the optimization is to be provided by analyzing the factors which are effective in giving dimension to the units, in abstract condition (computerized).*

**Keywords:** *a model software, building facade unit, prefabrication, thermal and sound ınsulation, static behavior analysis, the facades of ındustrial buildings*

## Introduction

There are many studies on building modeling. They bring all the stages of construction closer to a predictable system. Building information modeling (BIM) is one of the most promising recent developments in the architecture, engineering, and construction (AEC) industry. With BIM technology, an accurate virtual model of a building is digitally constructed. This model, known as a building information model, can be used for planning, design, construction, and operation of a facility. It helps architects, engineers, and constructors visualize what is to be built in a simulated environment to identify any potential design, construction, or operational issues. BIM represents a new paradigm within AEC— one that encourages integration of the roles of all stakeholders on a project. The architecture, engineering, and construction (AEC) industry has long sought out techniques to decrease project cost, increase productivity and quality, and reduce project delivery time. Building information modeling (BIM) offers the potential to achieve these objectives (Azhar et al. 2008). When completed, the building

[*]Associate Professor, Konya Technical University, Turkey.
[±]Associate Professor, Istanbul University, Turkey.

information model contains precise geometry and relevant data needed to support the design, procurement, fabrication, and construction activities required to realize the building (Eastman et al. 2008).

The future of BIM is both exciting and challenging. It is hoped that the increased use of BIM will enhance collaboration and reduce fragmentation in the AEC industry and will eventually lead to improved performance and reduced project costs (Azhar 2011).

This study conducts analyses in order to determine (static) behaviors in terms of thermal, sound and conveying features expected from an element while forming the element cross-section in order to make use of "Coordination Dimensions" in defining the dimensions of reinforced concrete pre-fabricated facade elements which are used in industrial structures' facades (Wang-Dong et al. 2011). A computer software was created in order to conduct these analyses. For this software, Delphi was used. Delphi is a visual software development tool which was developed by Borland. It is Pascal-based and object-oriented (Lantim 1998). In the study, the "MT2 Prefabrike" program was prepared for dimensional analysis.

With the "MT2 Prefabrike" analysis program, analyses can be done on "thermal insulation, sound insulation, sizing and conveying properties (static)" for non-conveying reinforced concrete pre-fabricated and multi-layered facade elements used in Industrial structures' facades. For this purpose in this program, a "Program Flow Diagram" was prepared which indicates the relationship and transitions among data (Figure 1). This developed model works with the system outlined in the flowchart in Figure 1 and reaches the result. The model is definitively completed when all the stages in Figure 1 are concluded in accordance with the calculations.

**Figure 1.** *Flow Diagram for "MT2 Prefabrike" Analysis Program*

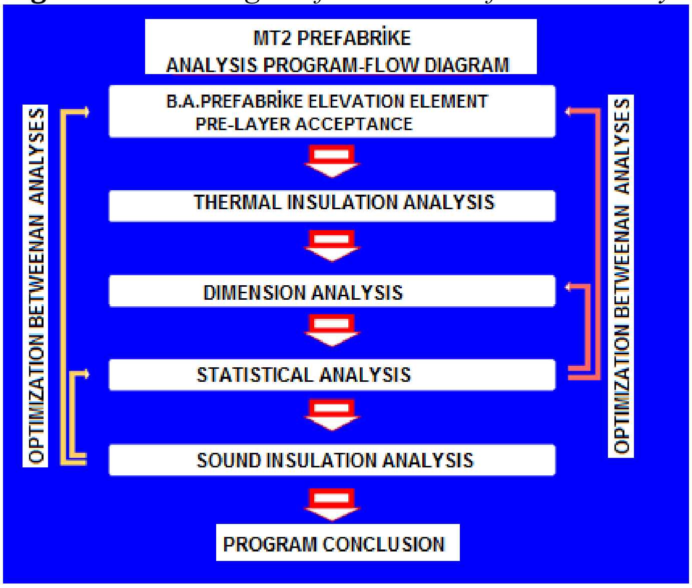

## Model Introduction and Application of Model

The limitations which define the dimensions of reinforced concrete pre-fabricated industrial structures should be regarded as data intended to standardize the element (Cansun 1989). The element has three dimensions, namely horizontal dimension (width), vertical dimension (height) and cross-section (Christiane et al. 2018).

### *Factors Which Affect the Cross-Section Size of Facade Elements*

In the "MT2 Prefabrike" program the analyses (thermal insulation, sizing, static and sound insulation) were represented in separate menus and these were optimized in their interactions among each other.

#### Heat Insulation of Facade Elements

Heat transmission coefficient in construction elements is expressed with the "U" symbol and its value is explained as "$W/M^2k$". It is expressed in "watt" units (Joule/sec). It describes air which transitions from a 1 $m^2$ surface to another surface under 10 $C^0$ temperature (TSE 825 1999, Chudley 1994).

For this reason, "MT2 Prefabrike" was prepared in line with the "thermal insulation requirements for buildings" directive which was published on 18 December 2013. Separating Turkey into five zones in terms of thermal insulation applications (Table 1), the directive prescribes that structures be insulated in accordance with environmental conditions and properties, and indicated of such insulation by drawing up a heat insulation project (TSE 825. 1999).

**Table 1.** *Heat Transmission Coefficients (U) of Facade Element According to Zones (Eriç 1994)*

| | $U_D$ (W/m²K) | $U_T$ (W/m²K) | $U_t$ (W/m²K) | $U_P$ (W/m²K) |
|---|---|---|---|---|
| Region-I | 0.66 | 0.43 | 0.66 | 1.8 |
| Region-II | 0.57 | 0.38 | 0.57 | 1.8 |
| Region-III | 0.48 | 0.28 | 0.43 | 1.8 |
| Region-IV | 0.38 | 0.23 | 0.38 | 1.8 |
| Region-V | 0.36 | 0.21 | 0.36 | 1.8 |

#### Example Solution Using the "MT2 Prefabrike" Software-Forming Facade Element Layers

The starting point for formation of the layers to be used in the whole analysis of the reinforced concrete pre-fabricated element is a selection in the main "thermal analysis" menu in the program. After this selection, an array of windows will be displayed on the screen. In the first window, the number of layers, which form the cross-section of the element, is entered (Figure 2). We can form a layer cross-section example like below, using values for material, thickness and related heat conductivities (Table 2).

**Figure 2.** *Layer Quantity Window for the Element in the "MT2 Prefabrike" Program*

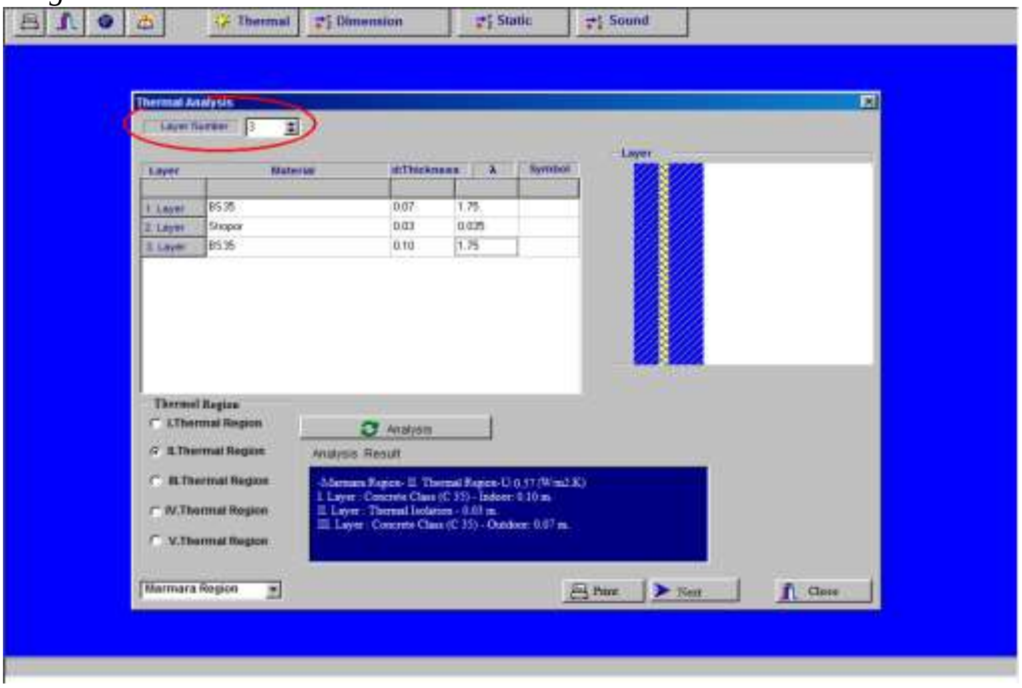


**Table 2.** *Sample Cross-Section Data Used in the Program*

| Layer | Material | Heat Conduc.(λ) | Thickness(d) |
|---|---|---|---|
| 1st Layer ................... | C(35) concrete ..... …….. | 1.75 kcal/m²hC° ........................... | 0.07 m. |
| 2nd Layer ................ | Thermal İnsulation .......... | 0.035 kcal/m²hC° ........... ................ | 0.03 m. |
| 3rd Layer ...................... | C(35) concrete ……..... | 1.75 kcal/m²hC° ........................... | 0.10 m. |

**Figure 3.** *Sample Cross-Section of the Element, to be Analyzed in the "MT2 Prefabrike" Program*

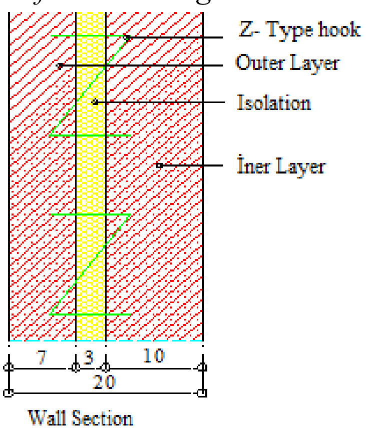

Together with the reinforced concrete pre-fabricated facade element's layers, the "Heat Conductivity Coefficient (λ)" will be automatically given in selection of each material from the material window, as seen in Figure 1. Afterwards, material thickness (m.) must be entered. Formation of the facade element's layers will also provide a representation for each material in the symbol window. Therefore the material can be recognized in the analyses; wall section layer has been given in Figure 3.

Thermal Zones

The program's menus feature a "thermal zone" parameter. In order to determine the thermal zone where the industrial structure is to be constructed, the only action required is to select the name of construction zone from the "Thermal Zone" parameter. The program will take this zone as the base and then show the "Heat Transmission Resistance (R=1/λ)'' m$^2$hC°/kcal" value for the zone, of which value can be used in inquiries.

Thermal Analysis

The analysis on expected thermal behavior from the facade element of reinforced concrete pre-fabricated industrial structures, that is, determining whether the element has suitable insulation according to selected thermal zone, can be conducted via pressing the "Analysis" button (Figure 2). The equation uses the below formula:

$$Ro \;= 1 / \lambda = (d1/\lambda) + (d2 / \lambda) + (d3 / \lambda) \qquad (1)$$

**Figure 4.** *Thermal Insulation Calculation Results in the "MT2 Prefabricated" Program*

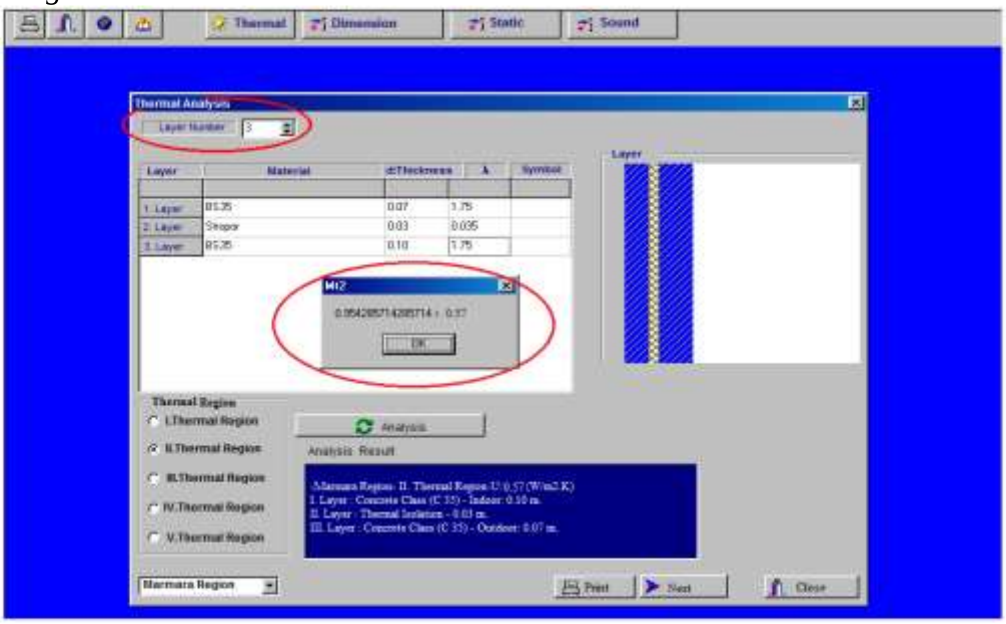

Analysis Results

This section of the program is shown in the menu called "Analysis Results" where all the results are displayed and the print outputs can be obtained. Here are the names of the materials that make up the layer, their thickness, the heat zone and the information that evaluates the suitability of the result. The results of the analysis are shown in Figure 4.

In the MT2 evaluation program, necessary feedbacks can be made by considering a dynamic structure for the case where appropriate values for the building site Heat Zone do not come out. The program has a "print" command window in which the analysis results can be printed. You can then proceed to the sizing analysis with the "Next" command button or you can exit the program with the "Close" command button.

*Factors Which Affect the Height of Facade Elements*

In reinforced concrete pre-fabricated industrial structures, the height of facade elements can be varied according to the structure's height and the element's position in the facade. For this reason, factors such as the height of the industrial structure, facade design and transport of the elements affect the outcome.

*Factors Which Affect the Width of Facade Elements*

The factors which affect the widths of reinforced concrete prefabricated industrial structures also include the factors that are to be evaluated in the computer program. These are factors such as the opening where the element will be positioned, joint width and joint tolerances, number of elements in the opening and whether to position the elements on the front or behind carriers. In facade element design, one of the most important factors which affect element width is the element's design alternatives. The design of the facade element is also directly related to the design of the building facade. Named "Modular Coordination", the system was derived from the Latin word "Modulus" (small scale) (Figure 5) (Escrig et al. 1996).

Artificial Neural Networks are systems made up of artificial nerve cells that imitate problem solving skills of biological nerve cells by communication and that only living things possess (Montali et al. 2017). These networks discover the connections among attributes inside the samples and can make it possible to classify a sample that they have never encountered before. The discovery process of connections among previous samples is called the training of artificial neural networks. The classification plays an important role for the accuracy of results.

However, when an appropriate solution is found for network classification during the process, it can be possible to focus on this solution. At this point, the artificial neural network algorithm is optimized with the help of the firefly algorithm, which is a powerful and fast optimization algorithm, in order to decrease this sticking possibility (Montali et al. 2017).

**Figure 5.** *Basic Module (M=10)*

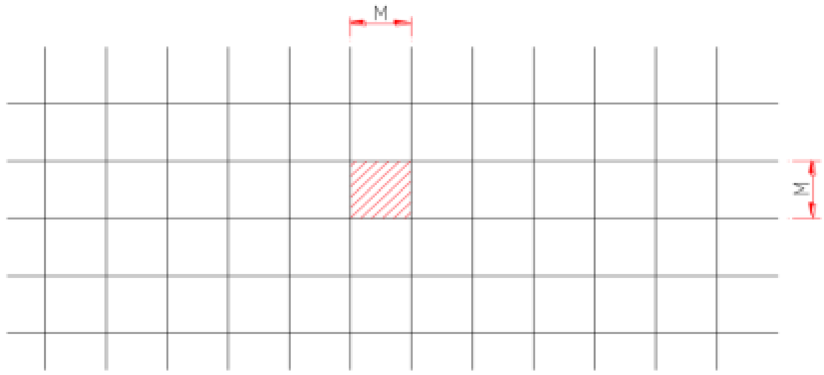


Reinforced concrete pre-fabricated facade elements are placed in (n) quantity into the shaft opening of the carrier system, therefore entering this structure. In the dimensional coordination, shaft opening (D) is obtained with multiple repetitions (n) of the basic module (M); (nxM) (Figure 5). Facade elements which are in relation to another, that is, which enter dimensional coordination, should be within coordination lines and their coordination dimensions should also be equal (Figure 6). It is called the "position line" which determines the location of the facade elements in dimensional coordination. We can express the position of the facade element in dimensional coordination in the following terms:

D = n x M Shaft opening (cm)
n = Basic module coefficient (quantity)
M=Basic Module (cm). Can be M, 2M, 3M, or 1.5M, 0.75M, 0.5M, etc. times of the basic module (Şener 1990).

The reinforced concrete prefabricated facade elements, which are used in industrial structures' facades, fit into the modular coordination and are placed into the shaft opening obtained. In order to make the facade element in a computer environment suitable to the needs of decision-makers, it is necessary to design in the direction of modular coordination principles. Elements are sized using M=10 cm, which is the basic module.

**Figure 6.** *The Position of Prefabricated Facade Element on the Modular Grid*

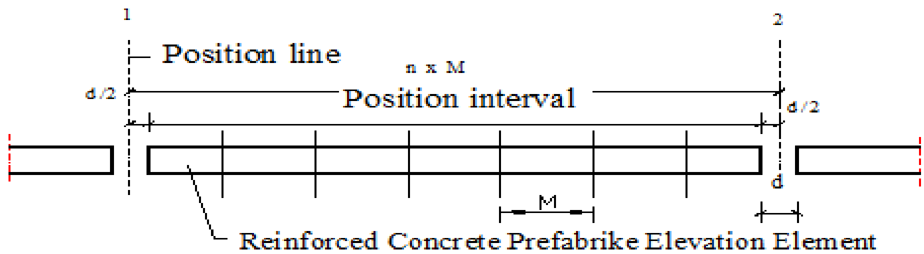


In order to be able to decide how many (n) multi-layered elements to produce and what the mould size, that is the net width (A), would be in reinforced concrete pre-fabricated, the element's position in the facade within the element design has to be determined. For this, two design alternatives, which are fundamental to the MT2 Prefabricated Computer program and affect the determination of the widest dimension of the element, are taken into consideration.

Design of Prefabricated Facade Elements Between Columns

If reinforced concrete prefabricated facade elements are designed to be between load-bearing columns (Figures 7 and 8) below equation can be used, depending on the distance between columns, in order to calculate the net width of the element (A):

$$A = \frac{\mathrm{D} - [\left(\frac{\mathrm{b1}}{2}\right) + \left(\frac{\mathrm{b2}}{2}\right) + (\mathrm{n}+1)\mathrm{xd}]}{\mathrm{n}} \quad (2)$$

d=Joint width
D=Shaft opening measurement of load-bearing columns (cm)
A=Pre-fabricated facade element size
n=Number of elements
b=Column size

**Figure 7.** *Designing Prefabricated Facade Elements Between Columns*

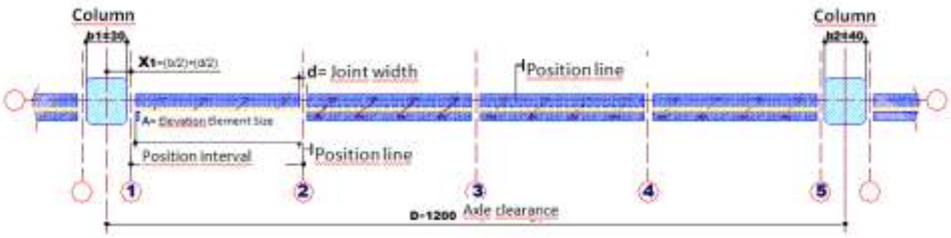


**Figure 8.** *Positioning Prefabricated Concrete Facade Element Between Columns*

In this program, the net element size (A) can be recalculated by changing the number of facade elements (n). The element size will then be calculated as “Facade Element Net Size” A=130.6 in the top right corner of the program. The program contains the “Analysis Results” section which shows all the data of the facade element and the net element size (A) according to this data. The program also has a graphical representation of the facade design of the facade element, with all the values written on the element (Figure 8).

When the process of finding the maximum size (A) of the program element is completed, the “Next” button can be pressed to move to the next step, or the analysis results can be printed out with the “Print” command. In addition, you can return to thermal analysis with the “Back” command for optimization at element size. You can use the “Close” message to exit the program.

*Designing Reinforced Concrete Prefabricated Facade Elements on the Front of the Columns*

If reinforced concrete pre-fabricated facade elements are designed to be on the front of load-bearing columns (Figure 9), below equation can be used, depending on the distance between columns, in order to calculate the net width of the element (A):

$$A = \frac{\mathrm{D-(nxd)}}{\mathrm{n}} \tag{3}$$

d=Joint width
D=Coordination size (Shaft opening size)
A=Pre-fabricated facade element size
n=Number of elements

**Figure 9.** *Designing Reinforced Concrete Prefabricated Facade Elements on the Front of the Columns*

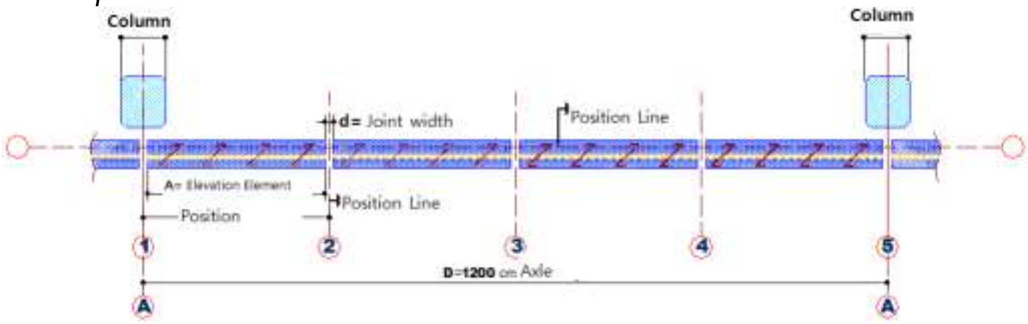


In this part of the program, an assessment can be made to determine the width dimension of the element directly involved in the production, lifting, transport, assembly processes of the front elements used in the reinforced concrete prefabricated industry structures and tool capacities.

In this part of the program, an assessment can be made to determine the width dimension of the element directly involved in the production, lifting, transport, assembly processes of the front elements used in the reinforced concrete prefabricated industry structures and tool capacities.

Analysis Results

The net element size (A) found at the end of the sizing analysis of reinforced concrete prefabricated multi-layer elements used in the facades of industrial structures will be visually included in the analysis results of the program. The "Analyze" window will show the facade design, the visual results and the results and evaluations of all the calculations. These data are shaft distance, coordination size, column width (b), joint tolerance width and calculated net element size (A) to be obtained from the mould.

*Load-Bearing (Static Structure) of Facade Elements*

From the production stage, a facade element needs a cross-section fitting that resists loads such as lifting, transport and wind effects. In order to resist these loads, the carrier inner-layer forming the element, the insulating material between and the outer layer move together.

This connection, which forms the cross section of the facade element, must form a rigid structure against the above static forces. In this section, the inner load-bearing layer of the element will be dealt with, which counteracts the static factors affecting the cross-sectional dimension of the element, the lifting forces, the loads that occur during transport and the wind effects.

Lifting Control

The position where the reinforced concrete pre-fabricated facade elements, which are used in industrial structures' facades, receive the most deflection risk, occurs at the moment when the element has to be lifted.

Facade elements are lifted from their hooks and a substantial load occurs in at this moment. This load delivers an equal momentum to both ends of the facade element, thanks to a balanced positioning of lifting hooks (Figure 10).

**Figure 10.** *Cross-Section and Lifting Points of Prefabricated Concrete Facade Elements*

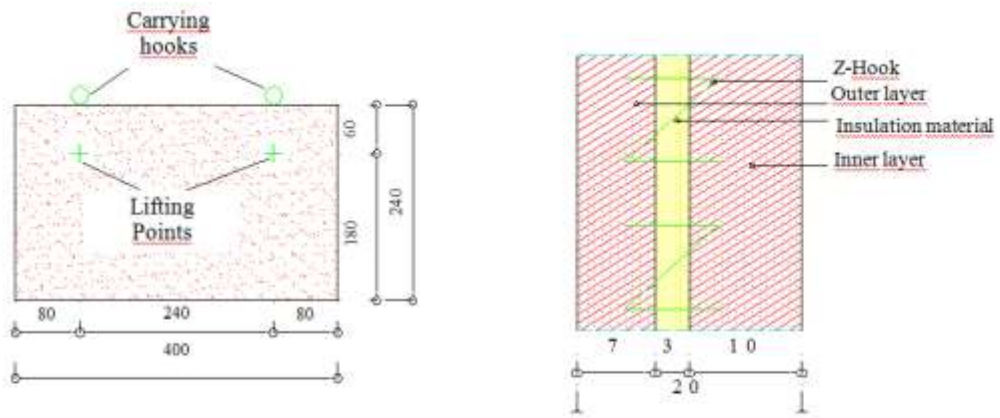

Equations 4, 5 or 6 can be used to calculate the lifting force received by the element (Figure 11).

σ=Tensile Stress
$\sigma = M/W$ (Kg/cm$^2$) (4)

Where:
$F_{ck}$=300 kg/cm$^2$ $f_{ct}$=150 kg/cm$^2$

$-M = (q \times l^2)/2$ (5)

$W = (L \times D^2)/6$ (6)

l=Abutment distance (cm)
L=Element width (cm)
D=Element cross-section (cm)
q=Spread load (t/m)

**Figure 11.** *Lifting Moments in Prefabricated Concrete Facade Elements*

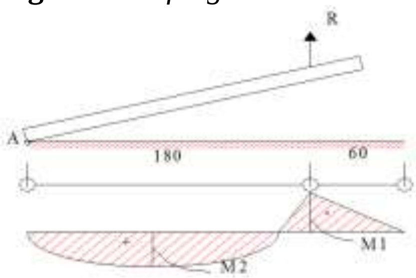


With the tensile stress calculation there will be an analysis of whether or not cracks will occur during lifting. This method can also be used in the computer program and the tensile strength can be calculated using equation 7:

$$[\sigma < 0.9 \sqrt{fci}\,] < 11.02 \text{ (Kg/ cm}^2)] \quad (7)$$

Where:
$0.9 \sqrt{fci}$=Maximum tensile stress for prestressed joint sections

fci=Pressure value on day "I" (kg/cm$^2$)
i=The age of the concrete at the moment of removal from the mold (Bakır 1990).

Bearing Control

After the production of the reinforced concrete pre-fabricated multi-layer facade elements used on the facades of industrial buildings, static calculations of the hooks must be made in order to be able to meet the loads coming to the transport hooks at the moment of transport to the construction site. This calculation is carried out as below for the "R" hooks seen in Figure 12 (Bakır 1990).

**Figure 12.** *Load on Bearing Hooks of Prefabricated Concrete Facade Elements*

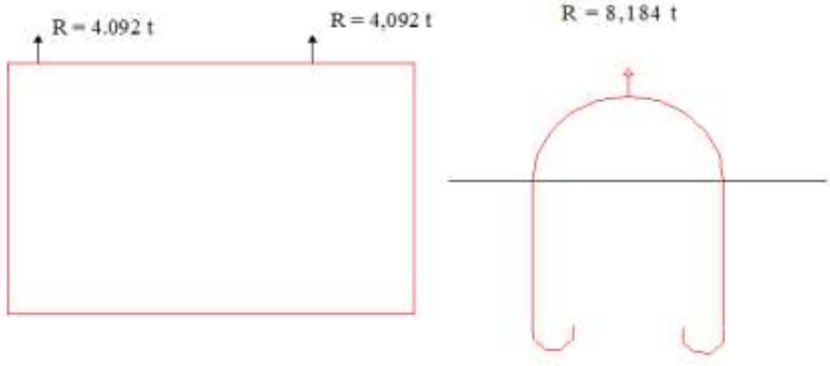


R=G/tons
Static load coeff.=4
R total= 4x R tons
R=Load on Bearing Hooks (tons)
G=Facade element weight (tons)

Wind Control

One of the problems facade elements can encounter after installation are Wind Impacts. The load resulting from Wind Impacts should be taken into account in the sizing analysis, although it is very small relative to the effect at the time of lifting (Figure 13).

**Figure 13.** *Wind Load on Prefabricated Concrete Facade Elements*

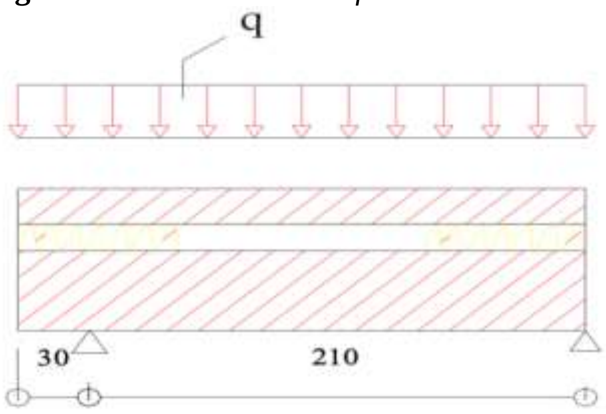


Calculations for the Tie Bars

In formation of cross-sections for Prefabricated Concrete Facade elements, tie bars are used between the outer layer and the inner layer. When these bars are placed, it is important that the cross-section is sufficient. Also, care must be taken to ensure that where the steel rods are placed have sufficient strength to support the building envelopes during lifting of the element. The highest pulling force on the tie rods will occur when the element is being lifted from the mould.

In “MT2 Prefabrike” static analysis program menu, at the very top, the element's total weight coming from its cross-section will be shown in two windows; the building envelope weight (Outer layer + Inner layer), and insulation weight.

Next there will be the window containing fck. and fct. values, which vary according to concrete class (C-35) (Figure 14). These values are decided upon during the "Thermal Analysis" stage by selecting concrete class during formation of building envelope layers. This is because all data of the program work in integration with one another.

Lifting Control Analysis

An analysis is made on the forces the element gets subjected to while it is lifted from the mould. This analysis is then shown in a window in the program menu. To do this, simply select the "Calculate" command in the lifting control analysis. This is because all data required for Lifting Control Analysis is also used commonly by "Thermal Analysis" and "Sizing Analysis".

**Figure 14.** *Data Connected to Concrete Class Used in Static Analysis*

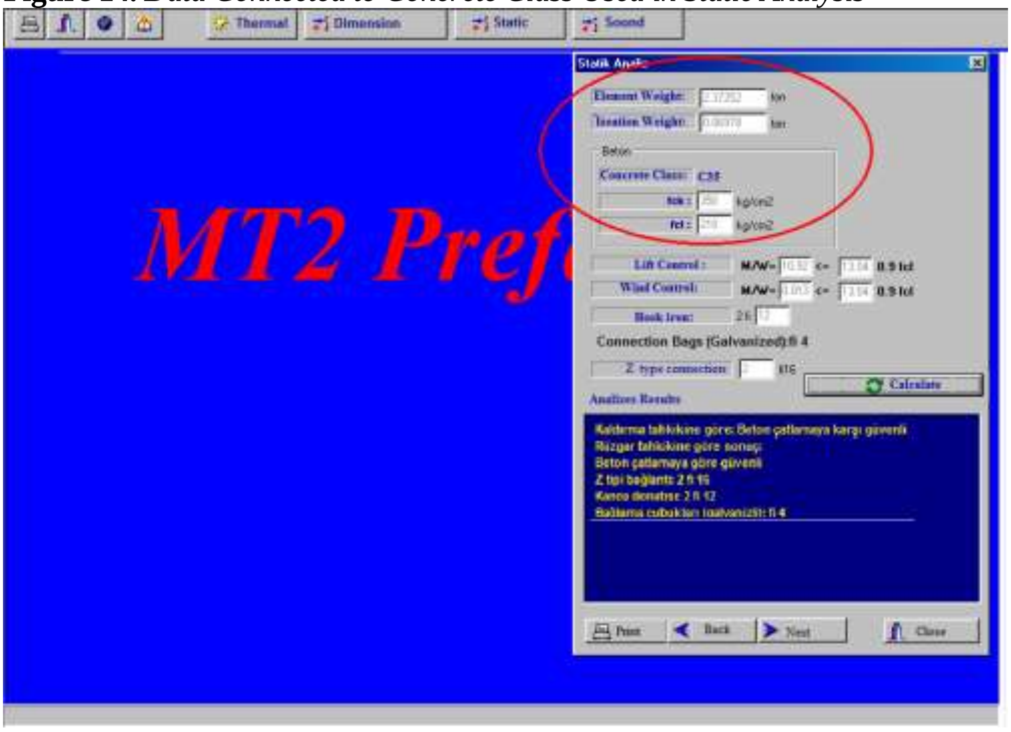


Bearing Control Analysis

In bearing control analysis, the hook fitting, which is expected to lift the element during the bearing action, will be calculated. The result will then be used to give the user the quantity of hook fitting and fitting diameter in the program menu. The result will be displayed in the "Hook Fitting" window. Since all values are taken from "Temperature and Sizing" analyses, here it will suffice to just use the "Calculate" command button.

Wind Control Analysis

In order to determine reinforced concrete prefabricated facade elements' behavior against wind loads, calculation results are displayed in the "Wind Control" window. If wind control calculations yield a result that is plausible against given dimensions, the program will not display any error messages. If M/W<0.9 fci, this means that a plausible size is selected and there will be no need to revise the size in the program.

Analysing Tie Bars

Diameters and quantity of the tie bars, which provide connection between inner and outer building envelope of reinforced concrete prefabricated facade elements, are displayed in a window in the program.

Analysis Results

The inquiries made with the "Static Analysis" of reinforced concrete prefabricated multi-layered facade elements used in industrial structures' facades are displayed in the "Analysis Results" window in the program. Here, the evaluation is based on whether any cracks will occur, using lifting and wind analyses. The number and diameter of hook fittings and binding reinforcements are also displayed in the Analysis window. If there is a negative result such as cracking of the concrete in evaluation, changes can be made to the size parameters of the element and the operation can be continued until a positive result is obtained. These parameters are: concrete class and the quantity of hook fittings—if cracking of the facade element cannot be prevented with these parameters, the user should go back to the sizing analysis and make changes in element quantity (n), element height (h) parameters. Then the statistical analysis is complete. Afterwards, pressing the "Next" command button in the right bottom corner for further analyses or the current analysis can be printed out using the "Print" command.

*Sound Insulation of Facade Elements*

The term "sound" is used for vibrations in the 16-20,000 Hz frequency range which the human ear can hear. ISO-acknowledged values are 20-20,000 Hz (ISO 1990).The National Academy of Sciences- National Research Council, Committee on Hearing, Bioacoustic Biomechanics (CHABA) determined sound emitting threshold for soundwave frequency zone as 20-12,000 Hz (Young 1988).

Sound insulation materials that form a cross-section of the "Reinforced Concrete Prefabricated" multi-layer facade elements provide insulation at different levels. In order to be able to make this decision, optimum decisions have to be given among some criteria. The most important of these is the level of sound proofing desired. If people work within the industry structure, the following levels of continuous, maximum volume will be needed depending on the hours of operation.

06.00 – 22.00 < 60 dB

22.00 – 06.00 < 50 dB (Young 1988).

For ease of understanding the effects of sound levels, the sound level (dB) of the sound sources given in Table 2 should be known. Table 3 gives acceptable background sound levels for human activities (Beranek and Ver 1992). In reinforced concrete prefabricated industry structures, the frequency with the largest amplitude, produced by two layers forming the cross-section by pressing against the insulation layer between, is called "natural frequency" (fr) (Simultaneous Vibration Frequency). The value of natural frequency depends on the zone weights of the two layers and the dynamic rigidity (s') of the insulation layer between and fr can be calculated using the below equation:

$$fr = 500 \sqrt{s'} \, [ (1/M1) + (1/M^2)] \text{ (Hz)} \quad (8)$$

Where:

fr= Natural frequency (Sim. Vib. Freq.) (Hz),
s'=Insulation layer dynamic rigidity ($kp/cm^3$)
M1 and M2=Zone weights of outer and inner layers ($kg/m^2$) (Table 6).
Dynamic Rigidity (s') of the insulation layer in the equation is called the elasticity of the insulation layer placed between the layers and used for sound damping.
s'=E/a ($kp/cm^3$)

Where:

E=Dynamic elasticity module ($kg/cm^2$) (Table 6)
a=Thickness of intermediate layer or space (cm)

**Table 3.** *Sound Levels from the Noise Sources (dB) (Young 1988)*

| | |
|---|---|
| Very light: 20 dB | Whisper, leaf rustling, background noise in broadcast studios |
| Light: 30 dB | Speaking with low voice, auditorium environment |
| Light: 40 dB | Private office, quiet house, quiet environment away from traffic |
| Moderate: 50 dB | Low-volume radio |
| Moderate: 60 dB | Speaking with moderate voice, noisy room |
| High: 70 dB | Medium noisy industry, medium noisy street |
| High: 80 dB | Noisy office |
| Very high: 90 dB | Police whistle, truck noise, noisy industry zone |
| Very high: 100 dB | High street noise |
| Deafening: 110 dB | Heavy industry, steel riveting |
| Deafening:120 dB | Thunder, airplane sound at departure |

**Table 4.** *Acceptable Background Audible Sound Levels in Areas with Human Activity (Beranek and Ver 1992)*

| Area Types | Approx. Sound Levels (dB) |
|---|---|
| Radio Broadcasting and Recording studios (Using microphone) | 18 |
| Concert hall, Opera houses etc. (For listening to light music) | 18-23 |
| Broad auditorium, Drama theater etc. (For very good listening conditions) | 28 |
| Radio-TV Broadcast and recording studios (Using closed microphone) | 33 |
| Small Auditoriums and theaters, Musical showrooms (For very good listening) or Conference halls for 50 people | 38 |
| Bedrooms, sleeping quarters, Hospitals, Apartments, Hotels, Motels vb. (For resting, sitting and sleeping), Small conference rooms, Classes, Libraries, Hospital rooms for 2-4 people (For good resting cond.), Living rooms in houses (Chatting while radio or TV is on) | 38-48 |
| Broad offices, Receptions, Retail stores, Stores, cafes, Dining houses, etc. (For barely good resting conditions) | 43-53 |
| Lobbies, Special working laboratories, Technical drawing and Engineering drawing rooms, General secretarial rooms (For full rest conditions) | 48-58 |
| Light food places, Industrial plant control rooms, Computer hardware rooms, Kitchens, Laundry (For barely good full resting conditions) | 53-63 |
| Shops, Garages etc. (For acceptable communication and phone communication centers) For locations with levels not recommended for any office and communication centers | 58-68 |
| For noisy working places or phone communication centers where verbal communication is possible, where sound is unwanted but it doesn't distract hearing | 63-78 |

The “Reinforced Concrete Prefabricated” facade elements used on the facades of ındustrial buildings, when they are multi-layered in cross-sectional dimension, the reinforced concrete outer and inner layers are connected to each other by tie bars. Therefore, while the section is being dimensioned, the sound insulation level calculation (R0) must be calculated taking into account sound bridges. The following equation can be used in calculations:

$$R_0 = 10\left[\log \frac{1}{\frac{fr^4}{f^4} + (n \times \sigma)}\right] \text{ dB} \quad (9)$$

Where:
F=Frequency, (Hz)
fr=Natural frequency of the facade element (Sim. Vibr. Freq.) (Hz)
n=Quantity of sound bridges
σ=Sound reflection degree

The sound reflection degree in the spot-sectioned sound bridges of the reinforced concrete prefabricated facade element can be calculated using the below formula:

$$\sigma = \frac{8}{\pi^2} \, x \, \frac{c^2}{f_g . S} \tag{10}$$

Where:
c=Sound spread speed in iron (m/s), (Table 5) (Özer 1979)
S=Cross section area of sound bridge ($cm^2$)
fg=Limit frequency of facade element's outer layer (Hz)

$$f_g = \frac{c^2}{2c_L . d} \tag{11}$$

d=The thickness of the outer layer of the facade element (m),
c= Sound spread speed in iron (m/s), (Table 5)
$c_L$=Vertical waves' spread speed in the plate (m/s), (Table 6)

**Table 5.** *Sound Spread Speed and Unit Weights in Some Materials*

| **Material** | **Sound Spr. Speed c(m/s)** | **Unit Weight (kg/m$^3$)** |
|---|---|---|
| Concrete | 4000 | 2000 |
| Aluminum | 5200 | 270 |
| Lead | 1300 | 11340 |
| Steel | 1000-4000 | 7800 |
| Cork | 500 | 200 |
| Air (- 15$^0$) | 330-350 | 1.2 |
| Water | 1453 | 1000 |

In the "Reinforced Concrete Prefabricated" industrial constructions, it is also necessary to take into consideration the door or window clearance inside the element in order to be able to calculate the sound insulation level using the factors affecting the cross-sectional dimension of the facade member. Because of the sound insulation in the element section, the improvement provided within the industry structure should not be adversely affected by the door or window opening. In this respect, the sound insulation level of the door or window (R1) must also be included in the calculation. If the gaps such as doors and windows in the facade element are lower than the sound damping (insulation) capability of the facade element, the structure will be adversely affected. A reinforced concrete prefabricated facade element's sound insulation (Rkp) with a door or window in it can be calculated using below formula 12:

$$R_{kp} = R - 10 \log \left[ 1 + \frac{F1}{F0} \, x \, \left( 10^{\frac{R - R1}{10}} - 1 \right) \right] \text{(dB)} \tag{12}$$

Where:

F1=Surface area of door or window ($m^2$),
F0=Wall area including door or window ($m^2$),
R=The B.A. Prefabricated facade element's sound damping (insulation) rate (dB),
R1=Sound damping (insulation) of door or window (dB) (Table 7)

**Table 6.** *Constant Value of Some Building Materials (Özer 1979)*

| **Material** | **Bulk Density ($g/cm^3$)** | **Elasticity Module ($E=N/m^2$)** | **Vertical waves' Spread speed in plate** |
|---|---|---|---|
| High-dens. concrete | 2.0....2.4 | $(25...35).10^5$ | $3.4 . 10^3$ |
| Light concrete | 0.6....1,3 | $(2.......4).10^5$ | $1.7 . 10^3$ |
| Amiant Cement | 2.0 | $28 . 10^5$ | $3.7 . 10^3$ |
| Plaster | 1.2 | $7 . 10^5$ | $2.4 . 10^3$ |
| Brick | (1.8....2.0) | $16 . 10^5$ | $(2.5....3) . 10^3$ |
| Lime Stuff | 1.7 | $44.10^5$ | $1.6 . 10^3$ |
| Glass | 2.5 | $60.10^5$ | $4.9 . 10^3$ |
| Flake boards | 0.6....0.7 | $4,6 .10^5$ | $2.7 . 10^3$ |
| Plexiglass | 1.2 | $5.6.10^5$ | $2.2 . 10^3$ |
| Glass Foam | 0.13....1.6 | $(1.3....1.6).10^5$ | $3.1 . 10^3$ |
| Aluminum | 2.7 | $72 .10^5$ | $5.2 . 10^3$ |
| Lead | 11.3 | $17.10^5$ | $1.3 . 10^3$ |
| Steel | 7.8 | $210.10^5$ | $5.1 . 10^3$ |

**Table 7.** *Sound Damping Rates of Windows (R) (Beranek and Ver 1992)*

| **Window Type** | **Avg. Sound Damping** | **Rate ( R )** |
|---|---|---|
| | With elastic webbing | Without elastic webbing |
| Simple Window | ~ 20 dB | ≤ 25 dB |
| Double-Glazing | ~ 25 dB | ≤ 30 dB |
| Double Casement | ~ 20 dB | ≤ 40 dB |

In double glass (layer) door and window formation, the g x a >100 formula should be watched.

Where:
g=Layer area weight ($kg/m^2$) (Table 4)
a=Distance between layers.

<u>Example Solution with "MT2 Prefabrike" Program</u>

While the dimensional analysis of the "reinforced concrete prefabricated" facade elements used in the industrial buildings' facades is done, another thing to be considered in determining the section size is the sound insulation performance of the element. When the sound performance of the element cross-section is measured, some data must also be entered into the program. These are:

Outdoor Air Sound (dB): In order to be able to measure which facade element is able to attenuate a high level sound, the outside air sound must be entered as data in the "Outside Air Sound (dB)" window of the program. These values are shown in Table 4.

Frequency (fr): By measuring the frequency of the environment, the obtained value must be added to the window of the "frequency (fr)" in the program.

Working Hours of Industry Structure: It is necessary to decide which of the activities in the industry structure will be carried out in the daytime or nighttime environment and to check the options indicated in the program window. Because the program will calculate the sound level for these two separate media separately and will thus analyze them separately. The element cross-section will be sized in such a way as to produce a suitable working environment inside against this outside air noise.

Sound attenuation measure (Rpk) calculations of the facade element will be done as such:

1. Night (22.00-06.00) Rpk<50 dB
2. Day (06.00-22.00) Rpk<60 dB

*Only those sections that meet these conditions will give the appropriate analysis report.*

Door/Window: When the element cross-section is determined, there are a number of factors that affect the outcome of the above analyses and should not be overlooked in the program. These are the Door/Window gaps in the element. The program offers options for these too. If there is a door/window opening in the front element, the combination criteria in terms of the dimensions of the opening and the sound technique of the doors and windows are also offered to the user as an option.

The program makes all insulation calculations according to these preferences. The facade element section can be verified until the sound insulation reaches the appropriate values and the program can continue to feed back until proper insulation is obtained.

By entering the above data, the program is then ready to perform sound insulation analysis. If the data is changed for sound insulation analysis, the result will change. If the outside air volume is high (140 dB) as in the above example, the operation will start with the "Analysis" command button and the dimensions of this element will be "Not suitable" in terms of the sound technique (Rpk) (Figure 15).

Analysis Results

This section is used to evaluate all of the previous study stages (Temperature, Sizing, Static). It will display the precautions to be taken according to the results obtained. If, as in the above example, the sound insulation performance of the facade element is not sufficient and the message "Not suitable" is received, then in the Analysis Results section, the necessary precautions will be taken to take precautions. Some precautions are:

- The thickness of sound insulation material can be increased.

- The door/window opening of the façade member may be reduced or removed if possible.
- Door/window joining technique options can be reviewed.
- Frequency can be lowered.
- The outdoor noise level can be reduced.

If all of this is inadequate, the process should be re-checked by adding a high-sound-insulation material to the section of the "Reinforced Concrete Prefabricated" facade element. For this, the "Heat", "Size" and "Static" analyzes of the element are repeated until the sound analysis.

**Figure 15.** *The Program's "Not Suitable" Analysis Window*

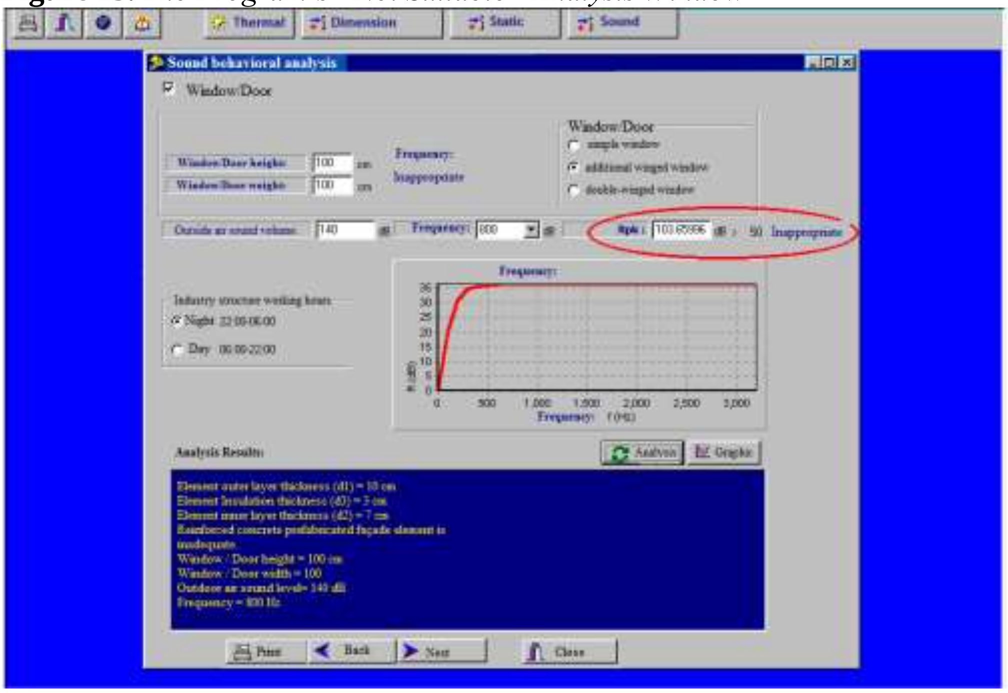


Sound Damping Rate/Frequency Graphic

After the sound insulation performance of the front element is made with the "Analysis" command button, the Frequency (f=Hz) Graph will be drawn in the program Sound Damping Rate (R=dB) based on the last found values of the element. It will suffice to press the "Graphic" command button for this. When the "graphic" command button is pressed the program will prepare the graphic which indicates the relation between "Sound damping rate R(dB) and Frequency f (Hz)" (Figure 16). This graphic will come to the computer screen as a separate window and will give the numerical values of the breakpoints. In other words, "Sound Damping Rate" (R=dB) can be tracked according to "Frequency (fr)" changes. The Graphic's "Zoom" function can be used for detailed views. This procedure will be completed with analyses and the user will be able to select "Back", "End", "Close" or "Print" command buttons to finish the process.

**Figure 16.** *The Program's "Graphic" Window for Sound Insulation*

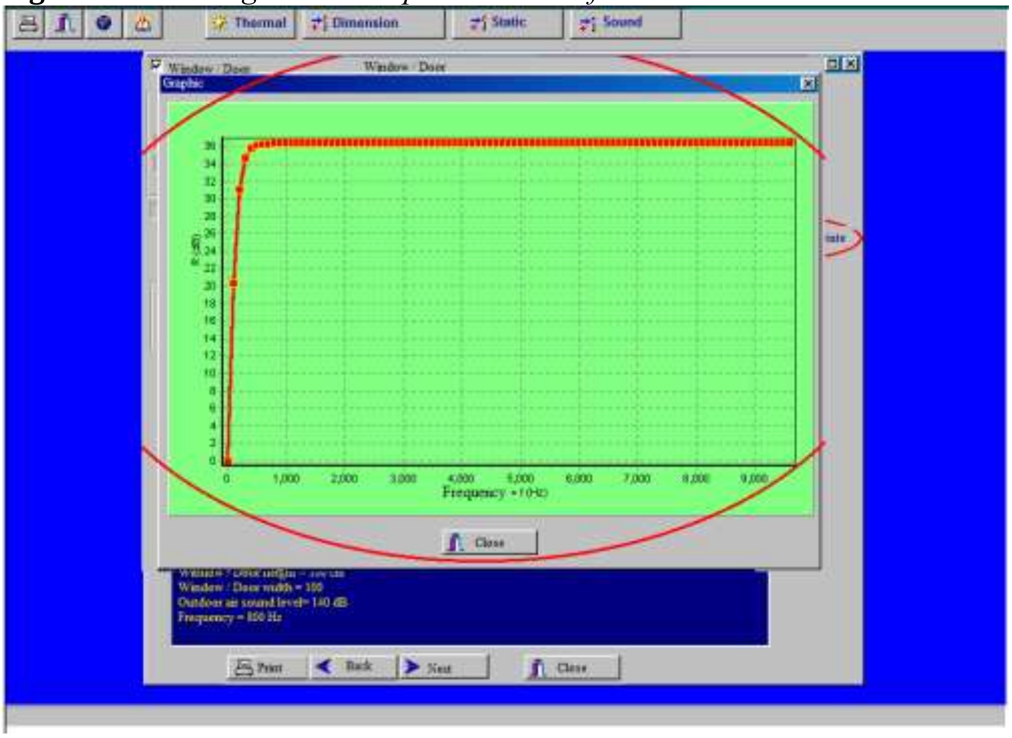


## Conclusion

This model software is prepared for multi-layered and non-carrier reinforced concrete. Prefabricated facade elements used in facades of Industrial Structures. For this software, firstly the dimensional performance and behaviors expected from the front elements were defined and the factors affecting them were determined. Later, calculations on the factors affecting dimensions of facade elements:

- Thermal insulation
- Coordination dimensions
- Carrying properties (static)
- Sound insulation feature can be made and optimum results can be obtained by evaluating these calculations. The results can be displayed in the "MT2 Prefabrike" analysis program in a virtual world window.

This model software will play an important role in giving product decisions before production of facade element. These are:

1. The facade element will have the required "Thermal Insulation" fittings for application everywhere in Turkey.

2. According to the design form of the element on the facade, “Coordination Dimension” (A) will be calculated and it will facilitate the necessary infrastructure preparations for the production of the element.
3. With optimization of the “Element’s Carrying Features” (static) risks of breaks and cracks can be eliminated.
4. Industrial structures will have “Sound Insulation” fittings to continue to function well in noisy environments.

This “MT2 Prefabricated” dimensional analysis program, developed for “Reinforced Concrete. Prefabricated Facade Elements”, is also a “Model” in terms of reducing diversity of dimensional behaviors expected from “Reinforced Concrete Prefabricated” structural members and facilitating “Standardization” approaches.

With this software, it is aimed to bring a correct view to the problem of the misunderstood standard concept of prefabricated building elements and is exemplified on a model.

## References

Azhar S (2011) Building Information Modeling (BIM): trends, benefits, risks, and challenges for the AEC industry. *American Society of Civil Engineers* 11(3).

Azhar S, Nadeem A, Mok JYN, Leung BHY (2008) Building information modeling (BIM): a new paradigm for visual interactive modeling and simulation for construction projects. In *Proceedings of the First International Conference on Construction in Developing Countries*, 435–446. Karachi, Pakistan.

Bakır E (1990) *Design principles guide of prefabricated reinforced concrete buildings.* Ankara: Prefabricated Association.

Beranek LL, Ver, IL (1992) Noise and vibration control engineering. In *Principle and Aplications*. USA.

Cansun O (1989) *Curtain wall.* Lecture Notes. İstanbul: Department of Building, İ.T.Ü. Faculty of Architecture.

Christiane MH, Davide L, Isaac G (2018) Parametric design of sculptural fibre reinforced concrete facade components: learning, adapting and prototyping. In *Proceedings of the 23rd International Conference of the Association for Computer-Aided Architectural Design Research in Asia (CAADRIA) 2018,* volume 2, 319–328.

Chudley R (1994) *Construction technology.* Second Edition. Pearson India.

Eastman C, Teicholz P, Sacks R, Liston K (2008) *BIM handbook: a guide to building information modeling for owners, managers, designers, engineers and contractors*. New York: Wiley.

Eriç M (1994) *Building physics and materials*. Istanbul: Literature Publications 2.

Escrig F, Brebbia CA (1996) *Mobile rapidly assembled structure-II.* Southampton: Bookcraft Limited.

International Standardization Organization – ISO (1990) *Accoustics - Determination of occupational noise exposure and estimation of noise-induced hearing impairment*. ISO 1999.2. Geneva, Switzerland.

Lantim D (1998) *Delphi 3*. Computer Software. Paris: Eyrolles.

Montali J, Overend M, Pelken PM, Sauchelli M (2017) *Knowledge-based engineering applications for supporting the design of precast concrete facade panels.* In *DS 87-6 Proceedings of the 21st International Conference on Engineering Design (ICED 17)*, volume 6, 131–139. Vancouver, Canada.

Özer M (1979) *Building acoustics and sound insulation*. Istanbul: Arpaz Publishing.

Şener H (1990) *Open Systems in Industrialized Building*. Architecture Print Workshop. Istanbul: İ.T.Ü. Faculty of Architecture.

TSE 825 (1999) *Thermal insulation requirements for buildings.* Ankara: T.C. Bayındırlık ve İskan Bakanlığı.

Wang-Dong Y, Qiang C, Ni L (2011) *A framework-based model of software construction.* In *IEEE 2nd International Conference on Software Engineering and Service Science*, DOI=10.1109/ICSESS.2011.5982310.

Young RW (1988) *Optimum levels for reporting community noise.* Washington, USA: Private Communication.